The huntingtin protein in Huntington disease

Schut, M.H.

The huntingtin protein in Huntington disease

Menno Schut

Colophon
Cover: Menno H. Schut and John K. Fransz
Layout: M.H. Schut
Printing: Ipskamp
ISBN: 978-94-028-0703-5

The work described in this thesis was financially supported by grants from the Prinses Beatrix Spierfonds (WAR08-08) and the LUMC Bontius stichting.

The huntingtin protein in Huntington disease

Proefschrift

ter verkrijging van
de graad van Doctor aan de Universiteit Leiden,
op gezag van Rector Magnificus prof.mr. C.J.J.M. Stolker,
volgens besluit van het College voor Promoties
te verdedigen op woensdag 20 september 2017
klokke 15:00 uur

door

Menno Harm Schut
geboren te Voorburg
in 1980

Promotor:

Prof. Dr. G.J.B. van Ommen

Co-promotor:

Dr. W.M.C. van Roon-Mom

Leden promotiecommissie:

Prof. Dr. A.M. Aartsma-Rus

Prof. Dr. R.A.C. Roos

Prof. Dr. Y. Temel (Maastricht UMC)

Dr. E.A.J. Reits (AMC Amsterdam)

"Life is enormously about luck"

John Cleese (College Tour, 2014)

Thesis Contents

Chapter 1

General Introduction

Choreatic movement disorders such as Syndenham's chorea (also known as St Vitus dance) have been described since the middle ages [1]. The accompanying symptoms were often associated with possession or a form of punishment, invariably leading to stigmatisation. The term "chorea" was first introduced by Paracelsus [2], who also disconnected the presumed link between choreatic movements and supernatural phenomena [3]. Huntington disease is a choreatic movement disorder with a long historical background [4]. Although the symptoms and familial occurrence associated with Huntington disease were described before in medical literature, the disease was named after George Huntington who gave a thorough description in his 1872 paper [5]. Unfortunately and especially due to the rise of eugenics in the first decades of the twentieth century, Huntington disease was also subject of severe stigmatization [6]. Currently, patients suffering from Huntington disease still perceive discrimination in various ways [7-10]. Obviously, Huntington disease and other choreatic movement disorders impose a profound psychological burden on patients and their surroundings. Therefore, research into therapeutic interventions that delay or even halt the onset of Huntington disease symptoms would be of great benefit.

1.1 Huntington disease

Huntington disease (HD) is an autosomal dominant genetic disorder that mainly affects the brain [11, 12]. Symptoms of HD are diverse and include weight loss, psychological and behavioral problems, clinical depression and a decrease in voluntarily motor ability [13-17]. HD is a rare disorder with a prevalence between 1:10.000 to 1:100.000 varying with the geographical location [18]. The most striking symptom of HD is the appearance of involuntarily choreatic movements [5, 12]. In classical cases, HD symptoms first appear around mid-life and HD progression usually lasts more than 10 years [12], with the cause of death being secondary complications [14, 19-21]. Clinically, the boundary between pre-symptomatic HD gene-carriers and symptomatic HD patients is diagnosed with the onset of motor symptoms. However, psychological and behavioural symptoms often precede clinical HD [22]. Furthermore, it is thought that neuronal dysfunction and death precede the onset of clinical symptoms by years [23]. Hence, techniques to monitor disease progression before onset are pursued [23-28]. Furthermore, biomarkers capable of monitoring HD related changes in an early stage in easy accessible tissue, such as the level of mutant huntingtin protein in cerebrospinal fluid [29, 30], or transcriptome analysis of peripheral blood [31, 32] are of particular importance.

1.1.1 The genetics of HD

After several decades of research, the HD gene was mapped to chromosome 4 [33, 34]. In 1993, the responsible mutation was mapped to 4p16.3 and was originally referred to as *IT15* (interesting transcript 15) [35] while now it is named the *huntingtin*-gene (*HTT*). The causative mutation in HD was found to be expansion of a CAG repeat present in the first exon of *HTT*, resulting in a mutant huntingtin (htt) protein with an elongated polyglutamine (polyQ)-stretch [35, 36]. An expansion length of 36 CAG's or more is considered mutant [37], and there is an inverse correlation between the age of clinical symptom onset (AoO) and length of the CAG repeat [37, 38]. Hence, subjects with relatively short expanded CAG repeats (between 36-39 CAG's) may, or may not show clinical symptoms during their life time. Therefore CAG expansions within this range are considered to invoke a "reduced penetrance" of the HD phenotype, while CAG repeats of 40 or more are considered to invoke full penetrance [39]. Correlation between AoO and the CAG-repeat is ~70%, and AoO can vary several decades between subjects with the same CAG repeat length [40]. Recently, several genetic factors have been identified that influence the age of disease onset with -1.6, -6.1 or +1.4 years respectively [41]. Neither AoO, nor CAG repeat length is correlated to the duration or severity of the disease [42, 43]. The HD phenotype of subjects that are homozygous for the HD mutation does not remarkably differ from heterozygous subjects [44, 45], which underlines the strong autosomal dominant nature of HD. The elongated CAG repeat in HD is meiotically unstable, and exhibits anticipation during intergenerational transmission [46, 47]. Elongation of the CAG-repeat is mainly associated with paternal transmission [46-49]. Maternal transmission of the CAG-repeat length is mainly associated with no effect, or shortening of the repeat [48, 49], but CAG repeat elongation by maternal transmission is possible [50]. In addition, instability of

the CAG repeat in post-mitotic neurons was observed in HD mouse models and human HD subjects [51]. Meiotic and mitotic instability of CAG repeats have also been reported for other polyQ diseases such as SCA-1 [52], and SCA-7, [53], but not for Spinal Bulbar Muscular Atrophy (SBMA) [54]. This variability suggests a link between CAG stability and the specific gene. CAG repeat instability has been linked with DNA damage and repair mechanisms [55, 56], and chromatin remodelling [57]. The general population harbours a certain degree of longer, but non-HD associated CAG repeat lengths between 27 and 35 (intermediate CAG-repeat length). For example, 5,8% of the general population of British Columbia was found to carry an intermediate CAG repeat [58]. Due to intergenerational instability of the CAG-repeat, intermediate CAG-repeats are a risk of generating more *de novo* HD-cases [59]. Some debate regarding the question if intermediate CAG repeats could invoke an HD phenotype as well [60, 61] is currently ongoing. However, in these cases it is unclear if the observed phenotype is directly linked to the CAG repeat or due to a phenocopy [62], or even an unrelated phenotype [63].

1.1.2 HD pathology

Post-mortem brain pathology of HD can be divided into five grades (o, i, ii, iii, iv) as defined by VonSattel [64]. The primary region of pathology is the striatum **(Figure 1A)**. Striatal degeneration is already apparent on MRI-scans in pre-symptomatic HD-gene carriers [65]. Cortical involvement in HD pathology is associated with brain weight [66]. On a cellular level, neurons are specifically affected by HD pathology [64]. A subset of medium spiny neurons expressing preproenkephalin are preferentially affected early in the disease [67], when other neuronal subtypes are spared [68]. There is a large degree of variation in the pattern of neuronal loss between HD subjects, which could explain variances in HD “motor” or “mood” phenotypes [69-71]. A key pathological hallmark of HD is the presence of protein aggregates (**Figure 1B** and [72, 73]). The presence of aggregates within the cell nucleus was linked to the polyQ-length [74-76]. The exact role of these aggregates in HD pathology remains elusive. On one hand, delivery of polyQ aggregates in the nucleus of Cos-7 or PC12 cells was pathogenic for the cell [77] and transfer of htt aggregates between neuronal cells is possible through tunneling nanotubes [78]. Furthermore, aggregates were shown to sequester other cellular proteins such as transcription factors [79, 80], RNA binding proteins [81] and several vesicle-associated proteins [82]. This suggests that aggregates are pathologic by interfering with the cellular functions for which the co-aggregated proteins are important. However, the selective pattern of striatal degeneration does not correlate with the observation that aggregates are predominantly found in cortical tissue and neuronal cells that are less vulnerable for mutant htt [83, 84], and it has been shown that aggregate formation can be beneficial for cells [85, 86].

1.1.3 Juvenile HD

In juvenile HD (jHD), HD symptoms occur at an early age. The exact definition of jHD is a matter of debate [87], but is generally defined as an AoO lower than 20 years [12]. Juvenile HD is rare with a prevalence among the general HD population of approximately 5% [88]. As AoO is influenced by the CAG repeat length [40], jHD is associated with exceptionally long CAG repeats of over 55 [12]. Subjects with jHD are more likely to exhibit the Westphal-variant of HD clinical symptoms [89] which differ from classical HD, and include rigidity and bradykinesia [90-92].

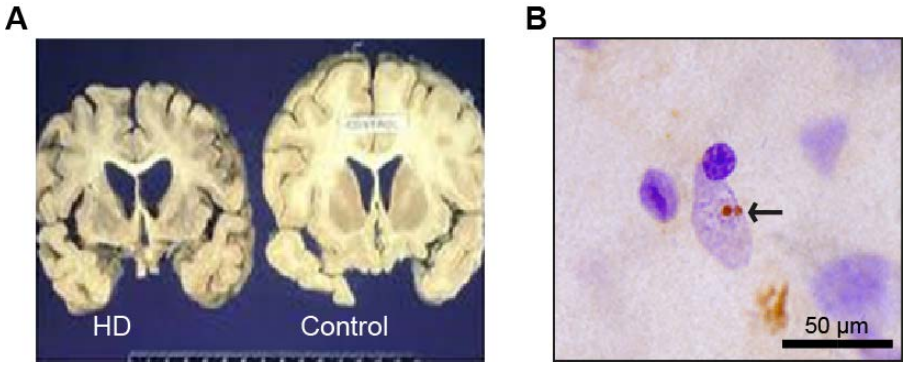

Figure 1 – HD Pathology

(A) Coronal sections of *post mortem* brain tissue from a late-stage HD patient versus a control subject. Within the HD-brain, enlargement of the ventricles, severe degeneration of striatal tissue and cortical atrophy is observed. *Image courtesy by Prof. Dr. Raymund A.C. Roos*. (**B)** DAB staining of *post-mortem* human HD brain tissue. Huntingtin aggregates indicated by an arrow. Cell nuclei are Nissl counterstained. *Image courtesy by Dr. W.M.C. van Roon-Mom.*

1.2 The huntingtin protein

Huntingtin (htt) is a large protein containing 3144 amino acids with a molecular weight of approximately 348 kD [35]. Evidence suggests full-length htt has an elongated "superhelical" tertairy structure [93]. Immunohistochemistry on monkey and human brain indicate that htt is predominantly present within the cytoplasm of neurons throughout different brain regions with larger neurons bearing a stronger signal [94-97]. Nuclear localization of htt was more abundant with HD subjects [95]. The normal huntingtin protein has many functions [98] within several cellular processes including mitosis [99], autophagy [100-102], vesicular transport through interaction with the dynein-complex [103-107], regulation of transcription [108, 109], transport of TrkB receptors [110] and transport of brain derived neurothropic factor (BDNF) [111]. Huntingtin has an anti-apoptotic effect [112], associated with the prevention of Pak2-cleavage [113]. The htt protein is essential for embryonic development. Morpholino-mediated knockdown of *HTT* in *Xenopus* frogs resulted in altered neuronal development and a paralysed phenotype [114]. Double knockout (htt^{-}/htt^{-}) mice did not survive past 7.5 days of embryonic development [115]. Interestingly, expression of mutant *HTT* within (htt-/htt-) mice rescued embryonic lethality implying that the mutant htt protein retains functionality [116]. This

implies a toxic gain-of-function mechanism such as impairment of transcription [117], defective actin remodelling [118], mitochondrial functioning [119-121], or endosomic vesicle formation [122] as an underlying cause for HD pathology. However, additional effects from loss of normal htt function cannot be excluded [123, 124].

1.2.1 Expression of normal and mutant huntingtin mRNA and protein

Huntingtin is expressed in all areas of the brain and all cell types of the brain which does not explain the region-specific HD pathology. Using northern blotting, expression of *HTT* RNA was detected throughout the brain and several peripheral human and rat tissues (heart, skeletal muscle, placenta, lung, liver, kidney and pancreas) [125]. This ubiquitous expression of *HTT* RNA was also shown using *in situ* hybridization on human brain tissue [126]. In concordance, the htt protein was also detected throughout the human brain [94, 97], as well as in several peripheral rat tissues (lung, spleen, kidney, thymus, liver and testes) [94], and in human derived myoblasts, fibroblasts and lymphoblasts [127-129]. Knowledge on the expression levels of the wild-type versus mutant htt allele in individual subjects is limited and not always consistent. Using qPCR against the 5' UTR, no significant difference between wild-type versus mutant *HTT* RNA was found in human cortical and striatal brain tissue [130]. Also, total *HTT* mRNA levels in lymphoblastoid cells were the same between HD patients and controls [131]. On the other hand, higher levels of mutant *HTT* mRNA with respect to wild-type *HTT* mRNA were detected with qPCR against SNP rs362307 in human cortical and striatum tissue samples [132]. Translation of mutant *HTT* mRNA into the mutant protein was suggested to be upregulated by increased interaction of the MID1-PP2A protein complex with the elongated CAG repeat [133]. Two antisense transcripts (*HTTAS_v1* and *HTTAS_v2*) are present at the *HTT* locus. Expression of *HTTAS_v1* was shown to reduce *HTT* transcripts in HEK293 and SH-SY5Y HD cell models. However, levels of the *HTTAS_v1* antisense transcript is suggested to be reduced in HD subjects [130]. The elongated polyQ-repeat results in a slightly larger protein, but also invokes atypical structural properties yet to be defined that further decrease mobility in an SDS-PAGE gel [134]. Hence, it is possible to separate wild-type htt from mutant htt on gel and visualize both forms separately. Western blot results on lymphoblasts indicated that longer polyQ repeats resulted in lower expression of the corresponding mutant htt protein [97]. Although no statistical analysis was performed by Hu *et al*, their western blots results on different human-derived HD fibroblasts also indicated a lower expression of the mutant htt protein [135]. Western blot studies in post-mortem human cortex and cerebellar tissue indicated that expression-levels of wild-type and mutant htt are comparable [36, 95]. Somatic mosaicism, the presence of genetically distinct cells within the same organism [136], was shown in HD mouse models and human HD subjects [51]. Somatic mosaicism can be observed on western blot by the presence of multiple protein bands that do not correspond to degradation products or post-translational modifications [36].

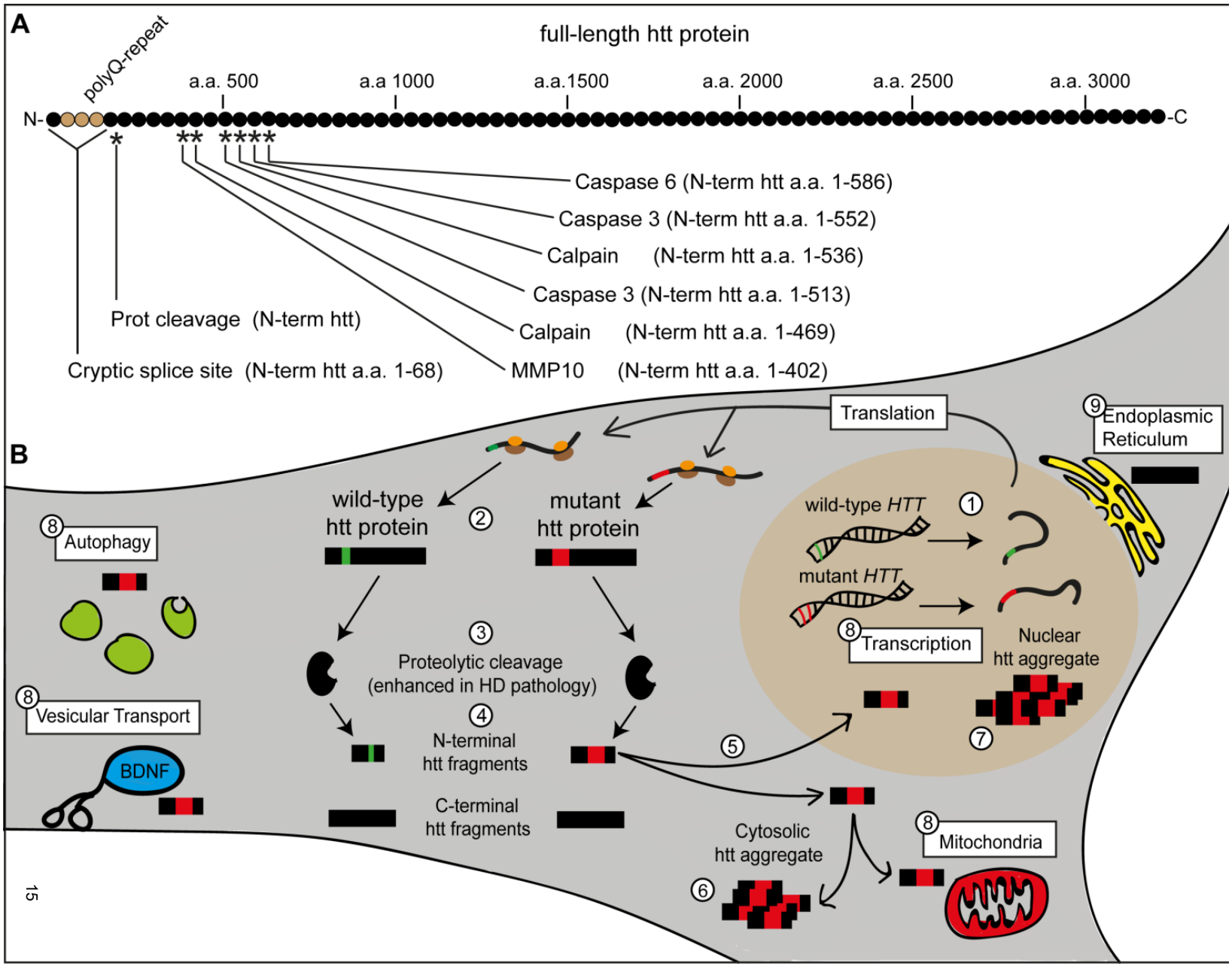

Figure 2 – Huntingtin fragments and HD cellular pathology.
(A) Full-length htt with polyQ-repeat and N-terminal proteolytic cleavage sites indicated. "a.a." = amino acid. **(B)** Huntingtin fragments within the cell. (1) Transcription of the wild-type *huntingtin* gene (normal CAG-repeat, green) and mutant *huntingtin* gene (expanded CAG-repeat, red) results in wild-type and mutant *HTT* mRNA. Subsequent translation results in a wild-type htt protein with a normal polyQ-repeat (green), and a mutant htt protein with an expanded polyQ repeat (red) (2). Proteolysis (3) of wild-type and mutant htt protein results in N-, and C-terminal htt fragments (4). Cellular localization of mutant N-terminal htt fragments depends on their proteolytic origin. Smaller, and Caspase6 associated mutant N-terminal htt fragments migrate to the nucleus. Other fragments remain in the cytosol, or the perinuclear region (5). Huntingtin aggregates are formed in the cytosol (6) and the nucleus (7). Soluble mutant N-terminal htt fragments interfere in various cellular processes (8), while C-terminal htt fragments (without polyQ repeat) interfere with the endoplasmic reticulum (ER, 9).

1.2.2 N-terminal huntingtin protein fragments

The first 17 htt amino acid domain (N17-htt) with the sequence MATLEKLMKAFESLKSF, that precedes the polyQ-repeat, plays an important role in HD pathology. N17-htt is associated with htt cellular distribution [137-139], has a high conformational flexibility [140] and is important for mutant htt aggregation [141-143]. The lysine residues can be either ubiquitinated or SUMOylated, where the latter is associated with HD pathology [144, 145]. N17-htt can be phosphorylated at serines S13 and S16, which has been associated with a reduction of mutant htt aggregation and a reduced HD phenotype in BACHD mice [146]. Directly after the polyQ-repeat, there is a poly proline repeat (polyP) which was suggested to be involved in the sequestering of additional proteins to htt aggregates [82]. The mutant htt protein is susceptible to degradation. Caspase-6, a protease associated with apoptosis is activated early in HD [147, 148] and the elongated polyQ shortens the lifetime of the mutant htt protein, suggesting that the mutant protein is less stable [149]. Also, more proteolytic cleavage fragments of htt were shown in HD brain tissue [150], and **chapter 4**. The importance of N-terminal mutant htt protein fragments in HD pathogenesis has been well established. First, results in HD mouse models that contain full-length or N-terminal htt constructs indicate an increased toxicity for the N-terminal mutant htt fragments. This was illustrated by the different phenotypes exhibited by the R6/2, YAC128 and Hdh$^{Q150/Q150}$ HD mouse models. The R6/2 mouse model expresses the first exon of human *HTT* with 150 CAGs [151]. The R6/2 model has an average age of symptom onset between 9 to 11 weeks, with detectable intranuclear htt inclusions appearing after 7 weeks [152]. The YAC128 mouse model that expresses the full-length human *HTT* with 128 CAGs [153], shows a much milder HD phenotype. The YAC128 mouse has a lifespan beyond 18 months, shows an AoO after 3 months, a decrease in brain weight after 9 months and detectable intranuclear htt aggregates after 12 months. The H*dh*$^{Q150/Q150}$ mouse model expresses full-length murine htt with 150 Q's [154]. Compared with the R6/2 phenotype after 12 weeks, H*dh*$^{Q150/Q150}$ mice reached a comparable phenotype after 22 months. N-terminal mutant htt fragments not present in aggregates are mainly monomeric [155] and interfere with cellular processes such as transcription [117] and mitochondrial functioning [119]. In human *post-mortem* brain tissue, a difference in striatum-associated N-terminal htt fragments between controls and HD subjects was detected [150], further indicating an involvement of these fragments in HD pathology. Several N-terminal htt proteolytic cleavage sites have been identified. Huntingtin is cleaved between htt amino acids 104-114 as demonstrated in a mouse-rat neuroblastoma-glioma HD cell model [156, 157], and by matrix metalloproteinase 10 (MMP-10) at amino acid 402 in mouse striatal HD cell-line Hdh$^{111Q/111Q}$ [158]. Using a 293T (human kidney) cell model of HD, calpain cleavage sites were identified at htt amino acids 469 and 536 associated with mutant htt toxicity [159]. In addition, experiments with an HEK293 HD cell model indicated that there are two caspase-3 cleavage sites and one caspase-6 site, associated with HD pathology present at amino acid positions 513, 552 and 586 respectively [160]. The caspase 3 site at position 552 was additionally detected in human and mouse brain tissue [161]. Although the Caspase-3/6 associated N-terminal htt fragments are comparable in size, they behave differently within the cell. Caspase-6 is activated early in HD [147, 148] and Caspase-6, but not Caspase-3 cleavage was associated with HD pathology in the YAC128 mouse model [162]. Caspase-6 related N-terminal htt fragments localize

within the cell nucleus, whereas N-terminal htt fragments related to caspase-3$^{(a.a.552)}$ cleavage localized within the perinuclear region [163]. A comparison between mouse models expressing different N-terminal htt fragments showed that the caspase-3$^{(a.a.552)}$ N-terminal htt fragment resulted in a more severe phenotype than the caspase-6$^{(a.a.586)}$ N-terminal fragment [164]. In addition, abherrant htt protein fragments can also arise from non-proteolytic cleavage-related events. This was shown in the H*dh*$^{Q150/Q150}$ mouse model in which fourteen different N-terminal htt fragments were identified by western blotting, from which the smallest fragment was mapped to the protein part expressed by *HTT* exon 1 only [165]. Subsequent experiments indicate that the source of the exon1-htt fragment is an aberrant splicing event associated with increased binding of the SRSF6 splicing factor to expanded GAC repeats [166]. Recently, the C-terminal htt fragment not containing the polyQ-repeat that arises from htt cleavage was also shown to contribute to HD pathology by invoking endoplasmic reticulum (ER) stress through errant interaction with dynamin 1 [167].

1.3 HD therapeutic strategies

Currently, HD treatment is limited to alleviating symptoms resulting in a combination of therapies as each symptom mandates a different approach. The search for effective HD therapies is extensive and different intervention strategies are assessed [168], including the targeting of peripheral tissues [169], which circumvents the need for passing the blood-brain barrier (BBB) [170, 171]. A therapeutic intervention which directly targets the pathogenic mutant htt protein is expected to alleviate all HD symptoms, delay disease-onset and decrease the therapeutic burden on HD patients (**Figure 3a**). There are several different ways to target the mutant htt protein directly: directly lowering the expression levels of mutant htt, modification of the mutant htt protein product or blocking pathologically important domains **(Figure 3b)**. Selective lowering of mut *HTT* mRNA translation resulting in less mutant htt protein was demonstrated in human fibroblasts derived from HD patients using several types of oligonucleotide constructs including peptide nucleic acid (PNA) and locked nucleic acid (LNA) [135], small interfering RNA's (siRNA) [172, 173] and antisense oligonucleotides (AON) [174]. However, specificity for lowering the mutant allele without affecting the wild-type allele remains an issue with this approach, as lowering of wild-type huntingtin expression is unwanted [123]. Modification of the mutant *HTT* mRNA by means of AON mediated exon-skipping of the 3'part of *HTT* exon 12 was shown to produce a truncated mutant htt protein (htt-Δ12) lacking the pathologically important caspase-6 cleavage site [175]. Toxicity from this specific htt isoform is not expected as htt-Δ12 occurs naturally [176]. However, protein modification by exon skipping could have unexpected toxic effects depending upon the chosen strategy. Moreover, exon-skipping is not specific for the mutant *HTT* allele. The specificity-issue could be addressed by the use of antibodies. Antibodies or immunoglobulins have a high specificity for their antigen. There are several classes of classical antibodies (IgA, IgD, IgE, IgG and IgM) of which the IgG-class is the most abundant. The IgG class can be further divided into four subclasses, and is a "Y"-shaped tetramer of approximately 150 kDa consisting of two heavy chains and two light chains **(Figure**

4a, IgG1**)**. The epitope recognizing domain, responsible for antigen binding, is formed only after combination of the correct light-and heavy chain domains. Antibodies are currently utilized against a broad spectrum of different pathologies such cancer [177, 178], auto-immune diseases [179], poisoning [180], and they are evaluated as a potential therapy against the Ebola virus [181]. However, BBB crossing by antibodies is very limited due to their size [182]. It is possible to artificially remove domains from the antibody without affecting specificity and affinity for the epitope, thus creating a smaller antibody fragment called a single-chain antibody fragment, or scFv, **(figure 4a)** [183]. An scFv against the htt N17 domain of the htt protein was shown to counter mhtt aggregation in a HD cell model [184], suppress HD pathology in a HD *drosophilia* model [185], and to reduce HD pathology in the R6.1 HD mouse model [186].

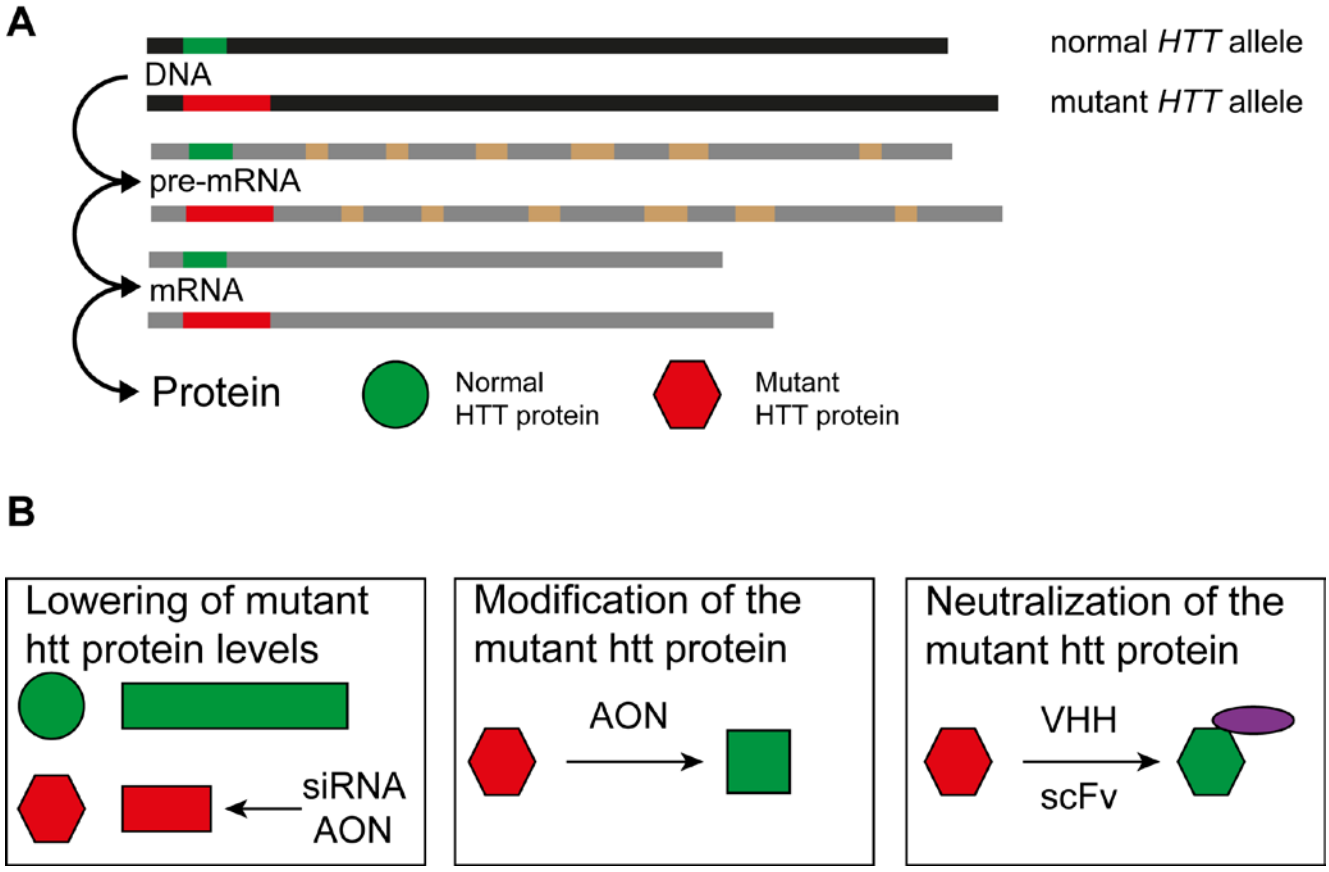

Figure 3 – Therapeutic strategies in Huntington disease

(A) Alleles for normal *HTT* (CAG-repeat indicated in green) and mutant *HTT* (expanded CAG repeat indicated in red) are first transcribed into pre-messenger RNA (pre-mRNA). Several post-transcriptional modifications of the pre-mRNA, including splicing of the introns (illustrated in brown) result in messenger RNA (mRNA) which is translated into either normal (green circle) or mutant (red hexagon) HTT protein. **(B)** Therapeutic strategies targeting expression levels or toxicity of the mutant huntingtin protein. *Specific lowering of mutant htt protein levels* by means of silencing the mutant *HTT* gene on the translational level using siRNA or AON. *Modification of the mutant huntingtin protein* by exon skipping during post-transcriptional modification. This results in a modified mutant huntingtin protein (green square) with fewer pathological properties. *Neutralization of the mutant huntingtin protein*. Antibody (VHH, scFv) binding of pathologically important domains on the mutant huntingtin protein could neutralize its toxicity.

1.3.1 VHH antibody fragments

In 1993, the same year as the discovery of the HD-gene, a unique antibody class lacking light chains was found in camelids [187]. These heavy chain-only (HCA) antibodies, also found in sharks (called IgNAR, [188]) consist of heavy chain dimers **(figure 4a).** The VHH antibody fragment is derived from the epitope recognizing domain of the HCA. The VHH has four framework-regions (FR1-4) that are important for protein integrity, and three hyper variable complement determining regions (CDR1-3) that are important for epitope selectivity and affinity **(figure 4b)**. Due to the lack of VH-VL interaction, the architecture of the VHH-domain is different compared with the IgG1-VH-domain [189]. VHH are versatile in their antigen binding capabilities. Crystal structures from a VHH in complex with lysozyme show that the CDR3 domain forms an extending “loop” allowing the VHH to preferentially bind the enzymatic cleft [190, 191], although VHH are also capable of binding flat surfaces using only the CDR3 [192]. In addition, VHH have several other advantages compared with conventional IgG antibodies: VHH are 16kD in size and stable [193, 194], VHH can be selected easily, intracellular expression of VHH is possible [195, 196], and VHH production in *E.Coli* cells is very effective [197].

1.3.2 Application of VHH antibody fragments

Due to their versatility, VHH have several possible medical applications. They are promising as a fast-acting antivenom against scorpion (*Androctonus australis hector*) poisoning [198, 199], or the prevention of endotoxin-induced sepsis [200]. VHH directed against the CD4 binding site of the gp120 envelope protein of HIV-1 show potential in blocking viral infectious capability [201, 202]. VHH also show potential as application against oculopharyngeal muscular dystrophy (OPMD), an autosomal dominant inheritable disease similar to HD as it is caused by expansion of an N-terminal polyA repeat of the polyadenylate binding protein nuclear 1 (PABPN1) protein resulting in mutant PABPN1 aggregation. Co-expression of an anti PABPN1 VHH (3F5) was capable of inhibiting mutant PABPN1 aggregation in a HeLa cell model and alleviating the phenotype of an OPMD drosophila model [196, 203]. For neuroscience, VHH are of interest because they are capable of crossing the blood-brain barrier (BBB) without the help of a carrier under certain circumstances [204]. BBB-crossing potential was demonstrated in an in-vitro BBB model for an anti-β amyloid VHH [205]. This VHH was shown to be capable of differentially recognizing parenchymal and vascular amyloid deposits which will aid in the differential diagnosis of Alzheimer's disease and cerebral amyloid angiopathy [206, 207]. VHH might also be applicable as a therapeutic, diagnostic or research tool for other neurological diseases such as HD.

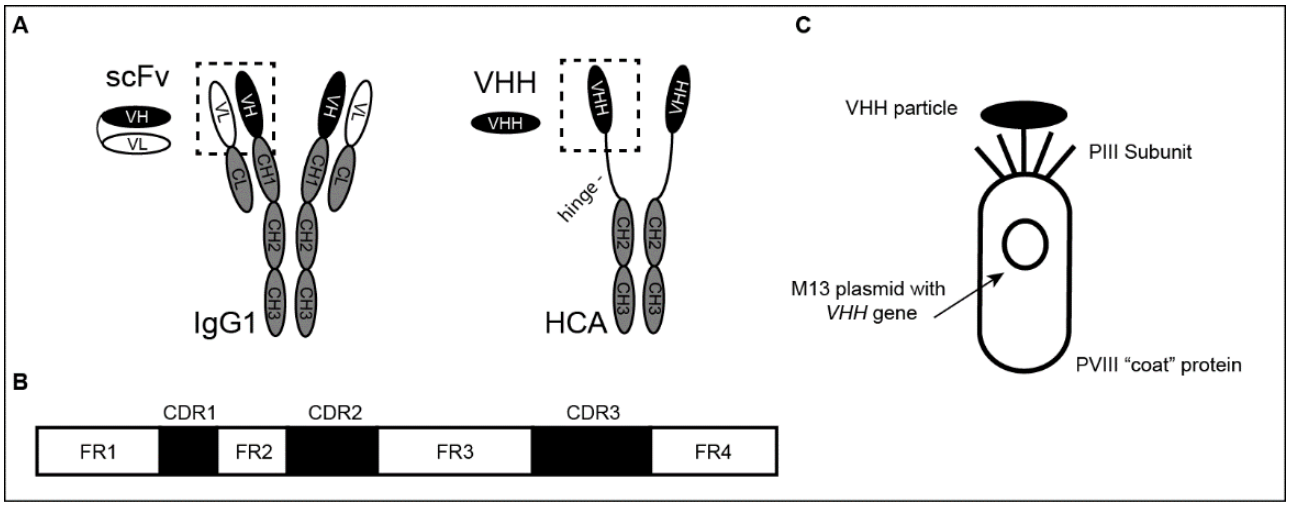

Figure 4 – Schematic overview of VHH antibody fragments.

(A) Immunoglobulin G antibodies (IgG1) consist of two heavy (H) and two light (L) chains. The H and L-chains consist of one (L) or three (H) constant regions (CL, CH1, CH2 and CH3), and one variable region (VL or VH) where the latter forms the antigen recognizing domain (dotted square). The scFv antibody fragment contains the IgG antigen recognizing domain connected by a peptide linker. Heavy chain antibodies (HCA) lack light chains and the CH1-domain from IgG is replaced by a hinge region that links the antigen recognizing domain (VHH, dotted square) with the CH2-domain. **(B)** VHH antibody fragments consist of four framework-regions (FR1, FR2, FR3 and FR4) that are mainly important for structural integrity, and three hyper-variable complementary determining-regions (CDR1, CDR2 and CDR3) that usually determine the epitope. **(C)** Illustration of an M13 phage-VHH particle (P-VHH). The VHH antibody fragment is attached to the PIII subunit while the corresponding *VHH* gene is present on the M13 plasmid encapsulated within the M13-phage particle. Western blot and ELISA with P-VHH as a primary antibody utilise secondary antibodies directed against the PVIII "coat" protein.

1.3.3 Selection of VHH antibody fragments

Because VHH are expressed from a single gene, cloning and selection of suitable VHH is straightforward. VHH can be selected by means of M13 phage-display [208, 209] with the VHH expressed as attachment to the pIII-subunit **(**Phage-VHH, **Figure 4C)**. The construction of a phage display library is illustrated in **Figure 5A** and could be performed either from non-immunized (naïve) [195, 196], or immunized [207, 210, 211] llama's (*Llama glama*). Selection from naïve libraries is expected to yield a higher diversity of binders compared with immunized libraries, but affinity of binders is expected to be lower due to the lack of affinity maturation against the antigen. It is possible however to enhance VHH binding affinity by artificial maturation [212]. The selection of suitable Phage-VHH from a phage display bank consists of one or more subsequent rounds of selection in which the antigen could be presented in several ways. **Figure 5B** shows a 2-round selection with antigen-capturing and antigen-panning.

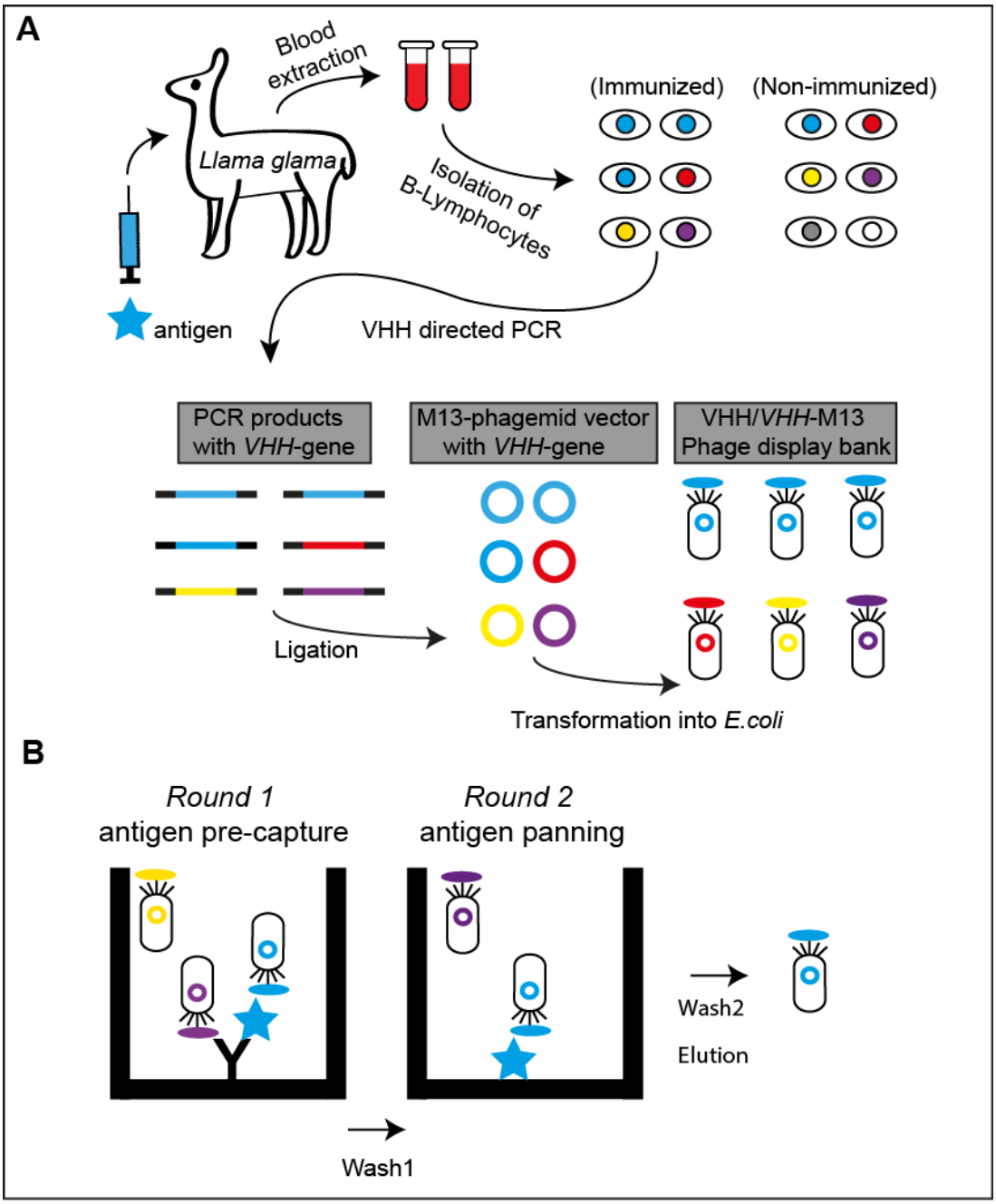

Figure 5 – Construction of llama VHH phage display library.

A B-lymphocytes containing *HCA* genes are extracted from llama (*Llama glama*) blood. Pre-immunization with the desired antigen (blue) generally results in more high-affinity binders, but lowers diversity of the library (Immunized versus non-immunized). Linear DNA fragments resulting from a PCR of the *VHH* genes within *HCA* are cloned into the M13-phagemid vector. The library of M13-VHH phagemid vectors is transformed into *Escherichia coli* cells for production of the different P-VHH particles that make up the llama phage display library. Antigen diversity is illustrated by color. **B** P-VHH selection using antigen pre-capture (round 1) involves the desired antigen bound to an antigen-specific IgG coated on a surface. Washing (wash1) removes any non-binding VHH. VHH binding the desired antigen and non-specific "background" binding VHH are retained. P-VHH selection using antigen panning (round 2) involves the antigen directly coated on a surface. Washing (wash2) now removes the "background" binding P-VHH from round 1, and retains P-VHH that bind the desired antigen that are subsequently eluted. Note: This illustration assumed a 2-round pre-capture/panning selection strategy.

1.4 Outline of this thesis

Although the causative mutation for HD has been known for over twenty years and a lot of subsequent research has been performed, not much is known about the huntingtin protein in human brain tissue. In **chapter 2** we have developed a screening-technique to pre-identify identical clone groups selected from Llama phage display libraries before sequencing. This technique was used in **chapter 3**, where we described VHH antibody fragments selected against N-terminal htt from a pre-immunized Llama phage display library. The selected VHH recognize htt at an N-terminal epitope, are capable binding full-length htt in human brain lysate, and might be used as a bio-imaging tool to track full-length htt or N-terminal htt protein fragments. In **chapter 4** we have looked at the effects of *post-mortem* delay, tissue preservation and subject variance on the profile of N-terminal htt protein fragments in human brain tissue. Our results show that *post-mortem* delay and tissue preservation affect signal strength, but the profile of N-terminal fragments is only minimally affected. Subject variance was shown to have a greater effect, underlining the importance of larger subject cohorts. In **chapter 5** we performed a pilot-study comparing htt aggregation in juvenile HD brain tissue versus adult brain tissue using a dot-blot assay. Our results suggest that the dot-blot assay is suitable for quantification of htt aggregates, and that htt aggregates in juvenile HD in cortical tissue is more abundant than in striatal tissue. In **chapter 6** we have assessed the levels of mutant versus wild-type HTT RNA and protein expression. We found that expression levels of both mutant htt RNA and protein were equal to or lower than wild-type. We also identified *HTTAS* in a fibroblast cell-line homozygous for HD, suggesting the HD antisense transcript levels are not changed when the repeat is expanded.

Reference list

1. T, S., *On St Vitus's dance. The works of Thomas Sydenham.* 1848.
2. Paracelsus, *Von den Krankheiten so die Vernunft berauben.* 1591.
3. Goetz CG, C.T., Lanska DJ., *History of chorea: Part 3 of the MDS-sponsored history of movement disorders exhibi.* 2000.
4. Wexler, A., *A brief prehistory of Huntington's disease.* J Huntingtons Dis, 2013. **2**(3): p. 231-7.
5. Huntington, G., *"On Chorea". Medical and Surgical Reporter of Philadelphia* Philadelphia 1872. **26**(15): p. 317–321.
6. Wexler, A., *Stigma, history, and Huntington's disease.* Lancet, 2010. **376**(9734): p. 18-9.
7. Barlow-Stewart, K., et al., *Verification of consumers' experiences and perceptions of genetic discrimination and its impact on utilization of genetic testing.* Genet Med, 2009. **11**(3): p. 193-201.
8. Bombard, Y., et al., *Perceptions of genetic discrimination among people at risk for Huntington's disease: a cross sectional survey.* BMJ, 2009. **338**: p. b2175.
9. Erwin, C., et al., *Perception, experience, and response to genetic discrimination in Huntington disease: the international RESPOND-HD study.* Am J Med Genet B Neuropsychiatr Genet, 2010. **153B**(5): p. 1081-93.
10. Penziner, E., et al., *Perceptions of discrimination among persons who have undergone predictive testing for Huntington's disease.* Am J Med Genet B Neuropsychiatr Genet, 2008. **147**(3): p. 320-5.
11. Mielcarek, M., *Huntington's disease is a multi-system disorder.* Rare Dis, 2015. **3**(1): p. e1058464.
12. Roos, R.A., *Huntington's disease: a clinical review.* Orphanet J Rare Dis, 2010. **5**: p. 40.
13. van Duijn, E., et al., *Neuropsychiatric symptoms in a European Huntington's disease cohort (REGISTRY).* J Neurol Neurosurg Psychiatry, 2014. **85**(12): p. 1411-8.
14. Hubers, A.A., et al., *Suicidal ideation in a European Huntington's disease population.* J Affect Disord, 2013. **151**(1): p. 248-58.
15. Hefter, H., et al., *Impairment of rapid movement in Huntington's disease.* Brain, 1987. **110 (Pt 3)**: p. 585-612.
16. David, A.S., et al., *Voluntary movement dysfunction in Huntington's disease and tardive dyskinesia.* Acta Neurol Scand, 1987. **75**(2): p. 130-9.
17. Aziz, N.A., et al., *Weight loss in Huntington disease increases with higher CAG repeat number.* Neurology, 2008. **71**(19): p. 1506-13.
18. Castilhos, R.M., et al., *Genetic aspects of Huntington's disease in Latin America. A systematic review.* Clin Genet, 2015.
19. Reyes, A., et al., *Pulmonary function in patients with Huntington's disease.* BMC Pulm Med, 2014. **14**: p. 89.
20. Heemskerk, A.W. and R.A. Roos, *Aspiration pneumonia and death in Huntington's disease.* PLoS Curr, 2012. **4**: p. RRN1293.
21. Heemskerk, A.W. and R.A. Roos, *Dysphagia in Huntington's disease: a review.* Dysphagia, 2011. **26**(1): p. 62-6.
22. Duff, K., et al., *Psychiatric symptoms in Huntington's disease before diagnosis: the predict-HD study.* Biol Psychiatry, 2007. **62**(12): p. 1341-6.
23. van den Bogaard, S., et al., *MRI biomarkers in Huntington's disease.* Front Biosci (Elite Ed), 2012. **4**: p. 1910-25.
24. van den Bogaard, S.J., E.M. Dumas, and R.A. Roos, *The role of iron imaging in Huntington's disease.* Int Rev Neurobiol, 2013. **110**: p. 241-50.
25. Sturrock, A., et al., *A longitudinal study of magnetic resonance spectroscopy Huntington's disease biomarkers.* Mov Disord, 2015. **30**(3): p. 393-401.
26. Sturrock, A., et al., *Magnetic resonance spectroscopy biomarkers in premanifest and early Huntington disease.* Neurology, 2010. **75**(19): p. 1702-10.
27. Huntington Study Group, P.I., et al., *Clinical-Genetic Associations in the Prospective Huntington at Risk Observational Study (PHAROS): Implications for Clinical Trials.* JAMA Neurol, 2015: p. 1-9.
28. Dumas, E.M., et al., *Reduced functional brain connectivity prior to and after disease onset in Huntington's disease.* Neuroimage Clin, 2013. **2**: p. 377-84.
29. Southwell, A.L., et al., *Ultrasensitive measurement of huntingtin protein in cerebrospinal fluid demonstrates increase with Huntington disease stage and decrease following brain huntingtin suppression.* Sci Rep, 2015. **5**: p. 12166.

30. Wild, E.J., et al., *Quantification of mutant huntingtin protein in cerebrospinal fluid from Huntington's disease patients.* J Clin Invest, 2015. **125**(5): p. 1979-86.
31. Mastrokolias, A., et al., *Huntington's disease biomarker progression profile identified by transcriptome sequencing in peripheral blood.* Eur J Hum Genet, 2015. **23**(10): p. 1349-56.
32. Mastrokolias, A., et al., *Increased sensitivity of next generation sequencing-based expression profiling after globin reduction in human blood RNA.* BMC Genomics, 2012. **13**: p. 28.
33. Gilliam, T.C., et al., *Localization of the Huntington's disease gene to a small segment of chromosome 4 flanked by D4S10 and the telomere.* Cell, 1987. **50**(4): p. 565-71.
34. Gusella, J.F., et al., *A polymorphic DNA marker genetically linked to Huntington's disease.* Nature, 1983. **306**(5940): p. 234-8.
35. *A novel gene containing a trinucleotide repeat that is expanded and unstable on Huntington's disease chromosomes. The Huntington's Disease Collaborative Research Group.* Cell, 1993. **72**(6): p. 971-83.
36. Aronin, N., et al., *CAG expansion affects the expression of mutant Huntingtin in the Huntington's disease brain.* Neuron, 1995. **15**(5): p. 1193-201.
37. Stine, O.C., et al., *Correlation between the onset age of Huntington's disease and length of the trinucleotide repeat in IT-15.* Hum Mol Genet, 1993. **2**(10): p. 1547-9.
38. Duyao, M., et al., *Trinucleotide repeat length instability and age of onset in Huntington's disease.* Nat Genet, 1993. **4**(4): p. 387-92.
39. Myers, R.H., *Huntington's disease genetics.* NeuroRx, 2004. **1**(2): p. 255-62.
40. Rosenblatt, A., et al., *Familial influence on age of onset among siblings with Huntington disease.* Am J Med Genet, 2001. **105**(5): p. 399-403.
41. Genetic Modifiers of Huntington's Disease, C., *Identification of Genetic Factors that Modify Clinical Onset of Huntington's Disease.* Cell, 2015. **162**(3): p. 516-26.
42. Roos, R.A., et al., *Duration of illness in Huntington's disease is not related to age at onset.* J Neurol Neurosurg Psychiatry, 1993. **56**(1): p. 98-100.
43. Kieburtz, K., et al., *Trinucleotide repeat length and progression of illness in Huntington's disease.* J Med Genet, 1994. **31**(11): p. 872-4.
44. Wexler, N.S., et al., *Homozygotes for Huntington's disease.* Nature, 1987. **326**(6109): p. 194-7.
45. Myers, R.H., et al., *Homozygote for Huntington disease.* Am J Hum Genet, 1989. **45**(4): p. 615-8.
46. Trottier, Y., V. Biancalana, and J.L. Mandel, *Instability of CAG repeats in Huntington's disease: relation to parental transmission and age of onset.* J Med Genet, 1994. **31**(5): p. 377-82.
47. Zuhlke, C., et al., *Mitotic stability and meiotic variability of the (CAG)n repeat in the Huntington disease gene.* Hum Mol Genet, 1993. **2**(12): p. 2063-7.
48. Aziz, N.A., et al., *Parent-of-origin differences of mutant HTT CAG repeat instability in Huntington's disease.* Eur J Med Genet, 2011. **54**(4): p. e413-8.
49. Kremer, B., et al., *Sex-dependent mechanisms for expansions and contractions of the CAG repeat on affected Huntington disease chromosomes.* Am J Hum Genet, 1995. **57**(2): p. 343-50.
50. Semaka, A., et al., *A new mutation for Huntington disease following maternal transmission of an intermediate allele.* Eur J Med Genet, 2015. **58**(1): p. 28-30.
51. Gonitel, R., et al., *DNA instability in postmitotic neurons.* Proc Natl Acad Sci U S A, 2008. **105**(9): p. 3467-72.
52. Koefoed, P., et al., *Mitotic and meiotic instability of the CAG trinucleotide repeat in spinocerebellar ataxia type 1.* Hum Genet, 1998. **103**(5): p. 564-9.
53. Stevanin, G., et al., *De novo expansion of intermediate alleles in spinocerebellar ataxia 7.* Hum Mol Genet, 1998. **7**(11): p. 1809-13.
54. Watanabe, M., et al., *Mitotic and meiotic stability of the CAG repeat in the X-linked spinal and bulbar muscular atrophy gene.* Clin Genet, 1996. **50**(3): p. 133-7.
55. Concannon, C. and R.S. Lahue, *Nucleotide excision repair and the 26S proteasome function together to promote trinucleotide repeat expansions.* DNA Repair (Amst), 2014. **13**: p. 42-9.
56. Jankowski, C., F. Nasar, and D.K. Nag, *Meiotic instability of CAG repeat tracts occurs by double-strand break repair in yeast.* Proc Natl Acad Sci U S A, 2000. **97**(5): p. 2134-9.
57. Simard, O., et al., *Instability of trinucleotidic repeats during chromatin remodeling in spermatids.* Hum Mutat, 2014. **35**(11): p. 1280-4.

58. Semaka, A., et al., *High frequency of intermediate alleles on Huntington disease-associated haplotypes in British Columbia's general population.* Am J Med Genet B Neuropsychiatr Genet, 2013. **162B**(8): p. 864-71.
59. Semaka, A., et al., *CAG size-specific risk estimates for intermediate allele repeat instability in Huntington disease.* J Med Genet, 2013. **50**(10): p. 696-703.
60. Groen, J.L., et al., *Late-onset Huntington disease with intermediate CAG repeats: true or false?* J Neurol Neurosurg Psychiatry, 2010. **81**(2): p. 228-30.
61. Kenney, C., S. Powell, and J. Jankovic, *Autopsy-proven Huntington's disease with 29 trinucleotide repeats.* Mov Disord, 2007. **22**(1): p. 127-30.
62. Herishanu, Y.O., et al., *Huntington disease in subjects from an Israeli Karaite community carrying alleles of intermediate and expanded CAG repeats in the HTT gene: Huntington disease or phenocopy?* J Neurol Sci, 2009. **277**(1-2): p. 143-6.
63. Killoran, A., et al., *Characterization of the Huntington intermediate CAG repeat expansion phenotype in PHAROS.* Neurology, 2013. **80**(22): p. 2022-7.
64. Vonsattel, J.P., et al., *Neuropathological classification of Huntington's disease.* J Neuropathol Exp Neurol, 1985. **44**(6): p. 559-77.
65. Tabrizi, S.J., et al., *Predictors of phenotypic progression and disease onset in premanifest and early-stage Huntington's disease in the TRACK-HD study: analysis of 36-month observational data.* Lancet Neurol, 2013. **12**(7): p. 637-49.
66. Hadzi, T.C., et al., *Assessment of cortical and striatal involvement in 523 Huntington disease brains.* Neurology, 2012. **79**(16): p. 1708-15.
67. Richfield, E.K., et al., *Preferential loss of preproenkephalin versus preprotachykinin neurons from the striatum of Huntington's disease patients.* Ann Neurol, 1995. **38**(6): p. 852-61.
68. Ferrante, R.J., et al., *Selective sparing of a class of striatal neurons in Huntington's disease.* Science, 1985. **230**(4725): p. 561-3.
69. Kim, E.H., et al., *Cortical interneuron loss and symptom heterogeneity in Huntington disease.* Ann Neurol, 2014. **75**(5): p. 717-27.
70. Nana, A.L., et al., *Widespread heterogeneous neuronal loss across the cerebral cortex in Huntington's disease.* J Huntingtons Dis, 2014. **3**(1): p. 45-64.
71. Thu, D.C., et al., *Cell loss in the motor and cingulate cortex correlates with symptomatology in Huntington's disease.* Brain, 2010. **133**(Pt 4): p. 1094-110.
72. Scherzinger, E., et al., *Huntingtin-encoded polyglutamine expansions form amyloid-like protein aggregates in vitro and in vivo.* Cell, 1997. **90**(3): p. 549-58.
73. DiFiglia, M., et al., *Aggregation of huntingtin in neuronal intranuclear inclusions and dystrophic neurites in brain.* Science, 1997. **277**(5334): p. 1990-3.
74. Becher, M.W., et al., *Intranuclear neuronal inclusions in Huntington's disease and dentatorubral and pallidoluysian atrophy: correlation between the density of inclusions and IT15 CAG triplet repeat length.* Neurobiol Dis, 1998. **4**(6): p. 387-97.
75. Legleiter, J., et al., *Mutant huntingtin fragments form oligomers in a polyglutamine length-dependent manner in vitro and in vivo.* J Biol Chem, 2010. **285**(19): p. 14777-90.
76. Li, S.H. and X.J. Li, *Aggregation of N-terminal huntingtin is dependent on the length of its glutamine repeats.* Hum Mol Genet, 1998. **7**(5): p. 777-82.
77. Yang, W., et al., *Aggregated polyglutamine peptides delivered to nuclei are toxic to mammalian cells.* Hum Mol Genet, 2002. **11**(23): p. 2905-17.
78. Costanzo, M., et al., *Transfer of polyglutamine aggregates in neuronal cells occurs in tunneling nanotubes.* J Cell Sci, 2013. **126**(Pt 16): p. 3678-85.
79. Kazantsev, A., et al., *Insoluble detergent-resistant aggregates form between pathological and nonpathological lengths of polyglutamine in mammalian cells.* Proc Natl Acad Sci U S A, 1999. **96**(20): p. 11404-9.
80. van Roon-Mom, W.M., et al., *Insoluble TATA-binding protein accumulation in Huntington's disease cortex.* Brain Res Mol Brain Res, 2002. **109**(1-2): p. 1-10.
81. Doi, H., et al., *RNA-binding protein TLS is a major nuclear aggregate-interacting protein in huntingtin exon 1 with expanded polyglutamine-expressing cells.* J Biol Chem, 2008. **283**(10): p. 6489-500.

82. Qin, Z.H., et al., *Huntingtin bodies sequester vesicle-associated proteins by a polyproline-dependent interaction.* J Neurosci, 2004. **24**(1): p. 269-81.
83. Kuemmerle, S., et al., *Huntington aggregates may not predict neuronal death in Huntington's disease.* Ann Neurol, 1999. **46**(6): p. 842-9.
84. Gutekunst, C.A., et al., *Nuclear and neuropil aggregates in Huntington's disease: relationship to neuropathology.* J Neurosci, 1999. **19**(7): p. 2522-34.
85. Arrasate, M., et al., *Inclusion body formation reduces levels of mutant huntingtin and the risk of neuronal death.* Nature, 2004. **431**(7010): p. 805-10.
86. Ravikumar, B., et al., *Inhibition of mTOR induces autophagy and reduces toxicity of polyglutamine expansions in fly and mouse models of Huntington disease.* Nat Genet, 2004. **36**(6): p. 585-95.
87. Gatto, E.M., et al., *Juvenile Huntington disease in Argentina.* Arq Neuropsiquiatr, 2015.
88. Quarrell, O., et al., *The Prevalence of Juvenile Huntington's Disease: A Review of the Literature and Meta-Analysis.* PLoS Curr, 2012. **4**: p. e4f8606b742ef3.
89. Westphal, *Ueber eine dem Bilde der cerebrospinalen grauen Degeneration ¨ahnliche Erkrankung des centralen Nervensystems ohne anatomischen Befund, nebst einigen Bemerkungen ¨uber paradoxe Contraction.* Archiv fur Psychiatrie und Nervenkrankheiten, 1883. **14**(1): p. 87–134.
90. Siesling, S., M. Vegter-van der Vlis, and R.A. Roos, *Juvenile Huntington disease in the Netherlands.* Pediatr Neurol, 1997. **17**(1): p. 37-43.
91. Ruocco, H.H., et al., *Clinical presentation of juvenile Huntington disease.* Arq Neuropsiquiatr, 2006. **64**(1): p. 5-9.
92. van Dijk, J.G., et al., *Juvenile Huntington disease.* Hum Genet, 1986. **73**(3): p. 235-9.
93. Li, W., et al., *Expression and characterization of full-length human huntingtin, an elongated HEAT repeat protein.* J Biol Chem, 2006. **281**(23): p. 15916-22.
94. Sharp, A.H., et al., *Widespread expression of Huntington's disease gene (IT15) protein product.* Neuron, 1995. **14**(5): p. 1065-74.
95. Sapp, E., et al., *Huntingtin localization in brains of normal and Huntington's disease patients.* Ann Neurol, 1997. **42**(4): p. 604-12.
96. Hoogeveen, A.T., et al., *Characterization and localization of the Huntington disease gene product.* Hum Mol Genet, 1993. **2**(12): p. 2069-73.
97. Gutekunst, C.A., et al., *Identification and localization of huntingtin in brain and human lymphoblastoid cell lines with anti-fusion protein antibodies.* Proc Natl Acad Sci U S A, 1995. **92**(19): p. 8710-4.
98. Cattaneo, E., C. Zuccato, and M. Tartari, *Normal huntingtin function: an alternative approach to Huntington's disease.* Nat Rev Neurosci, 2005. **6**(12): p. 919-30.
99. Godin, J.D., et al., *Huntingtin is required for mitotic spindle orientation and mammalian neurogenesis.* Neuron, 2010. **67**(3): p. 392-406.
100. Rui, Y.N., et al., *Huntingtin functions as a scaffold for selective macroautophagy.* Nat Cell Biol, 2015. **17**(3): p. 262-75.
101. Kegel, K.B., et al., *Huntingtin expression stimulates endosomal-lysosomal activity, endosome tubulation, and autophagy.* J Neurosci, 2000. **20**(19): p. 7268-78.
102. Ochaba, J., et al., *Potential function for the Huntingtin protein as a scaffold for selective autophagy.* Proc Natl Acad Sci U S A, 2014. **111**(47): p. 16889-94.
103. Caviston, J.P. and E.L. Holzbaur, *Huntingtin as an essential integrator of intracellular vesicular trafficking.* Trends Cell Biol, 2009. **19**(4): p. 147-55.
104. Caviston, J.P., et al., *Huntingtin facilitates dynein/dynactin-mediated vesicle transport.* Proc Natl Acad Sci U S A, 2007. **104**(24): p. 10045-50.
105. Caviston, J.P., et al., *Huntingtin coordinates the dynein-mediated dynamic positioning of endosomes and lysosomes.* Mol Biol Cell, 2011. **22**(4): p. 478-92.
106. Brandstaetter, H., A.J. Kruppa, and F. Buss, *Huntingtin is required for ER-to-Golgi transport and for secretory vesicle fusion at the plasma membrane.* Dis Model Mech, 2014. **7**(12): p. 1335-40.
107. White, J.A., 2nd, et al., *Huntingtin differentially regulates the axonal transport of a sub-set of Rab-containing vesicles in vivo.* Hum Mol Genet, 2015. **24**(25): p. 7182-95.

108. Zuccato, C., et al., *Huntingtin interacts with REST/NRSF to modulate the transcription of NRSE-controlled neuronal genes.* Nat Genet, 2003. **35**(1): p. 76-83.
109. Zuccato, C., et al., *Loss of huntingtin-mediated BDNF gene transcription in Huntington's disease.* Science, 2001. **293**(5529): p. 493-8.
110. Liot, G., et al., *Mutant Huntingtin alters retrograde transport of TrkB receptors in striatal dendrites.* J Neurosci, 2013. **33**(15): p. 6298-309.
111. Gauthier, L.R., et al., *Huntingtin controls neurotrophic support and survival of neurons by enhancing BDNF vesicular transport along microtubules.* Cell, 2004. **118**(1): p. 127-38.
112. Leavitt, B.R., et al., *Wild-type huntingtin protects neurons from excitotoxicity.* J Neurochem, 2006. **96**(4): p. 1121-9.
113. Luo, S. and D.C. Rubinsztein, *Huntingtin promotes cell survival by preventing Pak2 cleavage.* J Cell Sci, 2009. **122**(Pt 6): p. 875-85.
114. Haremaki, T., A. Deglincerti, and A.H. Brivanlou, *Huntingtin is required for ciliogenesis and neurogenesis during early Xenopus development.* Dev Biol, 2015. **408**(2): p. 305-15.
115. Duyao, M.P., et al., *Inactivation of the mouse Huntington's disease gene homolog Hdh.* Science, 1995. **269**(5222): p. 407-10.
116. White, J.K., et al., *Huntingtin is required for neurogenesis and is not impaired by the Huntington's disease CAG expansion.* Nat Genet, 1997. **17**(4): p. 404-10.
117. Li, S.H., et al., *Interaction of Huntington disease protein with transcriptional activator Sp1.* Mol Cell Biol, 2002. **22**(5): p. 1277-87.
118. Munsie, L., et al., *Mutant huntingtin causes defective actin remodeling during stress: defining a new role for transglutaminase 2 in neurodegenerative disease.* Hum Mol Genet, 2011. **20**(10): p. 1937-51.
119. Orr, A.L., et al., *N-terminal mutant huntingtin associates with mitochondria and impairs mitochondrial trafficking.* J Neurosci, 2008. **28**(11): p. 2783-92.
120. Shirendeb, U.P., et al., *Mutant huntingtin's interaction with mitochondrial protein Drp1 impairs mitochondrial biogenesis and causes defective axonal transport and synaptic degeneration in Huntington's disease.* Hum Mol Genet, 2012. **21**(2): p. 406-20.
121. Shirendeb, U., et al., *Abnormal mitochondrial dynamics, mitochondrial loss and mutant huntingtin oligomers in Huntington's disease: implications for selective neuronal damage.* Hum Mol Genet, 2011. **20**(7): p. 1438-55.
122. Li, X., et al., *Mutant huntingtin impairs vesicle formation from recycling endosomes by interfering with Rab11 activity.* Mol Cell Biol, 2009. **29**(22): p. 6106-16.
123. Dragatsis, I., M.S. Levine, and S. Zeitlin, *Inactivation of Hdh in the brain and testis results in progressive neurodegeneration and sterility in mice.* Nat Genet, 2000. **26**(3): p. 300-6.
124. Trushina, E., et al., *Mutant huntingtin impairs axonal trafficking in mammalian neurons in vivo and in vitro.* Mol Cell Biol, 2004. **24**(18): p. 8195-209.
125. Li, S.H., et al., *Huntington's disease gene (IT15) is widely expressed in human and rat tissues.* Neuron, 1993. **11**(5): p. 985-93.
126. Landwehrmeyer, G.B., et al., *Huntington's disease gene: regional and cellular expression in brain of normal and affected individuals.* Ann Neurol, 1995. **37**(2): p. 218-30.
127. Ciammola, A., et al., *Increased apoptosis, Huntingtin inclusions and altered differentiation in muscle cell cultures from Huntington's disease subjects.* Cell Death Differ, 2006. **13**(12): p. 2068-78.
128. De Rooij, K.E., et al., *Subcellular localization of the Huntington's disease gene product in cell lines by immunofluorescence and biochemical subcellular fractionation.* Hum Mol Genet, 1996. **5**(8): p. 1093-9.
129. Toneff, T., et al., *Comparison of huntingtin proteolytic fragments in human lymphoblast cell lines and human brain.* J Neurochem, 2002. **82**(1): p. 84-92.
130. Chung, D.W., et al., *A natural antisense transcript at the Huntington's disease repeat locus regulates HTT expression.* Hum Mol Genet, 2011. **20**(17): p. 3467-77.
131. Lee, J.M., et al., *Dominant effects of the Huntington's disease HTT CAG repeat length are captured in gene-expression data sets by a continuous analysis mathematical modeling strategy.* Hum Mol Genet, 2013. **22**(16): p. 3227-38.
132. Liu, W., et al., *Increased Steady-State Mutant Huntingtin mRNA in Huntington's Disease Brain.* J Huntingtons Dis, 2013. **2**(4): p. 491-500.

133. Krauss, S., et al., *Translation of HTT mRNA with expanded CAG repeats is regulated by the MID1-PP2A protein complex.* Nat Commun, 2013. **4**: p. 1511.
134. Preisinger, E., et al., *Evidence for a recruitment and sequestration mechanism in Huntington's disease.* Philos Trans R Soc Lond B Biol Sci, 1999. **354**(1386): p. 1029-34.
135. Hu, J., et al., *Allele-specific silencing of mutant huntingtin and ataxin-3 genes by targeting expanded CAG repeats in mRNAs.* Nat Biotechnol, 2009. **27**(5): p. 478-84.
136. Freed, D., E.L. Stevens, and J. Pevsner, *Somatic mosaicism in the human genome.* Genes (Basel), 2014. **5**(4): p. 1064-94.
137. Zheng, Z., et al., *An N-terminal nuclear export signal regulates trafficking and aggregation of Huntingtin (Htt) protein exon 1.* J Biol Chem, 2013. **288**(9): p. 6063-71.
138. Maiuri, T., et al., *The huntingtin N17 domain is a multifunctional CRM1 and Ran-dependent nuclear and cilial export signal.* Hum Mol Genet, 2013. **22**(7): p. 1383-94.
139. Rockabrand, E., et al., *The first 17 amino acids of Huntingtin modulate its sub-cellular localization, aggregation and effects on calcium homeostasis.* Hum Mol Genet, 2007. **16**(1): p. 61-77.
140. Kim, M.W., et al., *Secondary structure of Huntingtin amino-terminal region.* Structure, 2009. **17**(9): p. 1205-12.
141. Arndt, J.R., et al., *Lysine residues in the N-terminal huntingtin amphipathic alpha-helix play a key role in peptide aggregation.* J Mass Spectrom, 2015. **50**(1): p. 117-26.
142. Thakur, A.K., et al., *Polyglutamine disruption of the huntingtin exon 1 N terminus triggers a complex aggregation mechanism.* Nat Struct Mol Biol, 2009. **16**(4): p. 380-9.
143. Tam, S., et al., *The chaperonin TRiC blocks a huntingtin sequence element that promotes the conformational switch to aggregation.* Nat Struct Mol Biol, 2009. **16**(12): p. 1279-85.
144. Steffan, J.S., et al., *SUMO modification of Huntingtin and Huntington's disease pathology.* Science, 2004. **304**(5667): p. 100-4.
145. Kalchman, M.A., et al., *Huntingtin is ubiquitinated and interacts with a specific ubiquitin-conjugating enzyme.* J Biol Chem, 1996. **271**(32): p. 19385-94.
146. Gu, X., et al., *Serines 13 and 16 are critical determinants of full-length human mutant huntingtin induced disease pathogenesis in HD mice.* Neuron, 2009. **64**(6): p. 828-40.
147. Graham, R.K., et al., *Cleavage at the 586 amino acid caspase-6 site in mutant huntingtin influences caspase-6 activation in vivo.* J Neurosci, 2010. **30**(45): p. 15019-29.
148. Ehrnhoefer, D.E., et al., *p53 increases caspase-6 expression and activation in muscle tissue expressing mutant huntingtin.* Hum Mol Genet, 2014. **23**(3): p. 717-29.
149. Tsvetkov, A.S., et al., *Proteostasis of polyglutamine varies among neurons and predicts neurodegeneration.* Nat Chem Biol, 2013. **9**(9): p. 586-92.
150. Mende-Mueller, L.M., et al., *Tissue-specific proteolysis of Huntingtin (htt) in human brain: evidence of enhanced levels of N- and C-terminal htt fragments in Huntington's disease striatum.* J Neurosci, 2001. **21**(6): p. 1830-7.
151. Mangiarini, L., et al., *Exon 1 of the HD gene with an expanded CAG repeat is sufficient to cause a progressive neurological phenotype in transgenic mice.* Cell, 1996. **87**(3): p. 493-506.
152. Davies, S.W., et al., *Formation of neuronal intranuclear inclusions underlies the neurological dysfunction in mice transgenic for the HD mutation.* Cell, 1997. **90**(3): p. 537-48.
153. Slow, E.J., et al., *Selective striatal neuronal loss in a YAC128 mouse model of Huntington disease.* Hum Mol Genet, 2003. **12**(13): p. 1555-67.
154. Woodman, B., et al., *The Hdh(Q150/Q150) knock-in mouse model of HD and the R6/2 exon 1 model develop comparable and widespread molecular phenotypes.* Brain Res Bull, 2007. **72**(2-3): p. 83-97.
155. Cong, S.Y., et al., *Small N-terminal mutant huntingtin fragments, but not wild type, are mainly present in monomeric form: Implications for pathogenesis.* Exp Neurol, 2006. **199**(2): p. 257-64.
156. Lunkes, A., et al., *Proteases acting on mutant huntingtin generate cleaved products that differentially build up cytoplasmic and nuclear inclusions.* Mol Cell, 2002. **10**(2): p. 259-69.
157. Lunkes, A. and J.L. Mandel, *A cellular model that recapitulates major pathogenic steps of Huntington's disease.* Hum Mol Genet, 1998. **7**(9): p. 1355-61.
158. Miller, J.P., et al., *Matrix metalloproteinases are modifiers of huntingtin proteolysis and toxicity in Huntington's disease.* Neuron, 2010. **67**(2): p. 199-212.

159. Gafni, J., et al., *Inhibition of calpain cleavage of huntingtin reduces toxicity: accumulation of calpain/caspase fragments in the nucleus.* J Biol Chem, 2004. **279**(19): p. 20211-20.
160. Wellington, C.L., et al., *Inhibiting caspase cleavage of huntingtin reduces toxicity and aggregate formation in neuronal and nonneuronal cells.* J Biol Chem, 2000. **275**(26): p. 19831-8.
161. Wellington, C.L., et al., *Caspase cleavage of mutant huntingtin precedes neurodegeneration in Huntington's disease.* J Neurosci, 2002. **22**(18): p. 7862-72.
162. Graham, R.K., et al., *Cleavage at the caspase-6 site is required for neuronal dysfunction and degeneration due to mutant huntingtin.* Cell, 2006. **125**(6): p. 1179-91.
163. Warby, S.C., et al., *Activated caspase-6 and caspase-6-cleaved fragments of huntingtin specifically colocalize in the nucleus.* Hum Mol Genet, 2008. **17**(15): p. 2390-404.
164. O'Brien, R., et al., *Integration-independent Transgenic Huntington Disease Fragment Mouse Models Reveal Distinct Phenotypes and Life Span in Vivo.* J Biol Chem, 2015. **290**(31): p. 19287-306.
165. Landles, C., et al., *Proteolysis of mutant huntingtin produces an exon 1 fragment that accumulates as an aggregated protein in neuronal nuclei in Huntington disease.* J Biol Chem, 2010. **285**(12): p. 8808-23.
166. Sathasivam, K., et al., *Aberrant splicing of HTT generates the pathogenic exon 1 protein in Huntington disease.* Proc Natl Acad Sci U S A, 2013. **110**(6): p. 2366-70.
167. El-Daher, M.T., et al., *Huntingtin proteolysis releases non-polyQ fragments that cause toxicity through dynamin 1 dysregulation.* EMBO J, 2015. **34**(17): p. 2255-71.
168. Shannon, K.M. and A. Fraint, *Therapeutic advances in Huntington's Disease.* Mov Disord, 2015. **30**(11): p. 1539-46.
169. Carroll, J.B., et al., *Treating the whole body in Huntington's disease.* Lancet Neurol, 2015. **14**(11): p. 1135-42.
170. Palmer, A.M., *The role of the blood brain barrier in neurodegenerative disorders and their treatment.* J Alzheimers Dis, 2011. **24**(4): p. 643-56.
171. Palmer, A.M., *The blood-brain barrier.* Neurobiol Dis, 2010. **37**(1): p. 1-2.
172. Fiszer, A., et al., *Self-duplexing CUG repeats selectively inhibit mutant huntingtin expression.* Nucleic Acids Res, 2013. **41**(22): p. 10426-37.
173. van Bilsen, P.H., et al., *Identification and allele-specific silencing of the mutant huntingtin allele in Huntington's disease patient-derived fibroblasts.* Hum Gene Ther, 2008. **19**(7): p. 710-9.
174. Evers, M.M., et al., *Targeting several CAG expansion diseases by a single antisense oligonucleotide.* PLoS One, 2011. **6**(9): p. e24308.
175. Evers, M.M., et al., *Preventing formation of toxic N-terminal huntingtin fragments through antisense oligonucleotide-mediated protein modification.* Nucleic Acid Ther, 2014. **24**(1): p. 4-12.
176. Ruzo, A., et al., *Discovery of novel isoforms of huntingtin reveals a new hominid-specific exon.* PLoS One, 2015. **10**(5): p. e0127687.
177. Redman, J.M., G.T. Gibney, and M.B. Atkins, *Advances in immunotherapy for melanoma.* BMC Med, 2016. **14**(1): p. 20.
178. Scott, A.M., J.D. Wolchok, and L.J. Old, *Antibody therapy of cancer.* Nat Rev Cancer, 2012. **12**(4): p. 278-87.
179. Kawalec, P., et al., *Tumor necrosis factor-alpha antibodies (infliximab, adalimumab and certolizumab) in Crohn's disease: systematic review and meta-analysis.* Arch Med Sci, 2013. **9**(5): p. 765-79.
180. Theakston, R.D., *New techniques in antivenom production and active immunization against snake venoms.* Trans R Soc Trop Med Hyg, 1989. **83**(4): p. 433-5.
181. Misasi, J., et al., *Structural and molecular basis for Ebola virus neutralization by protective human antibodies.* Science, 2016.
182. Yu, Y.J. and R.J. Watts, *Developing therapeutic antibodies for neurodegenerative disease.* Neurotherapeutics, 2013. **10**(3): p. 459-72.
183. Robert, R., et al., *Engineered antibody intervention strategies for Alzheimer's disease and related dementias by targeting amyloid and toxic oligomers.* Protein Eng Des Sel, 2009. **22**(3): p. 199-208.
184. Lecerf, J.M., et al., *Human single-chain Fv intrabodies counteract in situ huntingtin aggregation in cellular models of Huntington's disease.* Proc Natl Acad Sci U S A, 2001. **98**(8): p. 4764-9.
185. Wolfgang, W.J., et al., *Suppression of Huntington's disease pathology in Drosophila by human single-chain Fv antibodies.* Proc Natl Acad Sci U S A, 2005. **102**(32): p. 11563-8.

186. Snyder-Keller, A., et al., *Early or late-stage anti-N-terminal Huntingtin intrabody gene therapy reduces pathological features in B6.HDR6/1 mice.* J Neuropathol Exp Neurol, 2010. **69**(10): p. 1078-85.
187. Hamers-Casterman, C., et al., *Naturally occurring antibodies devoid of light chains.* Nature, 1993. **363**(6428): p. 446-8.
188. Greenberg, A.S., et al., *A new antigen receptor gene family that undergoes rearrangement and extensive somatic diversification in sharks.* Nature, 1995. **374**(6518): p. 168-73.
189. Muyldermans, S., et al., *Sequence and structure of VH domain from naturally occurring camel heavy chain immunoglobulins lacking light chains.* Protein Eng, 1994. **7**(9): p. 1129-35.
190. Desmyter, A., et al., *Crystal structure of a camel single-domain VH antibody fragment in complex with lysozyme.* Nat Struct Biol, 1996. **3**(9): p. 803-11.
191. De Genst, E., et al., *Molecular basis for the preferential cleft recognition by dromedary heavy-chain antibodies.* Proc Natl Acad Sci U S A, 2006. **103**(12): p. 4586-91.
192. Desmyter, A., et al., *Antigen specificity and high affinity binding provided by one single loop of a camel single-domain antibody.* J Biol Chem, 2001. **276**(28): p. 26285-90.
193. van der Linden, R.H., et al., *Comparison of physical chemical properties of llama VHH antibody fragments and mouse monoclonal antibodies.* Biochim Biophys Acta, 1999. **1431**(1): p. 37-46.
194. Arbabi Ghahroudi, M., et al., *Selection and identification of single domain antibody fragments from camel heavy-chain antibodies.* FEBS Lett, 1997. **414**(3): p. 521-6.
195. Verheesen, P., et al., *Reliable and controllable antibody fragment selections from Camelid non-immune libraries for target validation.* Biochim Biophys Acta, 2006. **1764**(8): p. 1307-19.
196. Verheesen, P., et al., *Prevention of oculopharyngeal muscular dystrophy-associated aggregation of nuclear polyA-binding protein with a single-domain intracellular antibody.* Hum Mol Genet, 2006. **15**(1): p. 105-11.
197. Tanha, J., et al., *Selection by phage display of llama conventional V(H) fragments with heavy chain antibody V(H)H properties.* J Immunol Methods, 2002. **263**(1-2): p. 97-109.
198. Hmila, I., et al., *A bispecific nanobody to provide full protection against lethal scorpion envenoming.* FASEB J, 2010. **24**(9): p. 3479-89.
199. Hmila, I., et al., *VHH, bivalent domains and chimeric Heavy chain-only antibodies with high neutralizing efficacy for scorpion toxin AahI'.* Mol Immunol, 2008. **45**(14): p. 3847-56.
200. El Khattabi, M., et al., *Llama single-chain antibody that blocks lipopolysaccharide binding and signaling: prospects for therapeutic applications.* Clin Vaccine Immunol, 2006. **13**(10): p. 1079-86.
201. Gorlani, A., et al., *Llama antibody fragments have good potential for application as HIV type 1 topical microbicides.* AIDS Res Hum Retroviruses, 2012. **28**(2): p. 198-205.
202. Forsman, A., et al., *Llama antibody fragments with cross-subtype human immunodeficiency virus type 1 (HIV-1)-neutralizing properties and high affinity for HIV-1 gp120.* J Virol, 2008. **82**(24): p. 12069-81.
203. Chartier, A., et al., *Prevention of oculopharyngeal muscular dystrophy by muscular expression of Llama single-chain intrabodies in vivo.* Hum Mol Genet, 2009. **18**(10): p. 1849-59.
204. Muruganandam, A., et al., *Selection of phage-displayed llama single-domain antibodies that transmigrate across human blood-brain barrier endothelium.* FASEB J, 2002. **16**(2): p. 240-2.
205. Rutgers, K.S., et al., *Transmigration of beta amyloid specific heavy chain antibody fragments across the in vitro blood-brain barrier.* Neuroscience, 2011. **190**: p. 37-42.
206. Nabuurs, R.J., et al., *In vivo detection of amyloid-beta deposits using heavy chain antibody fragments in a transgenic mouse model for Alzheimer's disease.* PLoS One, 2012. **7**(6): p. e38284.
207. Rutgers, K.S., et al., *Differential recognition of vascular and parenchymal beta amyloid deposition.* Neurobiol Aging, 2011. **32**(10): p. 1774-83.
208. Sidhu, S.S., *Engineering M13 for phage display.* Biomol Eng, 2001. **18**(2): p. 57-63.
209. Marks, J.D., et al., *By-passing immunization. Human antibodies from V-gene libraries displayed on phage.* J Mol Biol, 1991. **222**(3): p. 581-97.
210. Goldman, E.R., et al., *Ricin detection using phage displayed single domain antibodies.* Sensors (Basel), 2009. **9**(1): p. 542-55.
211. Lafaye, P., et al., *Single-domain antibodies recognize selectively small oligomeric forms of amyloid beta, prevent Abeta-induced neurotoxicity and inhibit fibril formation.* Mol Immunol, 2009. **46**(4): p. 695-704.

212. Yau, K.Y., et al., *Affinity maturation of a V(H)H by mutational hotspot randomization.* J Immunol Methods, 2005. **297**(1-2): p. 213-24.

Chapter 2

Cost-effective HRMA pre-sequence typing of clone libraries; application to phage display selection

Barry A Pepers[1,2],Menno H Schut[1], Rolf HAM Vossen[1,3], Gert-Jan B van Ommen[1], Johan T den Dunnen[1,3] and Willeke MC van Roon-Mom[1*]

1 Center for Human and Clinical Genetics, Leiden University Medical Center, Albinusdreef 2, 2333ZA Leiden, The Netherlands

2 Department of Neurology, Leiden University Medical Center, Albinusdreef 2, 2333ZA Leiden, The Netherlands

3 Leiden Genome Technology Center, Leiden University Medical Center, Albinusdreef 2, 2333ZA Leiden, The Netherlands

* Corresponding author: Willeke M.C. van Roon-Mom, Department of Human Genetics, Leiden University Medical Center, Albinusdreef 2, 2333ZA Leiden, The Netherlands. Tel: +31 71 5269435; Fax: +31 71 5268285; Email: w.vanroon@lumc.nl

BMC Biotechnology (2009)

BMC Biotechnology

Methodology article

Cost-effective HRMA pre-sequence typing of clone libraries; application to phage display selection

Barry A Pepers[1,2], Menno H Schut[1], Rolf HAM Vossen[1,3], Gert-Jan B van Ommen[1], Johan T den Dunnen[1,3] and Willeke MC van Roon-Mom*[1]

Address: [1]Center for Human and Clinical Genetics, Leiden University Medical Center, Albinusdreef 2, 2333ZA Leiden, The Netherlands, [2]Department of Neurology, Leiden University Medical Center, Albinusdreef 2, 2333ZA Leiden, The Netherlands and [3]Leiden Genome Technology Center, Leiden University Medical Center, Albinusdreef 2, 2333ZA Leiden, The Netherlands

Email: Barry A Pepers - b.a.pepers@lumc.nl; Menno H Schut - m.h.schut@lumc.nl; Rolf HAM Vossen - r.h.a.m.vossen@lumc.nl; Gert-Jan B van Ommen - gjvo@lumc.nl; Johan T den Dunnen - ddunnen@lumc.nl; Willeke MC van Roon-Mom* - w.vanroon@lumc.nl

* Corresponding author

Published: 22 May 2009

BMC Biotechnology 2009, **9**:50 doi:10.1186/1472-6750-9-50

Received: 11 February 2009
Accepted: 22 May 2009

This article is available from: http://www.biomedcentral.com/1472-6750/9/50

Abstract

Background: Methodologies like phage display selection, *in vitro* mutagenesis and the determination of allelic expression differences include steps where large numbers of clones need to be compared and characterised. In the current study we show that high-resolution melt curve analysis (HRMA) is a simple, cost-saving tool to quickly study clonal variation without prior nucleotide sequence knowledge.

Results: HRMA results nicely matched those obtained with ELISA and compared favourably to DNA fingerprinting of restriction digested clone insert-PCR. DNA sequence analysis confirmed that HRMA-clustered clones contained identical inserts.

Conclusion: Using HRMA, analysis of up to 384 samples can be done simultaneously and will take approximately 30 minutes. Clustering of clones can be largely automated using the system's software within 2 hours. Applied to the analysis of clones obtained after phage display antibody selection, HRMA facilitated a quick overview of the overall success as well as the identification of identical clones. Our approach can be used to characterize any clone set prior to sequencing, thereby reducing sequencing costs significantly.

Background

Phage display libraries consist of small antibody fragments cloned into a display phage vector, allowing efficient antibody screening and production in a bacterial system [1,2]. Traditional antibodies are composed of a heavy- and a light-chain that need to recombine in a tetramer for the formation of a functional antibody. Because most of these random recombinations will yield non-functional antibodies, when produced as recombinant fragments in *E. coli*, isolation of effective antibodies demands extremely large phage libraries. *Camelidae* have, next to conventional antibodies, dimeric heavy chain antibodies (HCAb) that lack light chains [3]. The variable domain of the HCAb (VHH) has a single binding domain with a specificity and affinity similar to conventional antibodies [4,5]. In a phage display library, each phage displays a different antigen-binding domain on its surface. To isolate specific antibodies, phage particles from a library are bound to an antigen, recovered and used to infect fresh bacteria. Subsequently, phages go

through several rounds of epitope binding and re-infection resulting in an enrichment of binding phages. A perfect experiment will ultimately yield groups of phages, each encoding a different antibody directed against the starting antigen. The set of phages can be used together as 'polyclonal phages', individual phages as 'monoclonal phages'. After selection, individual VHH clones are characterized to determine their specificity by ELISA and their diversity by fingerprinting/sequencing. Although ultimate identification is done using clone-insert nucleotide sequencing, pre-sequence fingerprinting is performed to reduce cost. Phage display clones are usually analysed using restriction digestion of PCR amplified VHH insert, followed by agarose gel-electrophoresis [4]. However, this methodology is time consuming, labour intensive, has limited resolution and is not effective for the analysis of a large number of clones.

In the current study, we developed a protocol using high resolution melt curve analysis (HRMA) to visualise clonal diversity and study enrichment of clones after VHH-selection from a llama non-immune phage display library. Unlike the traditional application for melt curve analysis, where 1 base pair differences are detected through a change in melt temperature of a fully base-paired hybrid and mismatched hybrids, the current study uses differences in melt curve shape and the Tm of each melt curve to identify template nucleotide sequence similarities within a large group of unlike PCR fragments. Similar melt curve shapes represent similar DNA sequences and melt curves can be automatically and efficiently grouped using the available HRMA software.

Results

After two rounds of selection against an epitope spanning the first 548 amino acids of the huntingtin protein [6], 96 phages were picked and ELISA showed 25 positive and 71 negative wells. An optical density of 0.6 or higher was considered a positive result while the negative control was less than 0.1. Clone diversity was investigated using both HRMA and *Hin*fI restriction digestion of PCR-amplified clone inserts. As expected, since the PCR fragments had an average size of 600 bp, HRMA showed a wide range of melt profiles often containing multiple melting domains per fragment representing differences in nucleotide sequence. Representative results from 4 independent HRMA analyses are shown in Figure 1, a comparison of the ELISA and HRMA results are shown in Figure 2. Only the ELISA-positive clones are represented in this figure. There was a complete agreement of ELISA-positive and ELISA-negative clones with HRMA analysis. The 25 ELISA-positive clones belonged to 6 different groups, the largest

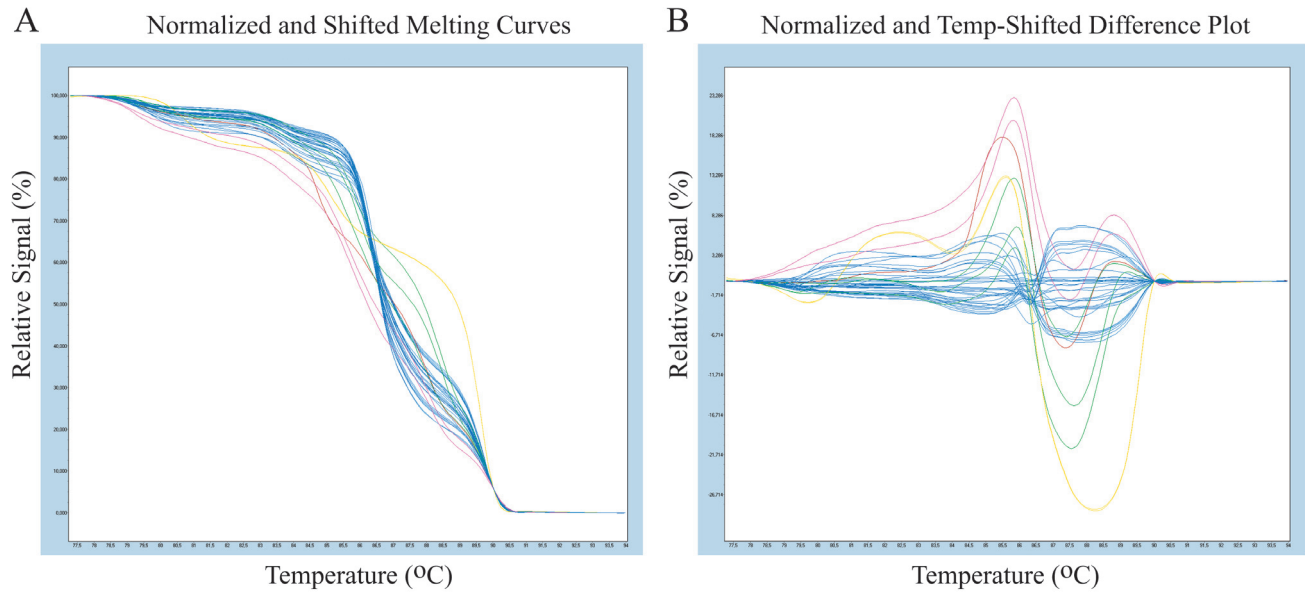

Figure 1

Grouping of clones by high resolution melt curve analysis (HRMA). A) Normalized and temperature shifted melt curves for the 25 samples that showed a positive result with ELISA. Samples with differences in their DNA sequences can be easily distinguished because of their different shaped melt curves. The different groups as assigned by HRMA are represented by different colours. B) Shows the same samples as in A. The differences in melt curve shapes are further analysed by using the sample with the highest melting temperature from the normalized and temperature shifted melt curves as a baseline in order to cluster samples automatically into groups that have similar melt curves. The different groups as assigned by HRMA are represented by different colours.

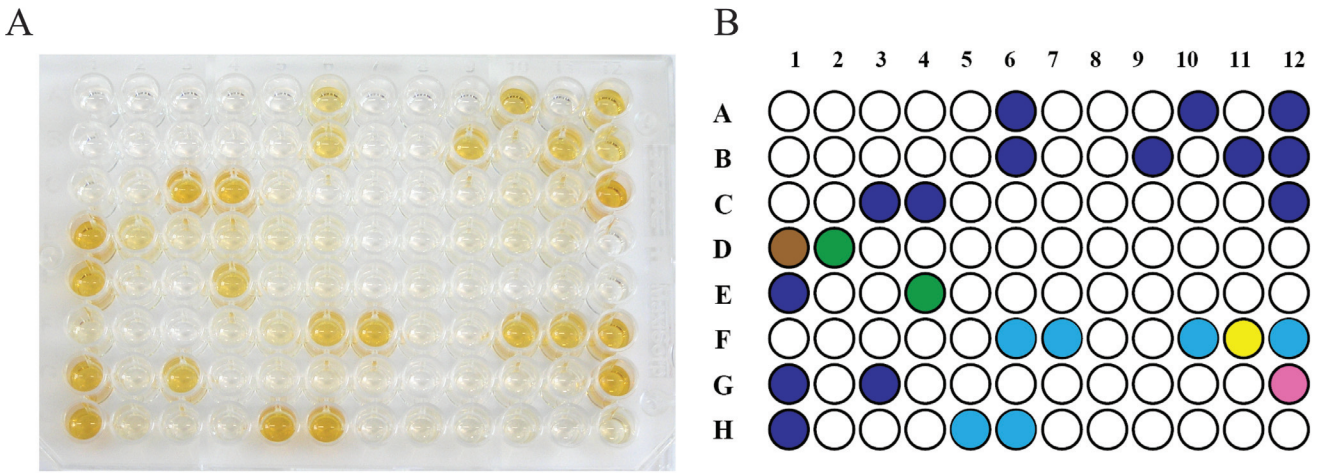

Figure 2
Comparison of ELISA results and high resolution melt curve analysis (HRMA). A) ELISA results for the 96 colonies selected from the phage display library. B) The different colours represent the different groups as assigned by HRMA. Only results for the ELISA positive clones are shown.

group contained 14 clones, one group 6 clones, one group 2 clones, and 3 groups contained a unique clone. Of the remaining 71 clones that showed a negative ELISA, 12 clones could not be analysed by HRMA because of a low PCR yield and/or low quality melting. The remaining 59 clones could be grouped into 20 different groups, consisting of one large group of 17 clones and three groups of 8, 6, and 4 clones, respectively. The remaining groups all contained 3 clones or less. All groups identified by restriction digestion fingerprinting were also identified by HRMA. Groups could overall be confirmed by nucleotide sequence analysis and PCR fragments were approximately 600 bp in length ranging from 552 to 607 bp with a Tm of either 85 or 86°C and a G/C content of 53 or 54%. The most common fragment length was 606 bp with a Tm of 86°C and a G/C content of 54%. Fragments with these characteristics were present in the majority of groups assigned by the software. As can be seen in Figure 3, HRMA even identified one additional group that was not seen with fingerprinting. However, as can be seen in the red HRMA group in Figure 3, occasionally, ELISA results and HRMA results did not agree with restriction digestion results. Sequencing showed that the red clone with the different digestion pattern was 2 bp different from the other clones in this HRMA group. These changes were outside the VHH encoding region and thus did not affect VHH binding characteristics. However, this 2 bp difference did change a *Hin*fI restriction site resulting in a different restriction pattern.

Discussion

HRMA has been used routinely for mutation scanning on patient samples with small fragments of equal size (up to 400 bp) that differ only 1 or a few nucleotides in sequence [7]. The temperature at which the probe-template hybrid melts, distinguishes between fully base-paired hybrids from mismatched hybrids. In the current study, we developed a protocol using HRMA to identify clonal origin of VHH fragments selected from a phage display library as an alternative for DNA fingerprinting. The protocol uses the differences in melt curve shape and Tm of each melt curve to identify template nucleotide sequence similarities within a large group of samples. Although the software used for HRMA was originally designed to detect 1 bp differences between two small fragments, our results demonstrate that it is also capable of accurately analysing melt curves from longer unlike PCR fragments. HRMA is a very efficient technique to obtain a quick overview and determine if clone selection was successful. From a successful selection experiment one expects several recurring clones. When all clones are different, no enrichment has taken place and clone selection has probably failed, when all clones are identical, the success is probably also doubtful. When the ELISA negative clones contain a large recurrent set, these clones might either be well-growing but have low-affinity/are non-specific (not interesting) or high affinity clones that somehow fail to produce enough VHH in order to obtain a positive ELISA signal (interesting). HRMA is also suitable to follow clone selection; initially one expects all clones to be different, with larger clone sets emerging in later rounds of selection. When comparing HRMA to digestion analysis of the VHH fragments, HRMA analysis is a more sensitive and efficient method to determine clonal similarity. All groups identified with restriction digestion fingerprinting could also be identified by HRMA and were overall confirmed by sequence analysis.

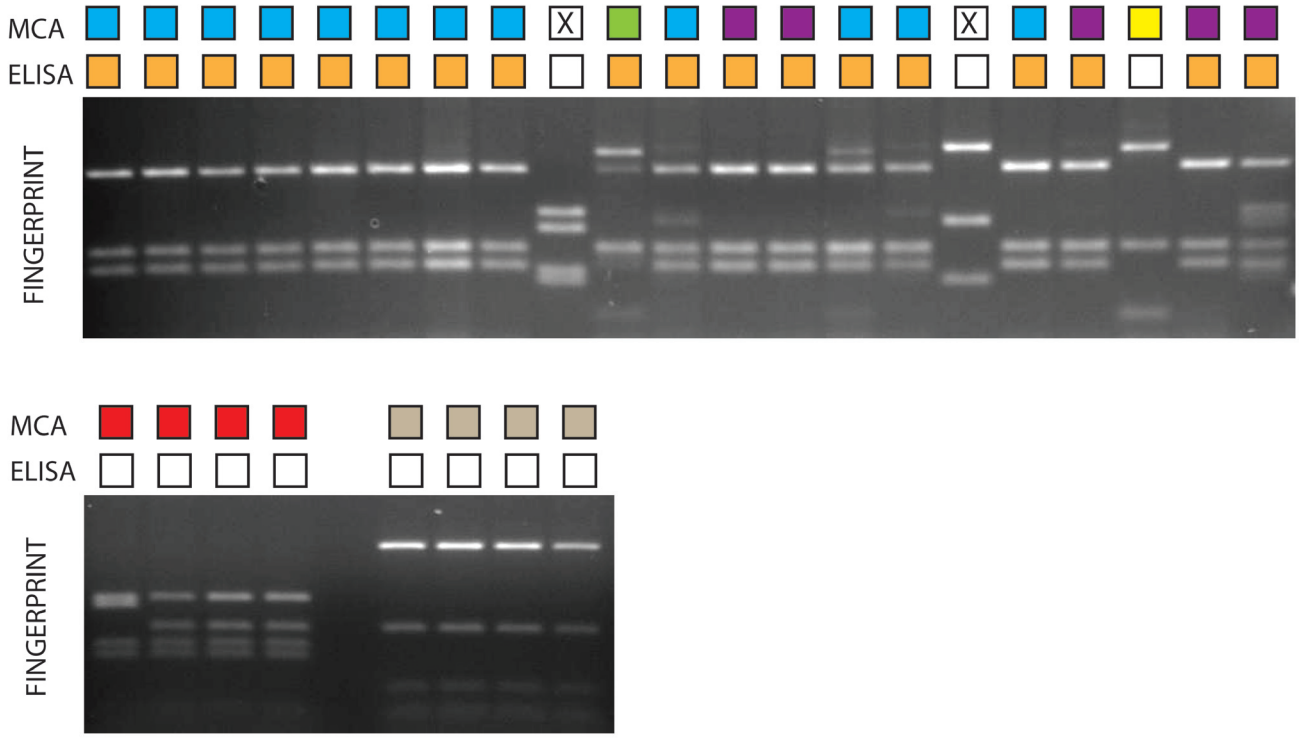

Figure 3
Comparison of ELISA results, high resolution melt curve analysis (HRMA) and restriction digestion analysis. Shown in the top row of the small square boxes are representative clones from groups as assigned by HRMA. The different colours indicate the different groups, and a cross indicates these samples could not be analysed because of a low quality melt curve. The second row of boxes indicates the ELISA results. A white box represents a negative ELISA result and an orange box indicates a positive ELISA result. The corresponding restriction digestion pattern for each sample is shown in the lower panel. HRMA identifies an additional group in the ELISA-positive clones (top panel sample 12,13, 18, 20 and 21) not identified by fingerprint analysis.

It is a simple and rapid method taking only two and a half hours to complete after PCR amplification. Furthermore, it is inexpensive, requiring only PCR, a DNA dye, and melting instrumentation. In the current study we have used the LightCycler480 for the final PCR amplification and melt curve analysis, however, any block cycler can be used for amplification and the subsequent melt analysis could then be performed with other high-resolution melting devices such as the LightScanner (Idaho Technology Inc, Salt Lake City, Utah). Multiple samples can be analysed simultaneously (HRMA facilitates analysis of up to 384 clones per microtitre plate) and groups can be assigned in an automated manner.

Conclusion

HRMA is very efficient to obtain a quick overview and determine if clone selection was successful. Similar groups of clones identified by restriction digestion fingerprinting were also identified by HRMA and were confirmed by nucleotide sequence analysis. HRMA is suitable for a wide variety of applications where verification and/or analysis of clonal diversity is essential, including determining clone diversity in a single-chain (sc) Fv phage library [8], analysis of clones obtained after *in vitro* mutagenesis [9], cDNA clones to determine allelic expression [10] and clones to determine methylation status of genomic regions [11].

Methods

ELISA and restriction digestion

Two consecutive rounds of selection were performed with a large non-immune VHH library as described previously [4,5] on the first 548 amino acids of the huntingtin protein [6]. From this selection, 96 individual colonies were randomly picked. To assess specific binding to the antigen of interest, ELISA was performed. In short, all 96 clones were grown first in 100 μl/well of growth medium (2xTY/Ampiciline/0,1% Glucose) for 4 hours at 37°C while shaking (220 rpm). Induction of VHH overproduction was then performed overnight after adding 20 μl of a 6 mM IPTG solution (in 2xTY/Ampiciline). A 96 well Maxisorp plate was coated with antigen overnight at 4°C. The

next day; Maxisorp plates were washed twice with 1× PBS and blocked for 30 min at room temperature with 4% non-fat milk in PBS. After blocking, 50 μl of 4% non-fat milk/PBS solution was added to each well. Plates containing the VHH's were spun down at 1200 g and 4°C for 15 minutes. From each well, 50 μl of VHH-containing supernatant was added to the corresponding well of the Maxisorp plate. The Maxisorp plate was then incubated for 2 hours at room temperature while shaking (900 rpm). After incubation the plate was rinsed 3 times with PBST and 3 times with PBS. For the detection of bound VHH's, 100 μl of a 1:1000 solution of anti-myc antibody (9E10, Santa Cruz) conjugated to Horse Radish Peroxidase (HRP) in 4% non-fat milk/PBS was added to each well. The Maxisorp plate was then incubated for 2 hours at room temperature while shaking (900 rpm). After incubation the plate was rinsed 3 times with PBS containing 0.05% Tween20 and subsequently 3 times with PBS. The reaction was developed by adding an OPD-H_2O_2 solution to each well followed by a 35 minutes incubation at room temperature under dark conditions. Reaction was stopped by adding 50 μl/well of 1 M H_2SO_4. Optical densities were measured at a wavelength of 490 nm using a plate reader (Biotek, Winooski, USA). To analyse clone inserts, PCR was performed on all 96 clones on a standard block cycler (Bio-Rad, Hercules, CA) using 1 μl of overnight culture with the following primers: M13R 5'-CAGGAAACAGCTATGAC-3' and MPE25WB 5'-TTTCTGTATGGGGTTTTGCTA-3'. Amplification was performed in 1× PCR buffer, 0.7 U FastStart Taq DNA polymerase (Roche, Mannheim, Germany), 200 μM dNTPs, 1 pmol of each primer in a reaction volume of 20 μl. Cycling conditions were 5 min at 95°C followed by 35 cycles of 40 sec at 95°C, 40 sec at 55°C and 1 min at 72°C, followed by a final incubation of 5 min at 72°C. DNA fingerprint analysis was performed on 10 μl PCR product digested for 2 hr at 37°C in a total volume of 20 μl containing, 1× reaction buffer and 1 U *Hin*fI (Fermentas, Burlington, Canada) and digests were run on a 3% agarose gel.

High resolution melt curve analysis

Amplification for HRMA was performed on 2 μl of 1:1000 dilutions of previously amplified clones using the same primers as in the first PCR reaction in a 10 μl reaction volume containing 1× LightCycler® High Resolution Melting Master (Roche), 2 mM $MgCl_2$, and 3 pmol of each primer. All samples were amplified in duplicate in the Lightcyler®480 (Roche) and this was followed by melt curve acquisition. Initial denaturation of 10 min at 95°C was followed by 30 cycles of 10 sec at 95°C, 30 sec at 55°C and 20 sec at 72°C. After a final extension of 5 min at 72°C, melt curve acquisition started with a hold of 1 min at 95°C followed by 1 min at 40°C and ramping from 60°C to 98°C at 1°C/sec with 25 acquisitions per °C. Grouping of the clones was done using the Genescanning module of the Lightcyler®480 Software Release 1.5.0 (Roche). The sample with the highest melting temperature was selected from the normalized and temperature shifted melt curves and used as baseline for the difference plot analysis. After the software had calculated the groups, they were checked manually to ensure that samples with identical melt curves were assigned to their appropriate groups. Because the software could only assign 8 groups at once, analysis was done three times. For the second and third round of analysis, all samples assigned to groups in the previous rounds were omitted until all samples had been clustered.

Competing interests

The authors declare that they have no competing interests.

Authors' contributions

BAP helped writing the manuscript, set up HRMA, performed ELISA and restriction digestion, MHS performed ELISA, restriction digestion analysis, and sequencing, RHAMV was instrumental in developing the HRMA method, GJBO participated in the design of the study JTD critically revised the manuscript and designed the study WMCRM wrote the manuscript and supervised the study.

Acknowledgements

The phage display library was kindly provided by Unilever Research Vlaardingen, The Netherlands. This work was partly funded by the CHDI Foundation.

References

1. Frenken LG, Hessing JG, Hondel CA Van den, Verrips CT: **Recent advances in the large-scale production of antibody fragments using lower eukaryotic microorganisms.** *Res Immunol* 1998, **149:**589-599.
2. McCafferty J, Griffiths AD, Winter G, Chiswell DJ: **Phage antibodies: filamentous phage displaying antibody variable domains.** *Nature* 1990, **348:**552-554.
3. Hamers-Casterman C, Atarhouch T, Muyldermans S, Robinson G, Hamers C, Songa EB, *et al.*: **Naturally occurring antibodies devoid of light chains.** *Nature* 1993, **363:**446-448.
4. van Koningsbruggen S, De Haard H, de Kievit P, Dirks RW, van Remoortere A, Groot AJ, *et al.*: **Llama-derived phage display antibodies in the dissection of the human disease oculopharyngeal muscular dystrophy.** *J Immunol Methods* 2003, **279:**149-161.
5. Verheesen P, de Kluijver A, van Koningsbruggen S, de Brij M, de Haard HJ, van Ommen GJ, *et al.*: **Prevention of oculopharyngeal muscular dystrophy-associated aggregation of nuclear poly(A)-binding protein with a single-domain intracellular antibody.** *Hum Mol Genet* 2006, **15:**105-111.
6. Martindale D, Hackam A, Wieczorek A, Ellerby L, Wellington C, McCutcheon K, *et al.*: **Length of huntingtin and its polyglutamine tract influences localization and frequency of intracellular aggregates.** *Nat Genet* 1998, **18:**150-154.
7. Reed GH, Kent JO, Wittwer CT: **High-resolution DNA melting analysis for simple and efficient molecular diagnostics.** *Pharmacogenomics* 2007, **8:**597-608.
8. Tanaka T, Rabbitts TH: **Intrabodies based on intracellular capture frameworks that bind the RAS protein with high affinity and impair oncogenic transformation.** *EMBO J* 2003, **22:**1025-1035.
9. Kuroda T, Martuza R, Todo T, Rabkin S: **Flip-Flop HSV-BAC: bacterial artificial chromosome based system for rapid generation of recombinant herpes simplex virus vectors using two**

independent site-specific recombinases. *BMC Biotechnology* 2006, **6:**40.
10. Rangwala SH, Elumalai R, Vanier C, Ozkan H, Galbraith DW, Richards EJ: **Meiotically stable natural epialleles of Sadhu, a novel Arabidopsis retroposon.** *PLoS Genet* 2006, **2:**e36.
11. Wada Y, Miyamoto K, Kusano T, Sano H: **Association between up-regulation of stress-responsive genes and hypomethylation of genomic DNA in tobacco plants.** *Mol Genet Genomics* 2004, **271:**658-666.

Chapter 3

Selection and characterization of llama single domain antibodies against N-terminal huntingtin

Menno H. Schut[1], Barry A. Pepers[1], Rinse Klooster[2], Silvère M. van der Maarel[1], Mohamed el Khatabi[3], Theo Verrips[3], Johan T. den Dunnen[1,4], Gert-Jan B. van Ommen[1], Willeke M.C. van Roon-Mom[1*]

1 Department of Human Genetics, Center for Human and Clinical Genetics, Leiden University Medical Center, Albinusdreef 2, 2333 ZA Leiden, The Netherlands

2 Merus BV, Padualaan 8, 3584 CH Utrecht, The Netherlands

3 QVQ BV, Padualaan 8, 3584 CH Utrecht, The Netherlands

4 Leiden Genome Technology Center, Center for Human and Clinical Genetics, Leiden University Medical Center, Albinusdreef 2, 2333 ZA Leiden, The Netherlands

* Corresponding author: Willeke M.C. van Roon-Mom, Department of Human Genetics, Leiden University Medical Center, Albinusdreef 2, 2333ZA Leiden, The Netherlands. Tel: +31 71 5269435; Fax: +31 71 5268285; Email: w.vanroon@lumc.nl

Neurological Sciences (2015)

Neurol Sci (2015) 36:429–434
DOI 10.1007/s10072-014-1971-6

ORIGINAL ARTICLE

Selection and characterization of llama single domain antibodies against N-terminal huntingtin

Menno H. Schut · Barry A. Pepers · Rinse Klooster · Silvère M. van der Maarel · Mohamed el Khatabi · Theo Verrips · Johan T. den Dunnen · Gert-Jan B. van Ommen · Willeke M. C. van Roon-Mom

Received: 7 July 2014 / Accepted: 24 September 2014 / Published online: 8 October 2014

Abstract Huntington disease is caused by expansion of a CAG repeat in the *huntingtin* gene that is translated into an elongated polyglutamine stretch within the N-terminal domain of the huntingtin protein. The mutation is thought to introduce a gain-of-toxic function in the mutant huntingtin protein, and blocking this toxicity by antibody binding could alleviate Huntington disease pathology. Llama single domain antibodies (VHH) directed against mutant huntingtin are interesting candidates as therapeutic agents or research tools in Huntington disease because of their small size, high thermostability, low cost of production, possibility of intracellular expression, and potency of blood-brain barrier passage. We have selected VHH from llama phage display libraries that specifically target the N-terminal domain of the huntingtin protein. Our VHH are capable of binding wild-type and mutant human huntingtin under native and denatured conditions and can be used in Huntington disease studies as a novel antibody that is easy to produce and manipulate.

Keywords VHH · Huntington disease · PolyQ · N-terminal huntingtin · Huntingtin

Introduction

Huntington disease (HD) is caused by expansion of a CAG repeat within the first exon of the *huntingtin* gene (4p16.3) [1]. This mutation results in an expanded polyglutamine repeat (polyQ) at the N-terminus of the huntingtin protein (htt), causing HD pathology through a toxic gain-of-function mechanism [2]. Antibody binding could reduce toxicity of the mutant htt protein. Messer et al. showed that a single chain Fv antibody construct, selected against the first 17 N-terminal htt amino acids was capable of reducing HD pathogenesis in various HD models [3, 4]. In our study we make use of llama single domain antibody fragments called VHH [5]. VHH contain four framework regions (FR1–4) for structural integrity and three variable complement determining regions (CDR1–3) that usually determine epitope binding. VHH have distinctive advantages compared with other antibody classes. VHH are thermostable, only ~16 kD in size and their single domain nature simplifies selection and production [6, 7]. VHH have been used for diseases such as oculopharyngeal muscular dystrophy (OPMD), which shares characteristics with HD. OPMD is caused by expansion of a triplet repeat in the *PABPN1* gene that encodes for a polyalanine repeat at the N-terminus of the polyA binding nuclear 1-protein (PABN1). VHH binding to an α-helical domain of mutant PABN1 prevented aggregation [8], and alleviated OPMD

Electronic supplementary material The online version of this article (doi:10.1007/s10072-014-1971-6) contains supplementary material, which is available to authorized users.

M. H. Schut · B. A. Pepers · S. M. van der Maarel · J. T. den Dunnen · G.-J. B. van Ommen · W. M. C. van Roon-Mom (✉)
Department of Human Genetics, Center for Human and Clinical Genetics, Leiden University Medical Center, Albinusdreef 2, 2333 ZA Leiden, The Netherlands
e-mail: W.M.C.van_Roon@lumc.nl

R. Klooster
Merus BV, Padualaan 8, 3584 CH Utrecht, The Netherlands

M. el Khatabi · T. Verrips
QVQ BV, Padualaan 8, 3584 CH Utrecht, The Netherlands

J. T. den Dunnen
Leiden Genome Technology Center, Center for Human and Clinical Genetics, Leiden University Medical Center, Albinusdreef 2, 2333 ZA Leiden, The Netherlands

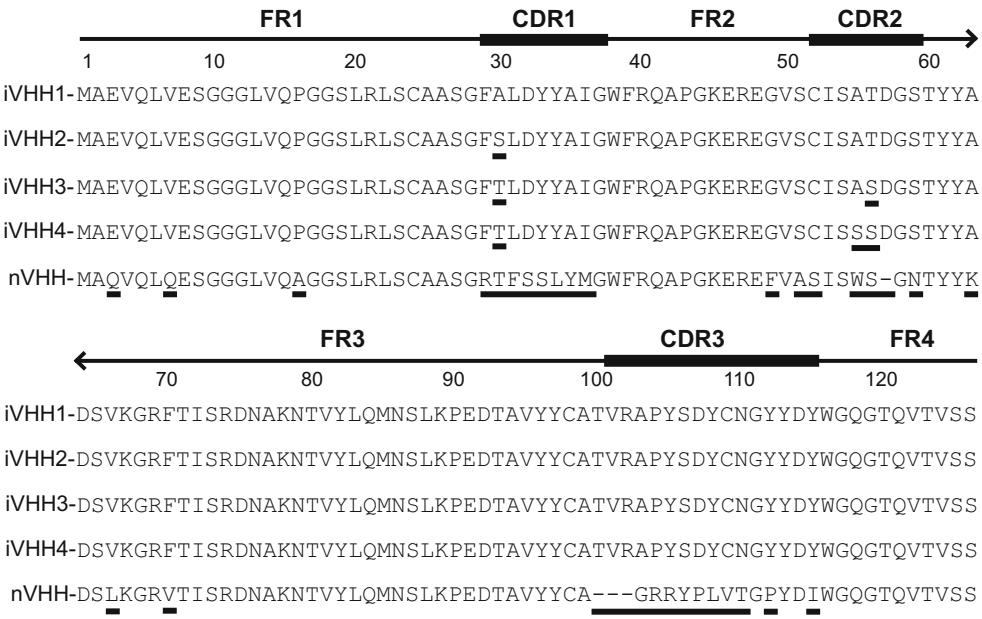

Fig. 1 VHH protein sequences. iVHH 1–4 were selected from an immunized llama phage display library. nVHH was selected from a non-immunized llama phage display library. *Underscored* amino acid position differs from iVHH1. Amino acid positions, framework (FR, *thin line*) and complementary determining regions (CDR, *thick line*) are according to Kabat [25]. −, deletion

pathology in a *drosophilia* model [9]. In the current study, we have selected VHH against the N-terminal domain of htt from llama phage display libraries. We show that high resolution melting curve analysis (HRMCA) [10] can successfully identify identical clones prior to sequencing. Our VHH can bind both endogenous and purified human wild-type and mutant htt at an epitope located between amino acids 49–148 and can co- immunoprecipitate htt from human HD brain lysates.

Results

Selection of VHH against N-terminal huntingtin

The phage-VHH (P-VHH) display library originated from llamas pre-immunized with an *Escherichia coli* produced N-terminal htt protein fragment consisting of the first 548 amino acids with 46 polyQs. We performed four different selections; each selection involved two rounds using either a wild-type or mutant N-terminal htt fragment. Enrichment of P-VHH after two rounds of selection was similar for direct coating or pre-capturing of N-terminal htt in the first round, with the optimal concentration being 5 µg N-terminal htt (Online Resource 1a). P-VHH output numbers of up to 3×10^4 were obtained. Screening ELISA revealed that on average, 20 % of selected clones bound htt (Online Resource 1b). Further screening by HRMCA (Online Resource 1c), followed by sequence analysis, revealed four

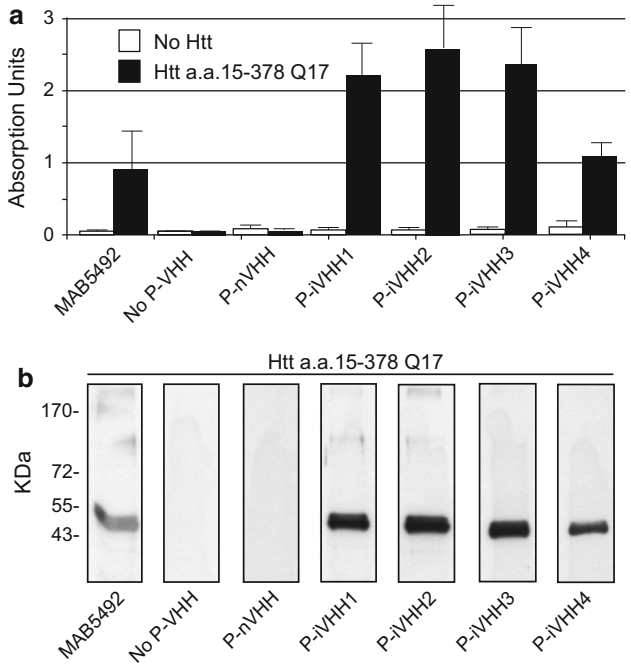

Fig. 2 VHH specificity for N-terminal htt. Assays were performed on a recombinant N-terminal htt fragment consisting of amino acids 15–378 with a polyQ length of 17 (htt a.a. 15–378 Q17). Positive control: MAB5492. Negative control: No P-VHH or P-nVHH. **a** ELISA on wells with (*black bars*), or without (*white bars*) N-terminal htt. *Bars* represent mean ELISA signal from two independent ELISA assays with standard deviation. Each assay was performed in triplicate. ELISA absorption units are measured at $\lambda = 490$ nm. **b** Western blotting on N-terminal htt. Blots were performed twice. *kDa* Molecular weight (kilodalton)

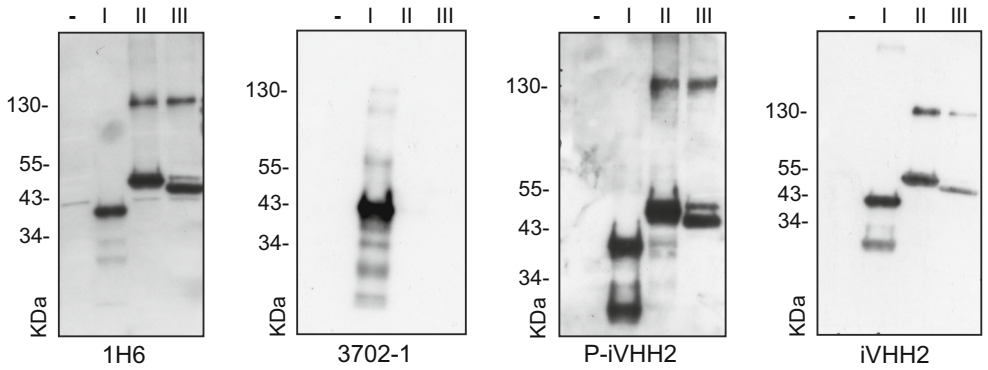

Fig. 3 VHH epitope determination. Western blots performed on no htt (−), htt a.a. 1–148 Q46 (I), htt a.a. 15–378 Q17 (II), and htt a.a. 49–415 (III). Primary antibody indicated below each blot. Blots were performed twice. *kDa* Molecular weight (kilodalton)

htt specific VHH, (immune)VHH1-4. These differed by one, two, or three amino acid substitutions in the CDR1 and CDR2, while the CDR3 was identical (Fig. 1). The negative control VHH (n-VHH) was selected previously from a naive llama phage display library [10].

Specificity of monoclonal iVHH for N-terminal huntingtin

To investigate if the iVHH specifically bind htt, we performed ELISA and western blot analysis on a normal and mutant N-terminal htt fragment using P-iVHH [11]. ELISA resulted in a positive signal for all P-iVHH (Fig. 2a, Online Resource 2a). P-iVHH1, 2 and 3 showed an equally strong ELISA signal, whereas P-iVHH4 gave a weaker signal. On western blot, all P-iVHH showed a band that matched the band obtained with the known htt antibody MAB5492 (Fig. 2b, Online Resource 2b). Western blotting results were in agreement with ELISA results.

Epitope determination of iVHH on N-terminal huntingtin

To determine the epitope of our iVHH, we performed western blotting using three different N-terminal htt fragments. Each fragment had a partially overlapping sequence with the next fragment (Fig. 3). All fragments were recognized by the 1H6 antibody [12] while 3702–1, that binds htt at the N-terminal 13 amino acids (Online Resource 3a), only recognized fragment I. All P-iVHH recognized all fragments (Fig. 3, Online Resource 3b) indicating that their epitope is located within the overlapping region of fragments I, II and III that consists of amino acids 49–148. Finally, western blotting with monomeric iVHH was performed. VHH were produced with an average concentration of 1.1 µg/µl. Western blotting using iVHH instead of P-iVHH recognized htt fragments I, II, and III but with less back ground staining.

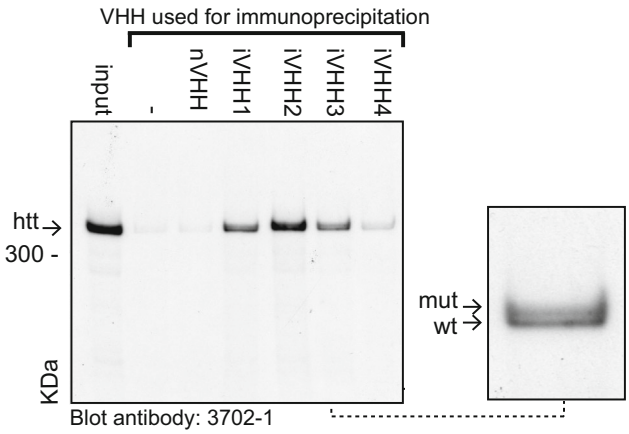

Fig. 4 Immunoprecipitation of endogenous human htt with VHH. Western blot analysis of VHH-htt immunoprecipitation complexes. VHH used for htt immunoprecipitation indicated at *top*, Input, 10 µg of brain lysate; –, No VHH. *Arrow* indicates full-length htt. *kDa* Molecular weight (kilodalton). Blot was analysed with 3702-1 anti htt antibody. *Right bracket* 3× enlargement of the iVHH3 immunoprecipitation result, showing wild-type (wt) and mutant (mut) huntingtin

iVHH detection of endogenous huntingtin in human HD brain lysates

Next, we analysed if our iVHH were capable of binding endogenous human htt. We performed immunoprecipitation experiments using monomeric iVHH and post-mortem human HD brain lysates. Non-specific binding of htt to the protA-beads without VHH (Fig. 4, –lane) was low. Immunoprecipitation in the presence of iVHH resulted in wild-type and mutant full-length htt band on western blot, while the negative control VHH (nVHH) did not show a full-length htt band (Fig. 4, Online Resource 4). This shows that, in concordance with previous ELISA and western blot results on N-terminal wild-type and mutant htt fragments, our iVHH recognize both wild-type and mutant endogenous full-length htt. Additionally,

Table 1 Construction of N-terminal Htt fragments

N-terminal htt fragment	Forward primer	Reverse primer
a.a. 1–318 (Q17/Q43)	TATGGCGACCCTGGAAA	GTCGACGAGCAGCACGCCAAGA
a.a. 15–378 (Q17/Q43)	CAAGTCCTTCCAGCAGCA	GTCGACGGCTCCGGTCACAACA
a.a. 49–415 (no polyQ)	GCCGCCTCCTCAGCTTC	GTCGACGCCACCAGACTCCTCCTT

a.a. amino acid, *Q17/Q43* polyQ stretch, *Underscored Sal*I-site

immunoprecipitation with iVHH4 was less efficient compared with the other iVHH.

Discussion

To our knowledge, our study is the first in which VHH have been selected against N-terminal htt protein fragments from an immunized llama phage display library. Monoclonal antibodies are increasingly used as therapeutic agents [13]. Proof of concept for using antibodies in HD has been provided [3, 4]. Whilst this is promising, there are high demands on any therapeutic or imaging antibody. Because HD is a brain disorder, it is important to cross the blood–brain barrier (BBB). Some VHH were able to cross the BBB [14, 15]. Also, VHH diffusion throughout the brain, and cellular uptake were demonstrated [15]. Although VHH selection from non-immune phage-VHH libraries is possible [16], selection from immune llama phage-VHH libraries is expected to yield more high-affinity binders because of affinity maturation. However, diversity will be less as affinity maturation selects for the strongest binder. This is reflected in our results. Our iVHH share a high degree of sequence homology. This indicates that the binding epitope of our iVHH is very similar. Our iVHH bind full-length and N-terminal htt in a native and denatured conformation. Binding characteristics for iVHH1-3 were comparable, whereas iVHH4 showed a lower binding efficiency. This is probably due to a single amino acid change in iVHH4 at position 55 in CDR2 where the a-polar alanine was replaced with a polar serine. Because both alanine and serine have side-chains of comparable sizes, it is conceivable that the lower binding efficiency of iVHH4 is due to a shift from an a-polar to polar amino acid. The epitope of all iVHH was mapped to a region between amino acids 49 and 148 downstream of the polyQ repeat, explaining why our iVHH bind both wild-type and mutant htt. In this region, htt contains several domains associated with HD pathogenesis. There is a proline rich region involved in sequestration of other proteins into htt aggregates [17]. Furthermore, proteolytic cleavage between amino acids 104 and 114 was linked with formation of intranuclear aggregates associated with increased toxicity [12]. Binding of our iVHH in this region could alleviate HD pathogenesis. However, it has to be noted that our huntingtin-specific VHH could also block neuroprotective properties of wild-type htt [18]. Additional research is needed to assess the therapeutic properties of our iVHH or their possible applications in HD research. We have demonstrated the feasibility of using VHH for immunoprecipitation, eliminating interference by IgG bands in the subsequent western blot [19]. Furthermore, since VHH have been used as imaging agent to stain amyloid-β deposits in vivo in an Alzheimer disease mouse model [20], our iVHH could be an interesting in vivo imaging tool in HD models to visualize the htt protein.

Materials and methods

N-terminal htt fragments

A *HTT* reference sequence with 23 polyQs was used. For PCR primers see Table 1. PCR products were ligated directly into the pGEM-T easy vector (Promega, Madison, WI, USA), digested with *Nco*I and *Sal*I (Fermentas, St. Leon-Rot, Germany), and ligated into a *Nco*I/*Xho*I (Fermentas) pre-digested pIVEX 1.3 vector. Clones were confirmed by sequence analysis. Htt protein fragments were produced with the RTS-100 wheat germ CECF kit (5 PRIME, Gaitersburg, MD, USA) using the ProteoMaster rapid translation system (Roche). To produce the N-terminal htt 1–148 Q46 protein fragment, the HD1955 pCI construct consisting of *HTT* nucleotides 1–1640 [21] was cloned into a pRP261 vector using the *Nco*I/*Sal*I restriction sites, and re-cloned into the pET28 vector using the *Bam*HI/*Sal*I restriction sites. The HD1955-pET28 construct was digested with *Xho*I and self-religated, resulting in the HD828-pET28 construct. Production and purification were performed in BL21 codon+ *E.coli* cells as described for VHH. To prevent aggregation, dialysis was performed in PBS + 0.5 % Sarkosyl (Sigma–Aldrich).

VHH selection

Selections were performed as described [16]. The first selection round involved a direct coating of NUNC maxisorp plates (Thermo fisher Scientific, Rochester, NY, USA)

with 10, 5, or 2.5 μg of antigen, or a pre-capturing of 10 μg antigen with 2, 1, or 0.5 μg of coated 1H6 antibody (Abnova, Taipei, Taiwan). Phage-VHH (P-VHH) from the first round were produced and purified as described [22] and subjected to a second round of selection with 5, 2.5, or 1 μg of directly-coated antigen. Purified P-VHH were stored at −20 °C in PBS containing 10 % glycerol. TG1 *E. coli* cells were infected with phage-VHH from the second selection round and plated on LB/Agar containing ampicillin. Ninety-four randomly selected clones were tested as described [10]. As secondary antibody for the screening ELISA, we used HRP conjugated mouse anti M13 (GE Healthcare, Buckinghamshire, UK). *VHH* DNA was purified using the Nucleospin Plasmid purification kit (Macherey–Nagel, Duren, Germany) according to manufacturer's instructions. DNA was sequenced using primer M13REV (CAGGAAA CAGCTATGAC). DNA to protein conversion: http://www.bioinformatics.picr.man.ac.uk/research/software/tools/sequenceconverter.html. VHH sequence alignment: http://www.ebi.ac.uk/Tools/msa/clustalW2.

VHH production

PCR was performed on M13 plasmid using primers iVHH-FW (CGGAATTCCTTTAGTTGTTCCA), and iVHH-Rev (CACATCATCATCACCATCACG), or nVHH-FW (CGCT GGATTGTTATTACTCGC) and nVHH-Rev (CCTCA GAACCCAAGACCA). PCR fragments were cloned into pUR5850 [23] by *Sfi*I and *Bst*EII (Fermentas) digestion and ligation. Clones were verified by sequence analysis and transferred into Neb5 *E. coli* for production. VHH were purified using the His6-tag with TALON metal affinity resin (Clontech, Mountain View CA, USA) according to the manufacturer's instructions using 50 mM NaPO4, 0.3 M NaCl, pH7 as wash buffer. Wash buffer with 150 mM imidazole was used as elution buffer. Pooled eluates were dialyzed against PBS using Cellu-Sep dialyze-tube MWCO 3500 (Interchim, MontluÇon, France). VHH production was checked on Coomassie staining (PageBlue, Thermo-Scientific) and western blotting against the VSV-tag. VHH was quantified with bicinchoninic assay (BCA, Thermo-Scientific). VHH were stored in 5 % glycerol at −20 °C.

ELISA

A 96-well NUNC maxisorp plate was coated with 0.1 μg/well of antigen. Staining was performed using P-VHH diluted 1:20, followed by HRP conjugated mouse anti M13 (Millipore Billerica, MA, USA). ELISA signal was visualized with *o*-Phenylenediamine (OPD, Sigma–Aldrich). Optical density at $\lambda = 490$ nm was measured using a plate reader (Biotek, Winooski, USA). The huntingtin-specific antibody MAB5492 (Millipore) was used as positive control.

Western blot

N-terminal htt fragments were run on a 10 % SDS-PAGE gel and proteins were blotted onto nitrocellulose membrane (#170-4159, Bio-Rad, Hercules, CA, USA). Blots were blocked with 4 % non-fat milk (Nutricia, Schiphol, The Netherlands) in TBST. Primary antibodies: 3702-1 (Epitomics, Burlinggame, CA, USA), MAB5492 (Millipore), 1H6 (Abnova, Taipei city, Taiwan), P-VHH or 20 ng/μl VHH. Blots probed with VHH were subsequently incubated with mouse anti VSV (Cell signalling). Secondary antibodies: HRP conjugated goat anti-mouse, goat anti-rabbit (Santa-Cruz), or mouse anti-M13 (Millipore). Bands were detected with Amersham ECL (#RPN 2132, GE healthcare) and Hyperfilm ECL (#28906837, GE healthcare).

Immunoprecipitation assay

Human post-mortem brain tissue from the middle temporal gyrus of a 67 year old female HD subject (CAG1: 15, CAG2: 42) was obtained with the families full consent and the ethical approval of the various institutional Ethics Committees. Post-mortem delay was 9 h. VHH (15 μg) was bound to 10 μl bed volume of protein A sepharose beads (GE Healthcare), and incubated for 90 min with 100 μg of post-mortem human HD brain tissue lysate in PBS. Western blot analysis of the VHH-htt complexes was performed as described above, where SDS-PAGE was performed according to [24].

Acknowledgments We thank Richard L. M. Faull and the Neurological Foundation of New Zealand Human Brain Bank for the HD post-mortem brain tissue. We thank Dr. Michael Hayden for the HD1955 (CAG44)-pCI construct. We thank Fausta Bankauskaite for technical assistance. This study was supported by a grant (WAR30808) from the Prinses Beatrix Spierfonds, and the Centre for Biomedical Genetics of the Netherlands.

Conflict of interest The authors declare no competing financial interests.

References

1. (1993) A novel gene containing a trinucleotide repeat that is expanded and unstable on Huntington's disease chromosomes.

The Huntington's Disease Collaborative Research Group. Cell 72(6): 971–983
2. Jacobsen JC, Gregory GC, Woda JM et al (2011) HD CAG-correlated gene expression changes support a simple dominant gain of function. Hum Mol Genet 20(14):2846–2860. doi:10.1093/hmg/ddr195
3. Wolfgang WJ, Miller TW, Webster JM et al (2005) Suppression of Huntington's disease pathology in Drosophila by human single-chain Fv antibodies. Proc Natl Acad Sci USA 102(32):11563–11568. doi:10.1073/pnas.0505321102
4. Snyder-Keller A, McLear JA, Hathorn T, Messer A (2010) Early or late-stage anti-N-terminal Huntingtin intrabody gene therapy reduces pathological features in B6.HDR6/1 mice. J Neuropathol Exp Neurol 69(10):1078–1085. doi:10.1097/NEN.0b013e3181f530ec
5. Hamers-Casterman C, Atarhouch T, Muyldermans S et al (1993) Naturally occurring antibodies devoid of light chains. Nature 363(6428):446–448. doi:10.1038/363446a0
6. van der Linden RH, Frenken LG, de Geus B et al (1999) Comparison of physical chemical properties of llama VHH antibody fragments and mouse monoclonal antibodies. Biochim Biophys Acta 1431(1):37–46
7. Arbabi Ghahroudi M, Desmyter A, Wyns L et al (1997) Selection and identification of single domain antibody fragments from camel heavy-chain antibodies. FEBS Lett 414(3):521–526
8. Verheesen P, de Kluijver A, van Koningsbruggen S et al (2006) Prevention of oculopharyngeal muscular dystrophy-associated aggregation of nuclear polyA-binding protein with a single-domain intracellular antibody. Hum Mol Genet 15(1):105–111. doi:10.1093/hmg/ddi432
9. Chartier A, Raz V, Sterrenburg E et al (2009) Prevention of oculopharyngeal muscular dystrophy by muscular expression of Llama single-chain intrabodies in vivo. Hum Mol Genet 18(10):1849–1859. doi:10.1093/hmg/ddp101
10. Pepers BA, Schut MH, Vossen RH et al (2009) Cost-effective HRMA pre-sequence typing of clone libraries; application to phage display selection. BMC Biotechnol 9:50. doi:10.1186/1472-6750-9-50
11. Liu B, Huang L, Sihlbom C et al (2002) Towards proteome-wide production of monoclonal antibody by phage display. J Mol Biol 315(5):1063–1073. doi:10.1006/jmbi.2001.5276
12. Lunkes A, Lindenberg KS, Ben-Haiem L et al (2002) Proteases acting on mutant huntingtin generate cleaved products that differentially build up cytoplasmic and nuclear inclusions. Mol Cell 10(2):259–269
13. Leavy O (2010) Therapeutic antibodies: past, present and future. Nat Rev Immunol 10(5):297. doi:10.1038/nri2763
14. Rutgers KS, Nabuurs RJ, van den Berg SA et al (2011) Transmigration of beta amyloid specific heavy chain antibody fragments across the in vitro blood-brain barrier. Neuroscience 190:37–42. doi:10.1016/j.neuroscience.2011.05.076
15. Li T, Bourgeois JP, Celli S et al (2012) Cell-penetrating anti-GFAP VHH and corresponding fluorescent fusion protein VHH-GFP spontaneously cross the blood-brain barrier and specifically recognize astrocytes: application to brain imaging. FASEB J 26(10):3969–3979. doi:10.1096/fj.11-201384
16. Verheesen P, Roussis A, de Haard HJ et al (2006) Reliable and controllable antibody fragment selections from Camelid non-immune libraries for target validation. Biochim Biophys Acta 1764(8):1307–1319. doi:10.1016/j.bbapap.2006.05.011
17. Qin ZH, Wang Y, Sapp E et al (2004) Huntingtin bodies sequester vesicle-associated proteins by a polyproline-dependent interaction. J Neurosci 24(1):269–281. doi:10.1523/JNEUROSCI.1409-03.2004
18. Dragatsis I, Levine MS, Zeitlin S (2000) Inactivation of Hdh in the brain and testis results in progressive neurodegeneration and sterility in mice. Nat Genet 26(3):300–306. doi:10.1038/81593
19. Landles C, Sathasivam K, Weiss A et al (2010) Proteolysis of mutant huntingtin produces an exon 1 fragment that accumulates as an aggregated protein in neuronal nuclei in Huntington disease. J Biol Chem 285(12):8808–8823. doi:10.1074/jbc.M109.075028
20. Nabuurs RJ, Rutgers KS, Welling MM et al (2012) In vivo detection of amyloid-beta deposits using heavy chain antibody fragments in a transgenic mouse model for Alzheimer's disease. PLoS ONE 7(6):e38284. doi:10.1371/journal.pone.0038284
21. Martindale D, Hackam A, Wieczorek A et al (1998) Length of huntingtin and its polyglutamine tract influences localization and frequency of intracellular aggregates. Nat Genet 18(2):150–154. doi:10.1038/ng0298-150
22. Marks JD, Hoogenboom HR, Bonnert TP et al (1991) By-passing immunization. Human antibodies from V-gene libraries displayed on phage. J Mol Biol 222(3):581–597
23. Verheesen P, ten Haaft MR, Lindner N et al (2003) Beneficial properties of single-domain antibody fragments for application in immunoaffinity purification and immuno-perfusion chromatography. Biochim Biophys Acta 1624(1–3):21–28
24. Hu J, Matsui M, Gagnon KT et al (2009) Allele-specific silencing of mutant huntingtin and ataxin-3 genes by targeting expanded CAG repeats in mRNAs. Nat Biotechnol 27(5):478–484. doi:10.1038/nbt.1539
25. Kabat E, Wu TT, Perry H et al. (1991) United States Public Health Services Publication No. 91-3242 (National Institutes of Health, Bethesda, MD)

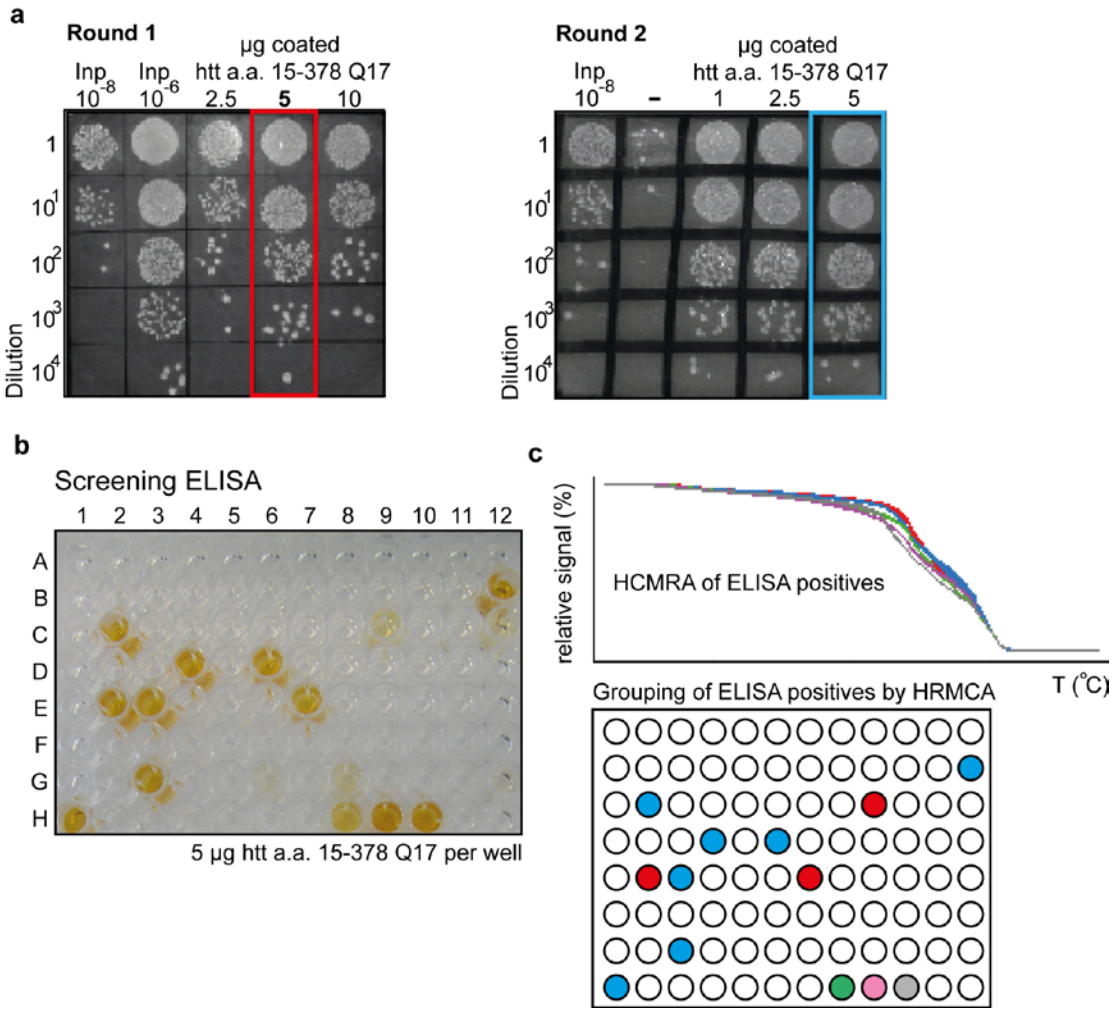

Electronic supplemental figure 1. Selection of P-iVHH by two rounds of panning against wild type N-terminal huntingtin.

a TG1 E.coli cells infected with P-VHH were diluted as indicated and spotted on agar medium selective for presence of P-VHH. Round 1: P-VHH from the llama phage display bank panned against three different concentrations of htt a.a. 15-378 Q17. Most P-VHH are recovered using 5 µg of N-term htt (indicated in red). Inp 10−6 / −8 = cells infected with whole phage display bank library diluted 106 or 108 x. Round 2: P-VHH from the most efficient first round selection were enriched and panned for a second time against htt a.a. 15-378 Q17 at indicated concentrations. Most P-VHH are recovered at a htt fragment concentration of 5 µg (indicated in blue). - = cells infected with enriched first round P-VHH selected against a blank well (background). Inp 10−8 = cells infected with whole round 1 P-VHH diluted 108 x. **b** Screening ELISA of 94 individual P-VHH clones from round 2. There were 13 (14%) ELISA positive clones (AU490>0.4) detected. **c** High resolution melting curve analysis (HRMCA) of ELISA positive clones revealed two groups of similar clones; blue (7 clones) and red (3 clones), and three unique VHH (green, pink and grey)

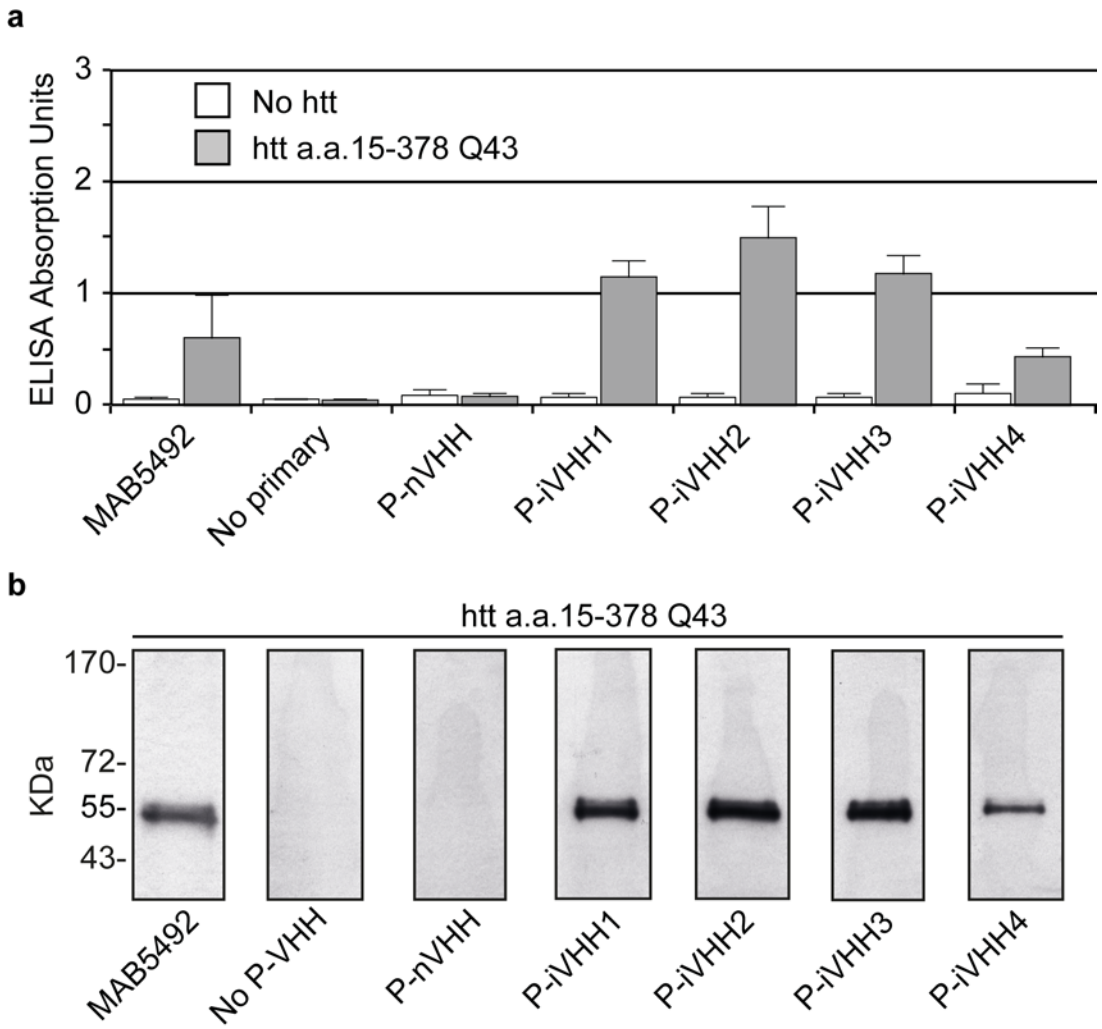

Electronic supplemental figure 2. Binding of P-VHH to N-terminal Htt fragment with elongated polyQ. Assays were performed on a recombinant N-terminal htt fragment consisting of amino acids 15 to 378 with a polyQ length of 43 (htt a.a. 15-378 Q43). Anti htt antibody MAB5492 served as positive control. Assays performed without P-VHH or the non-binding P-nVHH served as negative control. **a** ELISA with P-VHH on wells with (grey bars), or without (white bars) htt a.a. 15-378 Q43. Bars represent mean ELISA signal from two independent ELISA assays with standard deviation. Each assay was performed in triplicate. ELISA absorption units are measured at λ=490nm **b** Western blotting with P-VHH on htt a.a. 15-378 Q43. All blots were performed twice. kDa = running height in kilodalton.

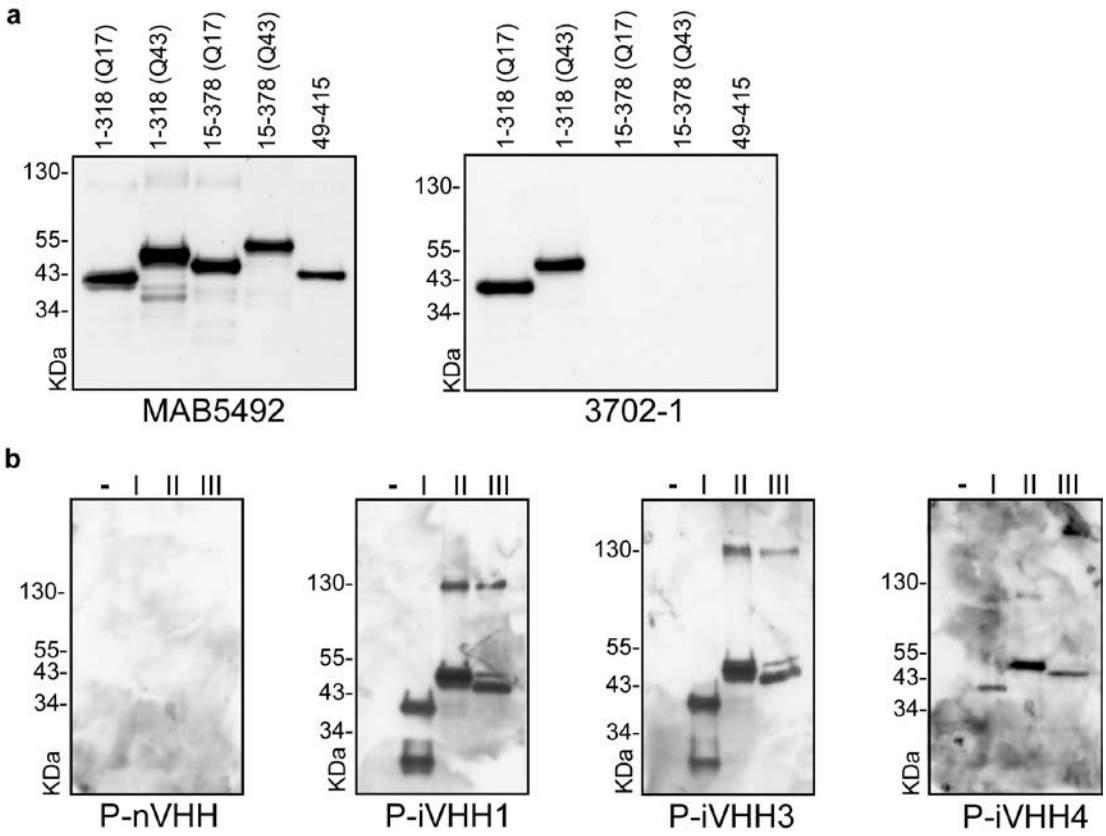

Electronic supplemental figure 3. Epitope determination of 3702-1 and VHH antibodies.

a Western blot on five different N-terminal htt fragments: htt a.a. 1 to 318 with wild type (Q17) and mutant (Q43) polyQ, htt a.a. 15 to 378 with wild type (Q17) and mutant (Q43) polyQ and htt a.a. 49-415 without the polyQ. MAB5492 (left bracket) binds all htt fragments. 3702-1 (right bracket) only binds htt a.a. 1 to 318 with either the wild type or mutant polyQ. **b** Epitope determination of P-iVHH1, 3 and 4. Fragments: I = N-terminal htt fragment with a.a. 1 to 148 with a mutant polyQ (Q46). II = N-terminal htt fragment with a.a. 15 to 378 with a wild type polyQ (Q17). III = htt fragment with a.a. 49 to 415 without polyQ stretch. - = no htt fragment. Blot performed with non-binding P-nVHH served as a negative control. All blots were performed twice.

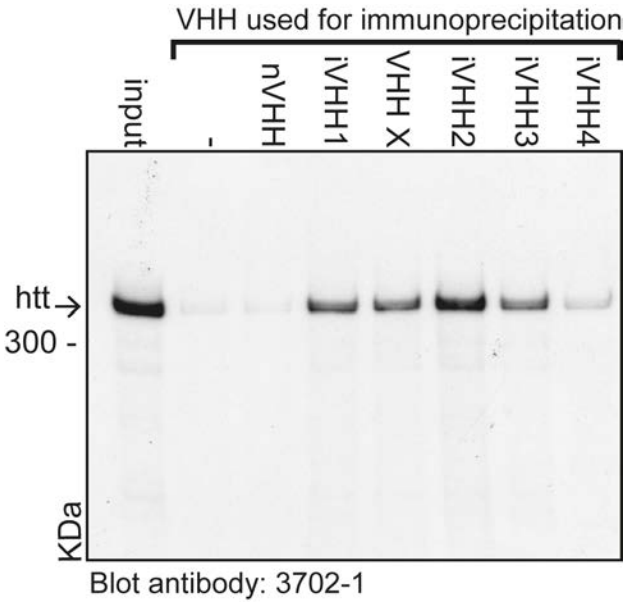

Electronic supplemental figure 4. Immunoprecipitation of human full length htt with VHH.
Input, -, nVHH, iVHH1-4 are shown in figure 4. VHH "X" corresponds to iVHH2 produced from the M13-vector. VHH produced from the M13-vector are less pure compared with VHH produced from pUR5850, hence the band intensity of VHH "X" is lower compared with iVHH2. Because the comparison between different VHH production vectors was outside the scope of this manuscript, we removed VHH X from figure 4.

Chapter 4

Effect of Post-Mortem Delay on N-terminal Huntingtin Protein Fragments in Human Control and Huntington Disease Brain Lysates

Menno H. Schut[1], Stefano Patassini[3], Eric H. Kim[3], Jocelyn Bullock[3], Henry J. Waldvogel[3], Richard L.M. Faull[3], Barry A. Pepers[1], Johan T.den Dunnen[1,2], Gert-Jan B. van Ommen[1], and Willeke M.C. van Roon-Mom[1*]

1 Department of Human Genetics, Leiden University Medical Center, 2333ZA Leiden, The Netherlands

2 Leiden Genome Technology Center, Leiden University Medical Center, 2333ZA Leiden, The Netherlands

3 Centre for Brain Research and Department of Anatomy with Radiology, University of Auckland, Auckland 1023, New Zealand

* Corresponding author: Willeke M.C. van Roon-Mom, Department of Human Genetics, Leiden University Medical Center, Albinusdreef 2, 2333ZA Leiden, The Netherlands. Tel: +31 71 5269435; Fax: +31 71 5268285; Email: w.vanroon@lumc.nl

Revised manuscript accepted for publication in PLOS ONE

Abstract

Huntington disease is associated with elongation of a CAG repeat in the *HTT* gene that results in a mutant huntingtin protein. Several studies have implicated N-terminal huntingtin protein fragments in Huntington disease pathogenesis. Ideally, these fragments are studied in human brain tissue but the use of human brain tissue comes with certain unavoidable variables such as post mortem delay, artefacts from freeze-thaw cycles and subject-to-subject variation. Knowledge on how these variables affect N-terminal huntingtin protein fragments in post mortem human brain is important for a proper interpretation of study results. The effect of post mortem delay on protein in human brain is known to vary depending on the protein of interest. In the present study, we have assessed the effect of post mortem delay on N-terminal huntingtin protein fragments using western blot. We mimicked post mortem delay in one individual control case and one individual Huntington disease case with low initial post mortem delay. The influence of subject-to-subject variation on N-terminal huntingtin fragments was assessed in human cortex and human striatum using two cohorts of control and Huntington disease subjects. Our results show that effects of post mortem delay on N-terminal huntingtin protein fragments are minor. Additionally, we show that one freeze-thaw cycle decreases the huntingtin western blot signal intensity, but does not introduce additional N-terminal huntingtin fragments. We conclude that subject-to-subject variation contributes more to variability in N-terminal huntingtin fragments than post mortem delay.

Introduction

Huntington disease (HD), is an autosomal dominant neurodegenerative disease that primarily affects the striatum and is caused by a CAG repeat expansion in the first exon of the *HTT* gene [1]. This results in a toxic huntingtin protein (htt) with an N-terminally expanded polyQ-stretch [2, 3]. Subsequent studies using HD mouse models with comparable polyQ-repeats expressing either N-terminal, or full length htt showed that N-terminal htt fragments invoke a more severe phenotype [4-6], with smaller fragments inducing the most severe phenotype [7, 8]. The htt N-terminal domain contains several proteolytic cleavage sites, some of which have been linked to HD pathology [9-12]. Results obtained from different mouse-models are sometimes conflicting. YAC128 mouse models expressing full length mutant htt resistant against caspase-3 or caspase-6 cleavage suggested that caspase-6 cleavage at amino acid 586 contributes more to HD pathogenesis than caspase-3 cleavage at amino acids 513 and 552 [13]. On the other hand, murine expression of the N552-htt fragment was shown to be more lethal compared with other caspase-associated htt fragments including N586-htt [7]. With regards to HD research on N-terminal htt protein fragments, it is important to note that studies in rat, mouse and post mortem human brain tissue have indicated that calpain-mediated proteolysis also occurs during post mortem delay (PMD) which is the time between death and tissue preservation. In rat brain, PMD-related fodrin calpain cleavage fragments were observed [14], and in mouse and human brain tissue PMD-related GSK-3 truncation by calpain was demonstrated [15]. Hence, it is important to distinguish biologically relevant N-terminal htt fragments from those that are formed during PMD. Available data on N-terminal htt protein

fragments in human post mortem brain is limited, but also indicates a role in HD pathology. N-terminal htt fragments in post mortem human HD striatum differ with post mortem human control striatum [16]. Also, the N552-htt fragment that is associated with HD pathology in a HD mouse model was detected in post mortem human HD and control brain tissue lysates [11]. Therapeutic strategies involving prevention of formation of N-terminal htt fragments are currently pursued [17]. However, extrapolation of results obtained in cell and animal models to the human brain is difficult. N-terminal htt fragments may vary between different biological systems [18]. Furthermore, research involving post mortem human brain tissue involves unavoidable variables that are difficult to control such as PMD, post mortem processing, and interpersonal variation. Effects of PMD on biological parameters have been well described [19]. In rat brain, synaptic density and vesicles decline after a PMD of 15hr, with subtle changes on synaptic structure [20]. Binding sites for forskolin, an activator for adenylate cyclase, were already reduced in rat striatum after a PMD of 4 hours [21]. PMD related effects vary between different molecules and proteins. No effect of PMD for up to 72 hours was observed for fatty acid molecules in post mortem human brain tissue [22]. PMD was shown to variously affect different proteins in mouse CNS [23]. A study on different post mortem human brain samples indicated that levels of synaptic proteins PSD-95 and syntaxin, but not synaptophysin, decline with PMD [24]. However, care must be taken when comparing different subjects with comparable PMD because PMD related effects might also vary between subjects [25, 26]. In the current study, we have assessed effects of PMD, freezing and inter-individual variation between human subjects on the profile of N-terminal htt fragments on western blot. Our study shows a small effect of artificially induced PMD on N-terminal htt fragments. Furthermore, one freeze-thaw cycle already adversely affected the western blot signal for huntingtin in human temporal lobe tissue, but did not result in the appearance of novel N-terminal htt fragments. Finally, analysis of nine control versus nine HD subjects matched for age, gender and PMD showed that there was more inter-individual variability in the profile of N-terminal htt fragments than the variability introduced by PMD.

Materials and Methods

Human brain tissue

Post mortem human cortical and striatal brain tissue from control and HD subjects was obtained from the Neurological Foundation of New Zealand Human Brain Bank, Centre for Brain Research, University of Auckland. The temporal lobe tissue was obtained 1 hour after surgery on a patient suffering from severe epilepsy. Tissue was obtained with the approval by the University of Auckland Human Participants Ethics Committee and informed consent from all families. See Table 1 for the complete list of samples with clinical information.

Human brain tissue for analysis of post mortem delay effects.

To mimic post mortem delay, tissue samples were taken from the main tissue specimen at regular time intervals (sampling). During sampling, tissue was left at room-temperature under sterile conditions. 1 ml of chilled homogenization buffer (150 mM Sucrose, 15 mM HEPES pH 7.9, 60 mM KCl, 0.5 mM EDTA pH 8.0, 0.1 mM EGTA pH 8.0, 1% Triton X-100) was added. Tissue was homogenized with a bullet blender (Next Advance) for 3 minutes, strength 8 using 0.5 mm stainless steel beads. Homogenized tissue was kept on ice for 1 hour and centrifuged cold at full speed for 10 minutes. Supernatant was aliquoted in 100 µl portions, snap-frozen and stored at -80˚C. To mimic post mortem delay with and without freeze-thaw cycle, the temporal lobe tissue was divided into two halves immediately after obtaining the tissue. One half was subsequently sampled, while the other was snap-frozen and stored at -80ºC according to [27] for 11 days before sampling.

Post mortem human brain tissue lysates.

For every subject, sensory/motor cortex and caudate nucleus tissue was collected separately. Per subject and region, 15 slides (thickness: 30 µm) of unfixed tissue were collected on glass slides with a cryostat-microtome (LEICA). Grey matter was scraped off, weighed and collected in 0.5 ml eppendorf tubes. 10 µl of chilled homogenization buffer was added per µg of tissue with a minimum of 200 µl. Tissue was homogenized with a bullet blender (Next Advance) for 3 minutes, strength 8 using 0.5 mm stainless steel beads. Homogenized tissue was kept on ice for 1 hour, centrifuged cold at full speed for 10 minutes. Supernatant was aliquoted in 100 µl portions, snap-frozen and stored at -80˚C.

Table 1 – Clinical information

Type	Number	Name	Age	Gender	PMD	CAG 1	CAG 2	Grade
HD	n.a.	HC107	75	M	3	43	19	3
Control	C1	H110	83	F	14	N.A.	N.A.	n.a.
Control	C2	H202	83	M	14	N.A.	N.A.	n.a.
Control	C3	H157	66	M	15	N.A.	N.A.	n.a.
Control	C4	H155	61	M	7	N.A.	N.A.	n.a.
Control	C5	H146	61	M	15	N.A.	N.A.	n.a.
Control	C6	H159	53	M	16.5	N.A.	N.A.	n.a.
Control	C7	H174	59	M	24.5	N.A.	N.A.	n.a.
Control	C8	H130	32	M	13	N.A.	N.A.	n.a.
Control	C9	H200	56	M	23	N.A.	N.A.	n.a.
HD	HD1	HC111	91	F	18	40	15	2
HD	HD2	HC137	83	M	13	41	17	1
HD	HD3	HC133	65	M	14	43	17	3
HD	HD4	HC134	62	M	9	43	18	2
HD	HD5	HC113	58	M	14	44	28	2
HD	HD6	HC120	51	M	15	46	10	2
HD	HD7	HC115	56	M	16	46	16	2
HD	HD8	HC132	32	M	14	47	17	1
HD	HD9	HC119	51	M	15.5	48	17	3

Age: Age in years at death. F: female, M: male. PMD: post mortem delay in hours. CAG1 = CAG repeat length of mutant allele, CAG2 = CAG repeat length of normal allele. N.A. Not assessed. n.a. Not applicable. HD grade according to [28]. Average age for control subjects = 61.6 ± 15.5 years, HD subjects = 61.0 ± 17.6 years. Average PMD for control subjects = 15.8 ± 5.3 hours, HD subjects = 14.3 ± 2.5 hours. Average CAG repeat length in HD subjects = 44.2 ± 2.7 CAGs (mutant allele), 17.2 ± 4.7 CAGs (normal allele).

Western Blotting.

100 µg of human brain lysate was used per sample. To detect full length htt, proteins were separated by SDS-PAGE according to the "shorter CAG repeats" protocol [29]. Proteins were transferred to a nitrocellulose membrane (Trans-Blot Turbo Transfer Pack Midi #170-4158, Bio-Rad, Hercules CA, USA) using the Trans-blot Turbo Transfer system (BioRad) with settings 2.5 A for 10 minutes. Blots were blocked with TBS containing 5% (w/v) non-fat milk (Nutricia, Schiphol, The Netherlands), and incubated with primary antibody 3702-1 (Epitomics, Burlinggame CA, USA) that binds the htt N17 terminus [30]. Secondary antibody goat anti rabbit IRDye800 (LI-COR, Lincoln, USA) diluted 1:5000 in TBS containing 5% non-fat milk (w/v). Blots were analyzed with the Odyssey infrared imaging system and Odyssey software version 3.0 (LI-COR). To detect htt fragments, proteins were separated by SDS-PAGE by running at 40 mA constant through the stacking gel and at 50 mA constant through the 10% separating gel alongside a protein size marker (PageRuler, Thermo Fisher, St Leon-Rot, Germany). Proteins were blotted onto either a nitrocellulose membrane for Control versus HD subjects (Trans-Blot Turbo Transfer Pack Midi #170-4158, Bio-Rad, Hercules CA, USA), or a PVDF-membrane for post mortem delay samples (Trans-Blot Turbo Transfer Pack Midi #170-4157), using the Trans-Blot Turbo Transfer System (Bio-Rad) with settings 1.0 A for 30 minutes. Blots were blocked with TBS containing 5% non-fat milk (Nutricia). For nitrocellulose-blots, primary incubation was performed with antibodies 3702-1 (Epitomics) and mouse anti β-actin. Secondary incubation

was performed with goat anti rabbit IRDye800 (LI-COR) and goat anti mouse IRDye680 (LI-COR). All antibodies were diluted 1:5000 in TBS containing 5% non-fat milk (Nutricia). Blots were analysed with the Odyssey reader and viewed using the Odyssey software version 3.0 (LI-COR) with the linear manual sensitivity set at 5, or 6 if blot was viewed at “high sensitivity”. For PVDF-blots, primary incubation was performed with antibody 3702-1 (Epitomics) diluted 1:1000. Secondary incubation was performed with a Goat anti Rabbit antibody conjugated with Horse Radish Peroxidase (Santa Cruz) diluted 1:10.000. Blots were visualized using ECL+ substrate (#32132, ThermoFisher Scientific), and Hyperfilm ECL (#28906837, GE healthcare). For the β-actin loading control, blots were stripped, re-blocked and incubated with mouse β-actin diluted 1:1000, followed by a Goat anti Mouse antibody conjugated with Horse Radish Peroxidase (Santa Cruz) diluted 1:10.000. Densitometric analysis was performed with image J. Intensities of relevant bands were reported as percentages of the total htt signal within the associated lane. Statistical significance (n=4) between timepoints was calculated in Excel using a paired T-test (two sided).

Results

Two wild-type N-terminal htt fragments increase with artificial PMD in control temporal lobe tissue.

To assess the effect of PMD on N-terminal htt fragments, we obtained human control temporal lobe tissue one hour post-surgery. One half was stored at -80ºC and the other half was sampled at regular time-intervals to mimic PMD (artificial PMD). Western blot analysis with an antibody that binds huntingtin at the N-terminal end showed no change in the full length htt signal, and a subtle gradual increase in band intensity compared with T=0 was observed for N-terminal htt fragments of 50 kDa (1,49% ± 1,12% on average), and 65 kDa (4,01% ± 1,53 on average) over an eight-hour time period **(Figs 1a and 1c)**. The increase became significant for the 65 kDa band at T=4. Next, we performed the same experiment using the frozen half of the temporal lobe. Here, we detected N-terminal fragments of the same molecular weight compared with the non-frozen tissue, but western blot bands corresponding to full-length and N-terminal htt fragments of more than 100 kDa became weaker with increasing artificial PMD **(Fig 1b)**. The relative intensities of the 50kDa and 65kDa bands at T=0hr from the frozen sample were higher compared to the non-frozen tissue at T=0hr. This difference was 2,06% ±1,38% (p=0.06) for the 50kDa band, and for the 65 kDa band the difference was 4,63% ± 1,88% ($p < 0.05$). Furthermore, we observed an increase in band intensity in the frozen sample after an artificial PMD of 8 hours for N-terminal htt fragments of 50 kDa (10,53% ±5,16%) and 65 kDa (13,33% ±2,04%) (**Fig 1d**) compared with T=0, that was already significant after 2 hours. This is in contrast to the subtle gradual increase observed in the non-frozen tissue. We did not detect additional N-terminal htt fragments that were introduced by the freeze-thaw cycle. This indicates that freezing of brain tissue affects htt signal strength, but not the profile of htt protein fragments in control brain tissue samples.

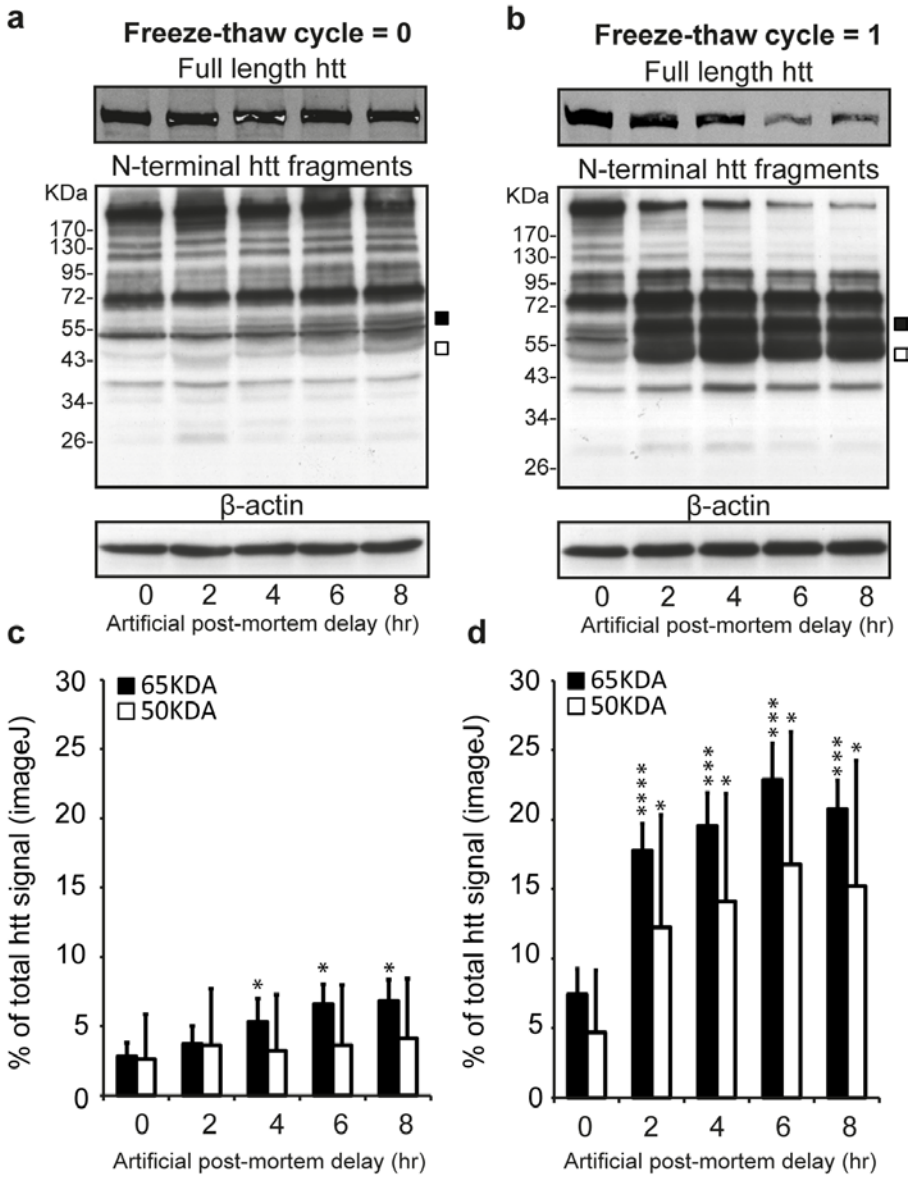

Fig 1. N-terminal huntingtin fragments in control temporal lobe tissue. Western blot analysis of temporal lobe tissue samples from tissue with no **(a)** and one freeze-thaw cycle **(b)** before sampling. Upper blot: full length htt. Middle and lower blot: N-terminal htt fragments with β-actin loading control. Squares: position of bands that increase with increasing artificial PMD (black = 65kDa, white = 50kDa). kDa = Molecular weight in kilodaltons, Artificial post mortem delay in hours (hr). **(c)** Image J quantification of PMD-related htt bands at indicated timepoints relative to total htt (0 freeze-thaw cycli). **(d)** Image J quantification of PMD-related htt bands at indicated timepoints relative to total htt (1 freeze-thaw cyclus). Columns represent the average of four independent western blots. Black columns: 65 kDa, White columns: 50 kDa. Error bars indicate standard deviation. * = P<0.05, *** = P<0.001, **** = P<0.0001.

Artificial PMD introduces N-terminal htt fragments in HD striatal tissue.

Using tissue from an HD subject with an initial PMD of 3 hours, we analyzed the effect of an increasing artificial PMD in human HD striatal tissue. Western blot analysis of full length htt showed two bands corresponding to wild-type and mutant huntingtin which is in agreement with findings in human HD fibroblast lysates [29]. Artificial PMD decreased band intensities of full-length htt and most N-terminal htt fragments in HD striatal tissue. However, we observed a band at 43 kDa that appeared after an artificial PMD of 24hr **(Fig 2a)**. Additionally, we were able to detect a band corresponding to a small N-terminal htt fragment (<26 kDa) that increased after 24hr, but this low molecular weight band could not reliably be quantified. ImageJ analysis of the 43 kDa band (**Fig 2b**) revealed a significant increase of 11,61% ±3,88% at T=30hr compared with T=24hr.

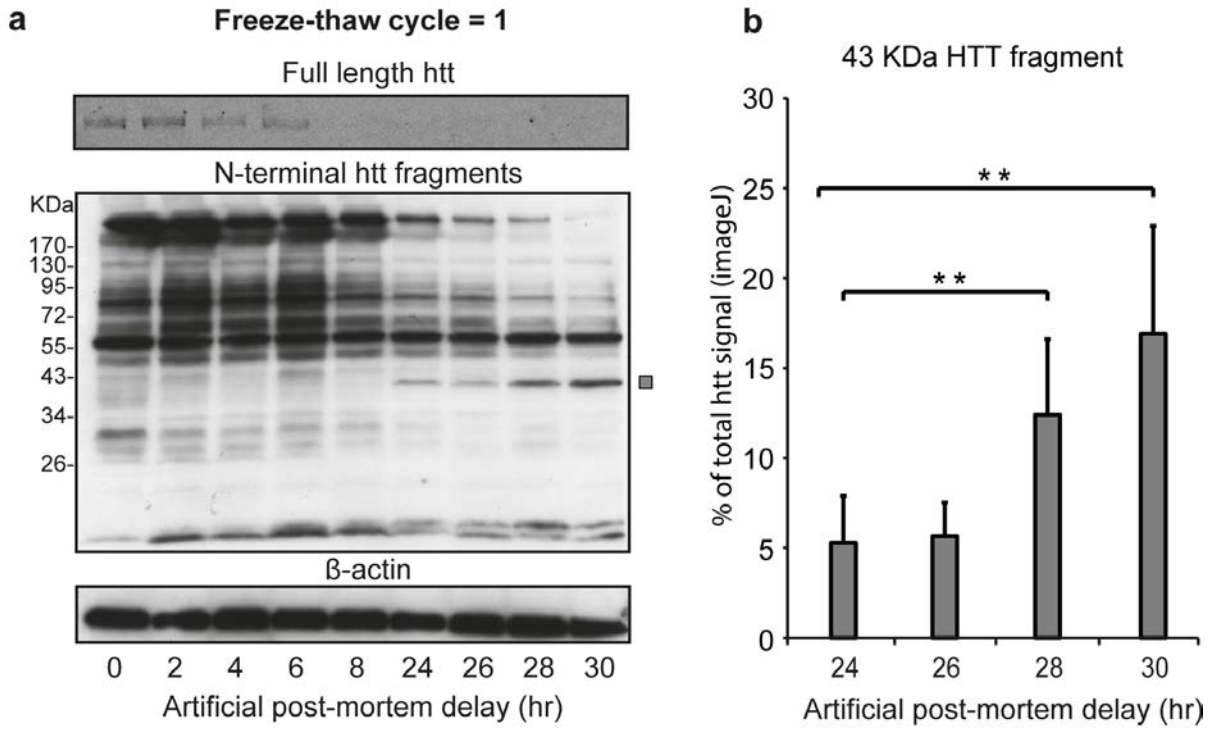

Fig 2. Effect of artificial post mortem delay on N-terminal huntingtin fragments in post mortem HD striatal tissue. (a) Western blot analysis of HD striatal tissue (1 freeze-thaw cyclus). Upper blot: full length htt. Middle and lower blot: N-terminal htt fragments with β-actin loading control. Gray square: Band increased with increasing artificial PMD. kDa = Molecular weight in kilodaltons, Artificial post mortem delay in hours (hr). **(b)** Image J quantification of the 43kDa band at indicated timepoints relative to total htt. Gray columns represent the average of four independent western blots. Error bars indicate standard deviation. **=P<0.01.

Huntington disease subjects show greater variation in full-length and N-terminal huntingtin protein fragment profiles.

Having identified N-terminal htt fragments that can be attributed to longer PMDs, we next analyzed N-terminal htt fragments in post mortem tissue in nine control subjects (mean age = 61.6 ± 15.5 years, mean PMD = 15.8 ± 5.3 hours) and nine HD subjects (mean age = 61.0 ± 17.6 years, mean age = 14.3 ± 2.5 hours). For further clinical information see **Table 1**. We observed that the western blot signal for full-length htt and N-terminal htt fragments was stronger in control subjects compared to HD subjects, and overall stronger in cortical tissue compared to striatal tissue, while no differences in the β-actin loading controls were observed **(S1 Fig)**. Therefore, for optimal comparison, western blot results for the HD subjects in Figures 3 and 4 are shown with the odyssey software configured at a higher viewing-sensitivity. In control cortical tissue, results were similar for subjects C2-C9 showing a consistent banding pattern with subtle interpersonal differences. The band-pattern for subject C1 was very different, showing relatively more N-terminal htt fragments below 55 kDa **(Fig 3a)**. In HD cortical tissue **(Fig 3b**), interpersonal variation was more prominent and subjects HD1, HD4 and HD5 showed a weaker N-terminal htt profile. Smaller N-terminal htt fragments below 55 kDa appeared more pronounced with respect to the total htt signal in HD cortical tissue compared with control cortical tissue **(S1 Fig)**. For both control and HD cortical subjects, western blot bands for N-terminal htt fragments were most prominent between 43 kDa and 95 kDa. This was in concordance with the N-terminal htt fragment profile induced by the artificial PMD of > 2 hours in temporal lobe tissue stored at -80°C **(Fig 1b)**. N-terminal htt fragments of 65kDa and 50kDa that were associated with PMD in temporal lobe tissue were detected in both control and HD cortical tissue. However, we did not observe a correlation with the PMD's of the different subjects.

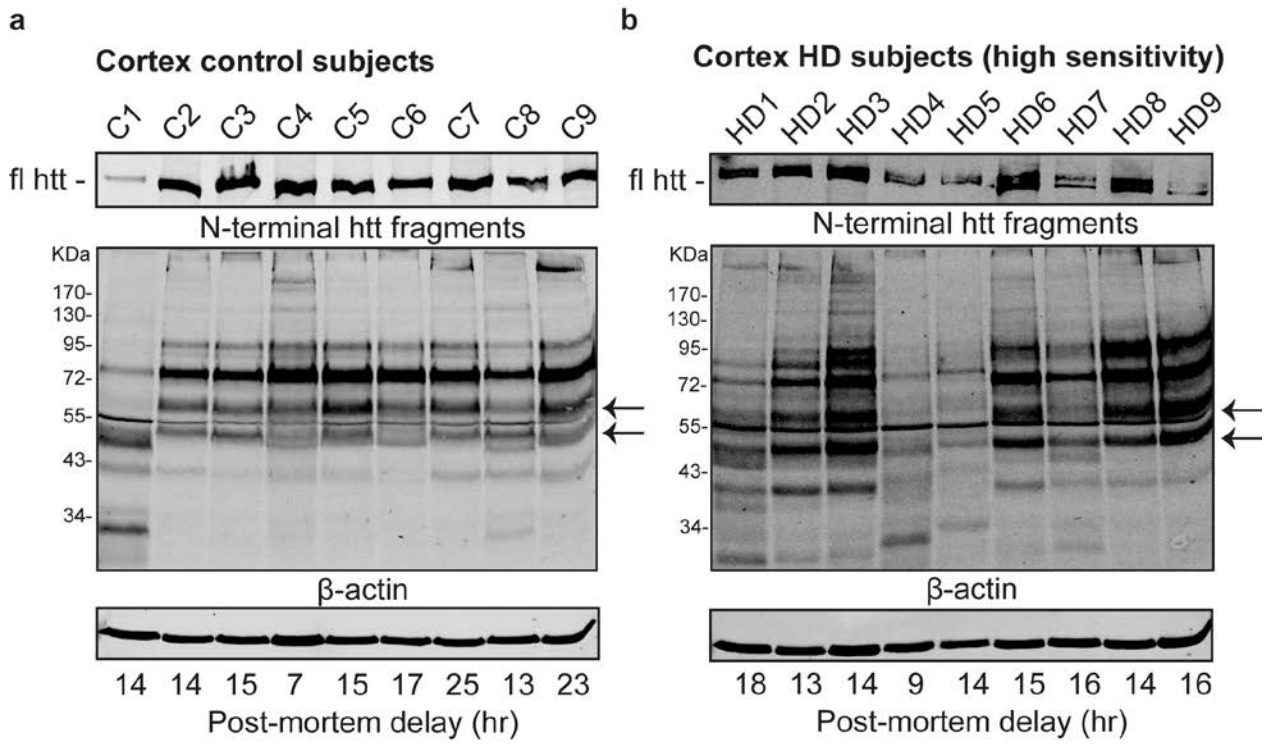

Fig 3. Comparison of N-terminal huntingtin fragments in post mortem control and HD cortex. Western blot analysis of **(a)** Control subjects, **(b)** HD subjects. Control and HD subjects were age, gender and post mortem delay matched. Upper blot: full length htt (fl htt). Middle and lower blot: N-terminal htt fragments with β-actin loading control. Arrows: position of bands associated with a post mortem delay related increase in intensity in non-HD temporal lobe tissue. kDa = Molecular weight in kilodaltons, Post mortem delay in hours (hr). High sensitivity: Blot analyzed at a higher viewing-sensitivity.

Next, we performed western blot on post mortem striatal tissue from the same control and HD subjects **(Fig 4)**. Between control subjects **(Fig 4a)** the N-terminal htt fragment profile was similar, but we observed some interpersonal variation in signal intensity. The overall htt western blot signal in striatum was weak for all HD subjects **(Figs 4b and S1)**. Between HD subjects the N-terminal htt fragment profile was similar with small interpersonal variation. Comparison between control and HD subjects for striatum revealed that the most prominent N-terminal htt fragment was detected at 80kDa in most control subjects, while in most HD subjects (HD1-HD6) the most prominent N-terminal htt fragment was detected at 55kDa. In subjects HD8-HD9, both 80kDa and 55kDa N-terminal htt fragments were detected equally. For control subjects, N-terminal htt fragments of similar sizes can be observed in both cortical and striatal tissue **(Figs 3a and 4a)**. On the other hand, in HD subjects the 55kDa N-terminal fragment is less prominent in cortical tissue compared with striatum **(Figs 3b and 4b).**

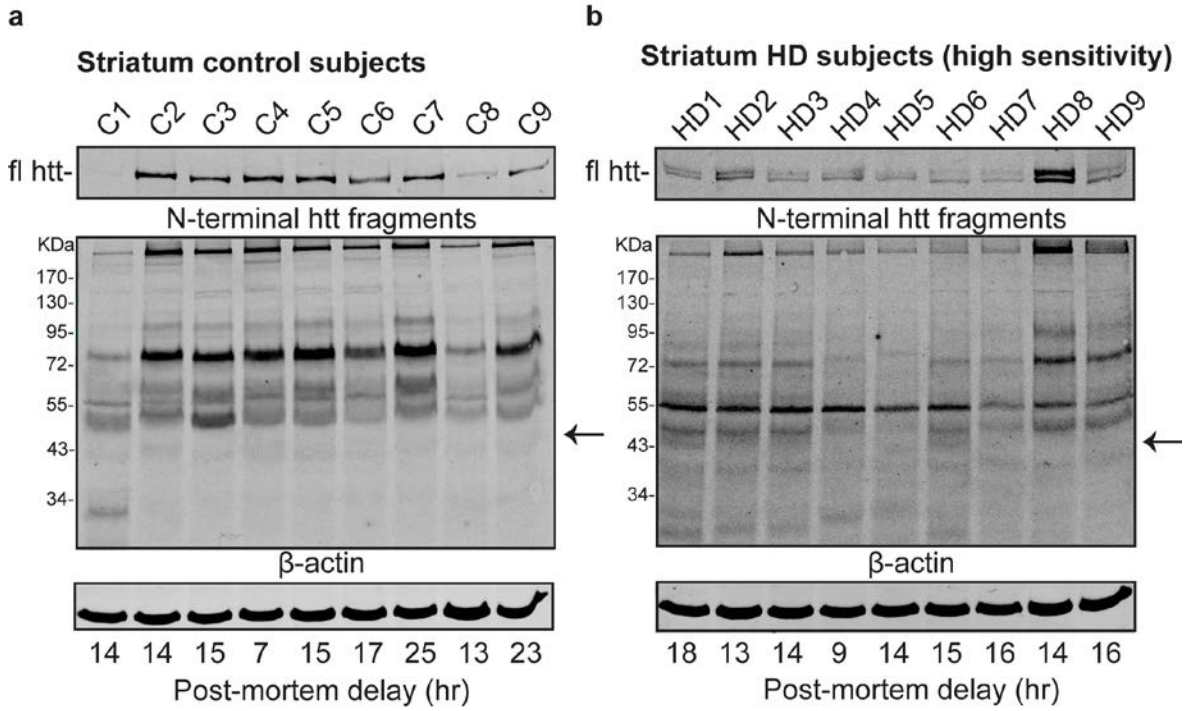

Fig 4. Comparison of N-terminal huntingtin fragments in post mortem control and HD striatum Western blot analysis of **(a)** Control subjects, **(b)** HD subjects. Control and HD subjects were age, sex and post mortem delay matched. Upper blot: full length huntingtin (fl htt). Middle and lower blot: N-terminal htt fragments with β-actin loading control. Arrow: position of bands associated with a post mortem delay related increase in intensity in HD striatal tissue. kDa = Molecular weight in kilodaltons, Post mortem delay in hours (hr). High sensitivity: Blot analyzed at a higher viewing sensitivity.

Discussion

In the current study we have examined PMD effects on N-terminal htt protein fragments in human brain tissue using western blot analysis on temporal lobe tissue obtained directly post-surgery from a control human subject. Our results show that increasing PMD resulted in a gradual increase of N-terminal htt fragment bands between 50 kDa-and 65 kDa on western blot. Other studies detected a similar N-terminal htt fragment of 50 kDa in post mortem human cortical brain tissue obtained from control subjects with a PMD of 9 to 16 hour [16, 18]. Within the context of our study, this 50kDa N-terminal htt fragment could be associated with PMD. However, other N-terminal htt fragments detected in [16, 18], and the caspase-3 related N-terminal htt fragment [11] detected in the cortex of human control subjects were not associated with PMD in our study. Our results further indicate that the effect of one freeze-thaw cycle on N-terminal htt fragments is quantitative, but not qualitative. We observed that one freeze-thaw cycle reduced the htt signal, especially for larger (>95 kDa) htt fragments and the full-length protein. Furthermore, PMD-related N-terminal htt fragments at 50kDa and 65kDa appeared at earlier time points for tissue that underwent one freeze-thaw cycle, suggesting their formation is enhanced due to freeze-thawing. However, no additional N-terminal htt fragments were observed due to freeze-thaw effects. Hence, the common practice of tissue storage at -80ºC and subsequent re-thawing for use is not expected to greatly influence study results on N-terminal htt fragments. This is an important finding because there is a well-established link between HD-pathology and small N-terminal htt fragments [7, 13]. Our experiments showed that artificial PMD gave rise to different N-terminal htt fragments in post mortem control temporal lobe tissue when compared with post mortem HD striatal tissue. This could suggest that PMD differently affects HD and control brains or different brain regions, but this difference might also be due to interpersonal differences between both subjects. The results on striatal tissue suggest that the 43 kDa band that is associated with PMD in HD striatum, appears between 8 and 24 hours. A striatal 43 kDa N-terminal fragment was reported before in HD striatum with PMD's of 9 to 16 hours [16]. In our cortical control and HD subjects, we observed inter individual differences in N-terminal htt fragments, especially for HD subjects. However, we did not observe a correlation between N-terminal htt bands and the PMD's of individual subjects. It is likely that the observed inter individual differences between subjects are mainly caused by other factors such as genetic or environmental factors. We did not observe different N-terminal htt fragment profiles between control and HD cortical tissue, which is in accordance with previous studies [16, 18]. However compared with these studies, we detected more larger N-terminal htt fragments. Possibly, this is due to the use of different subject-cohorts or western blotting protocols. In our striatal samples, the molecular weight of the most prominent N-terminal htt fragment differed between HD and controls. This suggests a difference in htt proteolytic cleavage in striatum between controls and HD. This is in agreement with [16] although Mende-Mueller et al reported N-terminal htt fragments of smaller sizes. We were probably not able to show these smaller N-terminal htt fragments due to the weak htt western blot signal obtained for HD striatal tissue. El-Daher et al, whom utilized the 4C8 antibody also observed weaker htt signals for HD striatum compared with controls [31]. On the other hand, studies using an anti N17 antibody did not observe a

difference in htt signal between control and HD striatum. [16, 18]. Hence, the observed difference in htt western blot signal between control and HD and cortex versus striatum could be due to variability between different human post mortem brain tissue specimens.

Conclusion

By mimicking PMD and a freeze-thaw cycle separately, we were able to provide an overview of expected effects on N-terminal htt fragments in post mortem human brain tissue. According to our results, PMD has a mild qualitative influence on N-terminal htt fragments because it introduces new fragments. A freeze-thaw cycle has a quantitative effect as it affects huntingtin signal strength. Hence, our study contributes to the correct interpretation of data on N-terminal htt fragments obtained from human post mortem brain tissue. Furthermore, our results show that subject to subject variation has a larger, both qualitative and quantitative effect on N-terminal htt fragments. Hence, our study underscores the need for larger subject cohorts in studies involving post mortem human brain tissue.

Acknowledgements

We would like to thank the Auckland City Hospital Neurosurgery department and the anonymous patient who were so kind to provide us with the post-surgery temporal lobe tissue. We also would like to thank the Neurological Foundation of New Zealand Human Brain Bank and all families involved for the post mortem human brain tissue. We thank Marika Eszes for technical assistance.

References

1. *A novel gene containing a trinucleotide repeat that is expanded and unstable on Huntington's disease chromosomes. The Huntington's Disease Collaborative Research Group*. Cell, 1993. **72**(6): p. 971-83.
2. Aronin, N., et al., *CAG expansion affects the expression of mutant Huntingtin in the Huntington's disease brain.* Neuron, 1995. **15**(5): p. 1193-201.
3. Duyao, M.P., et al., *Inactivation of the mouse Huntington's disease gene homolog Hdh.* Science, 1995. **269**(5222): p. 407-10.
4. Mangiarini, L., et al., *Exon 1 of the HD gene with an expanded CAG repeat is sufficient to cause a progressive neurological phenotype in transgenic mice.* Cell, 1996. **87**(3): p. 493-506.
5. Slow, E.J., et al., *Selective striatal neuronal loss in a YAC128 mouse model of Huntington disease.* Hum Mol Genet, 2003. **12**(13): p. 1555-67.
6. Woodman, B., et al., *The Hdh(Q150/Q150) knock-in mouse model of HD and the R6/2 exon 1 model develop comparable and widespread molecular phenotypes.* Brain Res Bull, 2007. **72**(2-3): p. 83-97.
7. O'Brien, R., et al., *Integration-independent Transgenic Huntington Disease Fragment Mouse Models Reveal Distinct Phenotypes and Life Span in Vivo.* J Biol Chem, 2015. **290**(31): p. 19287-306.
8. Waldron-Roby, E., et al., *Transgenic mouse model expressing the caspase 6 fragment of mutant huntingtin.* J Neurosci, 2012. **32**(1): p. 183-93.
9. Gafni, J., et al., *Inhibition of calpain cleavage of huntingtin reduces toxicity: accumulation of calpain/caspase fragments in the nucleus.* J Biol Chem, 2004. **279**(19): p. 20211-20.
10. Lunkes, A., et al., *Proteases acting on mutant huntingtin generate cleaved products that differentially build up cytoplasmic and nuclear inclusions.* Mol Cell, 2002. **10**(2): p. 259-69.
11. Wellington, C.L., et al., *Caspase cleavage of mutant huntingtin precedes neurodegeneration in Huntington's disease.* J Neurosci, 2002. **22**(18): p. 7862-72.
12. Wellington, C.L., et al., *Inhibiting caspase cleavage of huntingtin reduces toxicity and aggregate formation in neuronal and nonneuronal cells.* J Biol Chem, 2000. **275**(26): p. 19831-8.
13. Graham, R.K., et al., *Cleavage at the caspase-6 site is required for neuronal dysfunction and degeneration due to mutant huntingtin.* Cell, 2006. **125**(6): p. 1179-91.
14. Sorimachi, Y., K. Harada, and K. Yoshida, *Involvement of calpain in postmortem proteolysis in the rat brain.* Forensic Sci Int, 1996. **81**(2-3): p. 165-74.
15. Goni-Oliver, P., J. Avila, and F. Hernandez, *Calpain-mediated truncation of GSK-3 in post-mortem brain samples.* J Neurosci Res, 2009. **87**(5): p. 1156-61.
16. Mende-Mueller, L.M., et al., *Tissue-specific proteolysis of Huntingtin (htt) in human brain: evidence of enhanced levels of N- and C-terminal htt fragments in Huntington's disease striatum.* J Neurosci, 2001. **21**(6): p. 1830-7.
17. Evers, M.M., et al., *Preventing formation of toxic N-terminal huntingtin fragments through antisense oligonucleotide-mediated protein modification.* Nucleic Acid Ther, 2014. **24**(1): p. 4-12.
18. Toneff, T., et al., *Comparison of huntingtin proteolytic fragments in human lymphoblast cell lines and human brain.* J Neurochem, 2002. **82**(1): p. 84-92.

19. Ferrer, I., et al., *Brain banks: benefits, limitations and cautions concerning the use of post-mortem brain tissue for molecular studies.* Cell Tissue Bank, 2008. **9**(3): p. 181-94.
20. Petit, T.L. and J.C. LeBoutillier, *Quantifying synaptic number and structure: effects of stain and post-mortem delay.* Brain Res, 1990. **517**(1-2): p. 269-75.
21. Ross, B., et al., *Effects of post-mortem delay on high affinity forskolin binding sites and adenylate cyclase activity in rat and human striatum and cerebral cortex.* Brain Res, 1993. **629**(2): p. 225-30.
22. Fraser, T., H. Tayler, and S. Love, *Low-temperature improved-throughput method for analysis of brain fatty acids and assessment of their post-mortem stability.* J Neurosci Methods, 2008. **169**(1): p. 135-40.
23. Hilbig, H., et al., *Influence of post-mortem delay and storage temperature on the immunohistochemical detection of antigens in the CNS of mice.* Exp Toxicol Pathol, 2004. **56**(3): p. 159-71.
24. Siew, L.K., et al., *Measurement of pre- and post-synaptic proteins in cerebral cortex: effects of post-mortem delay.* J Neurosci Methods, 2004. **139**(2): p. 153-9.
25. Barrachina, M., et al., *Histone tail acetylation in brain occurs in an unpredictable fashion after death.* Cell Tissue Bank, 2012. **13**(4): p. 597-606.
26. Blair, J.A., et al., *Individual Case Analysis of Postmortem Interval Time on Brain Tissue Preservation.* PLoS One, 2016. **11**(3): p. e0151615.
27. Waldvogel, H.J., et al., *The collection and processing of human brain tissue for research.* Cell Tissue Bank, 2008. **9**(3): p. 169-79.
28. Vonsattel, J.P., et al., *Neuropathological classification of Huntington's disease.* J Neuropathol Exp Neurol, 1985. **44**(6): p. 559-77.
29. Hu, J., et al., *Allele-specific silencing of mutant huntingtin and ataxin-3 genes by targeting expanded CAG repeats in mRNAs.* Nat Biotechnol, 2009. **27**(5): p. 478-84.
30. Schut, M.H., et al., *Selection and characterization of llama single domain antibodies against N-terminal huntingtin.* Neurol Sci, 2015. **36**(3): p. 429-34.
31. El-Daher, M.T., et al., *Huntingtin proteolysis releases non-polyQ fragments that cause toxicity through dynamin 1 dysregulation.* EMBO J, 2015. **34**(17): p. 2255-71.

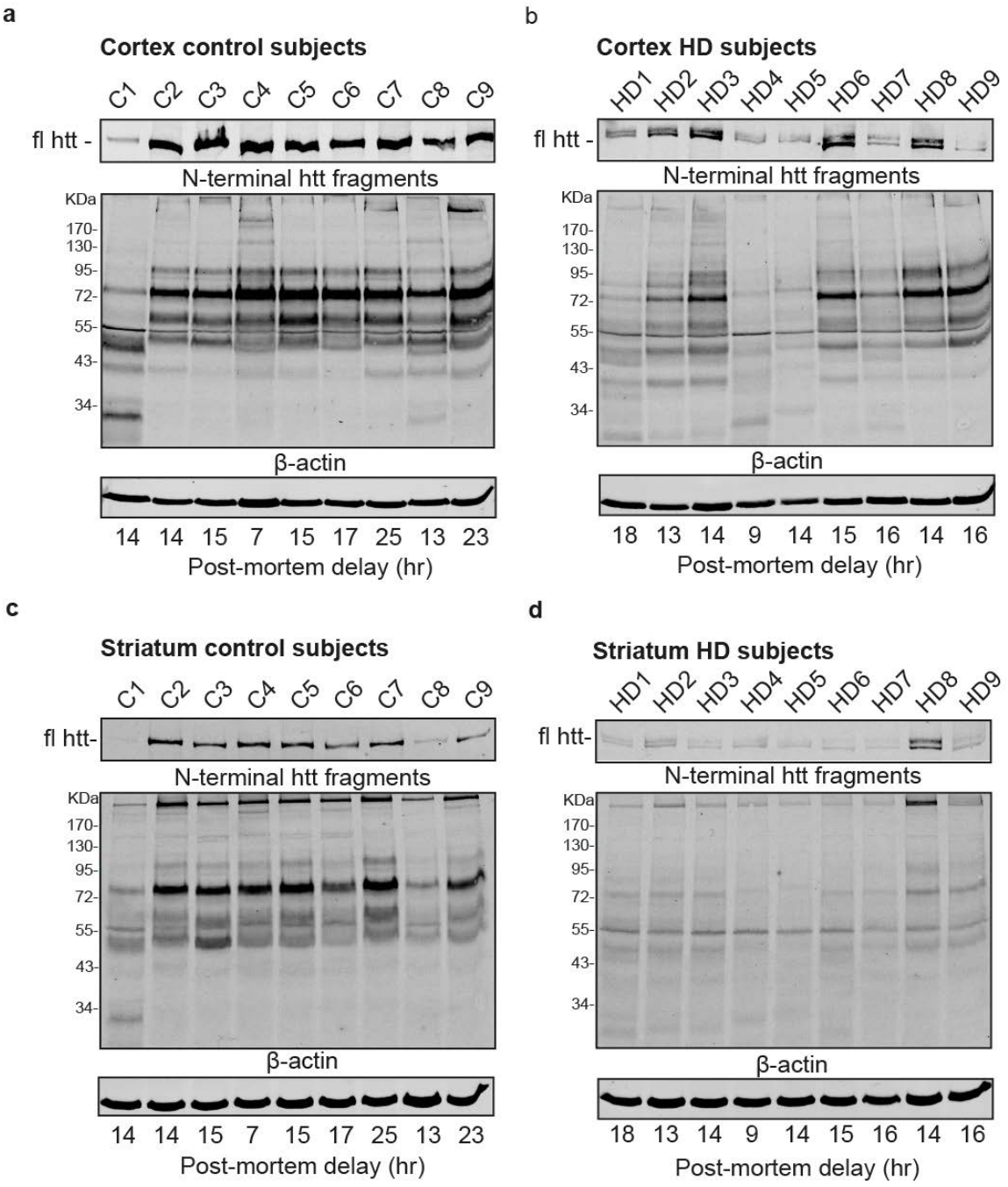

S1 Fig– Levels of N-terminal huntingtin fragments in cortical and striatal tissue.

All western blots shown at the same sensitivity. **(a)** Control subjects, Cortical region. **(b)** HD subjects, Cortical region. **(c)** Control subjects, Striatal region. **(d)** HD subjects, Striatal region. Control and HD subjects are age, sex and PMD matched. Upper blot :full length htt (fl htt). Middle blot: N-terminal htt fragments. Lower blot: β-actin. Post mortem delay in hours (hr).

Chapter 5

Huntingtin aggregation in adult onset and juvenile HD.

M.H. Schut[1], I. Hegeman[2], M. Eszes[3], R.L.M. Faull[3], G.J.B. van Ommen[1], and W.M.C. van Roon-Mom[1]

1 Department of Human Genetics, Leiden University Medical Center, Leiden, The Netherlands

2 Department of Pathology, Leiden University Medical Center, Leiden, The Netherlands

3 Centre for Brain Research and Department of Anatomy with Radiology, University of Auckland, Auckland, New Zealand

Partly published in GLIA (2017)

Abstract

The presence of protein aggregates within the brain is a key hallmark of Huntington disease. To better understand regional differences in HD pathology and the link with htt aggregation, it is important to quantify htt aggregates in different brain regions. In this small-scale pilot study we have assessed the correlation between the presence of insoluble htt protein as determined by the filter-trap assay, and counted aggregates in brain tissue sections. Our results indicate that the filter-trap assay is a promising technique to quantify protein aggregates in *post-mortem* human brain tissue.

Introduction

Huntington disease (HD) is an autosomal dominant neurodegenerative disease [1] caused by elongation of an exonic CAG-repeat within the *HTT* gene [2]. This mutation results in a mutant huntingtin protein (mutHtt) with an expanded polyglutamine repeat (polyQ) [3] that is prone to aggregation [4]. The presence of mutHtt protein aggregates is a key hallmark of HD [2, 5]. However, the link between mutHtt aggregates and HD pathology is elusive. A pathological role of mutHtt aggregates in HD has been suggested in some studies [6, 7]. However other studies suggests that mutHtt aggregate formation is beneficial for cells [8, 9], which indicates that soluble mutHtt is more toxic. The quantification of mutHtt aggregates in HD brain tissue should aid to further elucidate their role in HD pathogenesis. Quantification of protein aggregates can be performed by counting aggregates in tissue sections using a microscope, which is a cumbersome procedure. The filter-trap assay is a simple assay used to objectively quantify mutHtt aggregates [10] and has been used with PC12 cell lysates [11], and brain homogenates of R6/2 mice [12]. In this pilot study, we have used the filter-trap assay to quantify mutHtt aggregation in *post-mortem* human brain tissue. Our results indicate that there could be a correlation between the filter-trap assay and the number of aggregates as counted in tissue-sections. Furthermore, we found more mutHtt aggregates in cortical tissue compared with striatal tissue in one juvenile Huntington disease case which is in concordance with the immunohistochemistry results from [8]. Our results suggest that the filter-trap assay can be used to quantify mutHtt aggregates in *post-mortem* human brain tissue.

Materials and Methods

Post-mortem human brain tissue lysates.

Post-mortem human cortical and striatal brain tissue from control and HD subjects was obtained from the Neurological Foundation of New Zealand Human Brain Bank, Centre for Brain Research, University of Auckland and the department of pathology, Leiden University Medical Centre. Tissue was obtained with the approval of the institutes ethics committee and informed consent. Clinical information in **table 1**.

Table 1. Clinical information of subjects

Type	Subject	Grade	Gender	PMD	CAG	Age	A.o.O.
Control	H121	n.a.	F	6	18 : 23	64	n.a.
HD	HC105	1	F	9	15 : 42	67	47
HD	HD166	2	M	32	17 : 42	80	>70
HD	HD193	3	M	18	9 : 44	68	44
HD	HC90	3	M	NA	23 : 41	61	51
HD	HC140	3	M	22	17 : 40	62	44
HD	HC125	3	F	13	17 : 43	67	45
HD	HC139	3	F	5	14 : 41	67	15
jHD	HC104	3	M	15	18 : 53	40	15
jHD	HD29	NA	F	11	20 : 84	11	8
jHD	HD86	3	F	20	17 : 84	20	16
jHD	HD192	NA	M	NA	17 : 51	37	NA
jHD	HD208	NA	M	NA	15 : 68	37	~ 23

HD = Huntington disease, jHD = Juvenile Huntington disease, F=Female, M=Male, PMD = Post-mortem delay, A.o.O. = Age of onset, n.a. = not applicable. NA = not assessed.HD = subject with a mutant CAG repeat between 35 and 50. jHD = subject with a mutant CAG repeat of 50 or more.

Immunohistochemistry

Slide preparation: Tissue sections (thickness 8µm) were formalin fixed and embedded in paraffin. After paraffin removal, tissue sections were rehydrated and washed with PBS + Triton X-100. Sections were incubated in 50% methanol. Primary antibody (rabbit anti huntingtin): 3702-1 (Epitomics, Burlinggame CA, USA), or mouse anti htt EM48 (Millipore, Billerica MA, USA). Primary antibodies were diluted 1:500. Negative control: sections not incubated with a primary antibody. Secondary antibody: goat anti-rabbit or goat anti-mouse (Santa Cruz, Dallas TX, USA) diluted 1:1000. Streptavidin/DAB: Tissue sections were incubated with Streptavidin-HRP (diluted 1:2000 in 1% normal goat serum), followed by 10 minutes of incubation in DAB solution. Sections were Nissl-counterstained and examined for aggregates by microscope. Qualitative determination of aggregate abundance: Total number of aggregates for any combination of HD (adult-onset/juvenile), antibody (EM48/3702-1) and brain region (cortex/striatum) was subtracted by the number of aggregates counted in the corresponding negative control. The resulting number determines the qualitative abundance of aggregates where "+" = 1-5, "++" = 6-10, "+++" = 11-15, "++++" = > 15.

Preparation of insoluble protein fractions

Homogenization of human brain tissue sections: bullet blender (Next Advance, str 8, 3 min). Homogenization buffer: 150mM Sucrose, 15mM HEPES pH7.9, 60mM KCl, 0.5mM EDTA pH8 and 0.1mM EGTA pH8 (W/V ratio: 1:5). Added Triton X-100 (final concentration 1%). Stored on ice (1 hour). Preparation of pellet fraction: Homogenized tissue was centrifuged (14000rpm/10min) followed by 3x wash in wash-buffer (60mM Tris) subsequently followed by pellet-resuspension in 15% SDS and an o.n. incubation at 95ºC. The bicinchoninic (BCA) assay kit (Thermo Fisher Scientific,Waltham, USA) was used to determine protein concentration.

Filter-trap assay

Dot-blot: 100µg of pellet fraction in 300 µl of 15% SDS was applied onto a cellulose acetate membrane (Schleicher & Schuell,St Louis, USA, 0.2µm pore-size) with the Bio-Rad Bio-Dot apparatus (Bio-Rad, #1706545). Wash: 2x in 0.2% SDS. Fixation: 0.5% glutaraldehyde (20 min). Blocking of blot membranes was performed with 4% non-fat milk (Nutricia, Schiphol, The Netherlands) in TBST. Primary antibody (rabbit anti huntingtin): 3702-1, diluted 1:5000 (Epitomics). Secondary antibody: HRP conjugated goat anti rabbit, diluted 1:10000 (Santa Cruz). Visualization of results: ECL (#32106, ThermoFisher) and Hyperfilm ECL (#28906837, GE healthcare, Little Chalfond, United Kingdom). Quantification of signal intensity was performed with ImageJ-software. Results represent the average of three independent filter-trap assays.

Results

Immunohistochemistry reveals more huntingtin aggregates in juvenile HD compared with adult-onset HD tissue sections.

Immunohistochemistry was performed on four adult-onset HD subjects (HC90, HC125, HC139 and HC140, average age = 64.3y ±3.2y, average mutant CAG = 41.3 ± 1.3), and four juvenile HD subjects (HD86, HC104, HC192 and HD208, average age = 33.5y ±9.1y, average mutant CAG = 64.0 ± 15.3). In **Table 1**, a qualitative overview of the amount of aggregates in adult-onset HD or juvenile HD cases is shown. On average, htt aggregates were more abundant in the juvenile HD tissue sections.

Table 1 – Qualitative determination of aggregates in HD subjects

Adult-Onset HD	Cortex	Striatum	Juvenile HD	Cortex	Striatum
EM48	+	+	EM48	+++	+++
3702-1	+	+	3702-1	++++	+++

Immunohistochemistry was performed with either EM48 or 3702-1 as primary antibody.
Note: juvenile HD is defined here as any case with a CAG repeat of 50 or longer.

Insoluble huntingtin protein levels in Huntington disease subjects

For the filter-trap assay, we first used cortical brain tissue lysates from five HD subjects with increasing polyQ-repeats, and one non-HD subject as a negative control **(Figure 1)**. As expected, the negative control (H121) did not produce a significant signal indicating no insoluble huntingtin protein is present. Filter-trap analysis on the five HD subjects showed that the average signal-intensity per subject, as measured from three independent filter-trap assays, showed increased intensity of the filter trap assay dots with larger polyQ-repeats **(Figure 1)**. This was in agreement with the qualitative determination of aggregates in HD subjects shown in **table 1**.

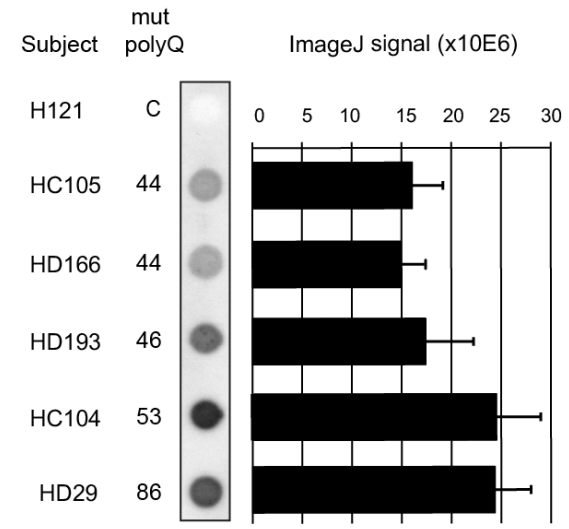

Figure 1 - Insoluble htt proteins in human adult-onset and juvenile HD brain tissue.

Left Filter-trap assay of SDS-insoluble htt protein in cortical human brain tissue of one control subject (H121), three adult-onset HD subjects (HC105, HD166, HD193) and two juvenile HD subjects (HC104, HD29). PolyQ-lengths shown next to dots. 100µg of protein was loaded per dot. Blots were probed with an anti htt antibody. Dot intensity indicates level of insoluble htt protein. *Right* Comparison of dot intensities per subject as determined with imageJ analysis. Black bars represent the average dot intensity from three independent dot blot assays. Standard deviation indicated by error bars.

Insoluble huntingtin protein in subject HD86 Cortex and Striatum

From one juvenile HD case we independently analyzed brain tissue lysates originating from the striatum and cortex using the filter-trap assay **(Figure 2)**. For this subject, our results clearly show a significant difference, with more insoluble huntingtin present in the cortical sample (**Figure 2**).

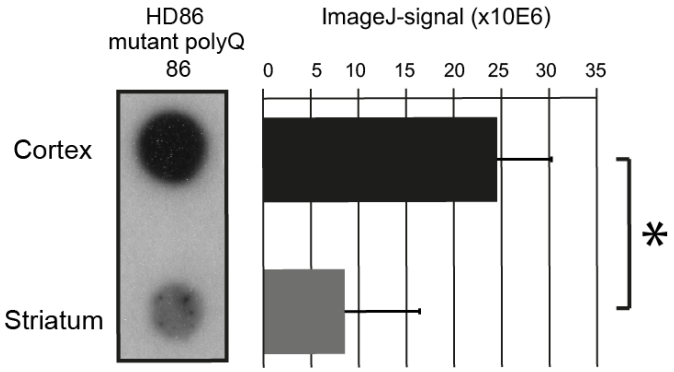

Figure 2 - Insoluble htt protein in cortex and striatum of juvenile HD subject HD86. *Left* Filter-trap assay of SDS-insoluble htt protein in cortical and striatal human brain tissue of one juvenile HD case. 100µg of protein was loaded per dot. Blots were probed with an anti htt antibody. Dot intensity indicates level of insoluble htt protein. *Right* Comparison of dot intensities per area as determined with imageJ analysis. Bars represent average dot intensity from three independent assays. Standard deviation indicated by error bars. * = P<0.05.

Discussion

The results of our pilot-study are encouraging for the use of the filter-trap assay in the quantification of protein aggregates in *post-mortem* human HD brain tissue. No discernible signal was obtained with the non-HD control subject which indicates that, despite the use of human brain material and the rigorous procedure to suspend the protein pellet, background is not an issue. We observed that the signal intensity for insoluble htt protein showed an increase with increasing polyQ repeats. One possible explanation is that increased polyQ repeats are more prone to aggregate formation [13]. The current study, does not elucidate whether the increased signal is due to more efficient aggregation of larger polyQ-repeats, or is merely mirroring differences in protein expression levels. In an earlier study, we have looked at soluble wild-type and mutant huntingtin protein levels in *post-mortem* human HD brain tissue [14]. Results from that study indicate that soluble mutant huntingtin protein levels were lower for juvenile HD cases. This suggests an inverse correlation between levels of aggregated and soluble mutant huntingtin, which is in accordance with results obtained by Baldo *et al* [12]. In addition, we demonstrated the filter-trap assay's ability to assess differences in the level of insoluble htt protein within different brain regions. The difference in insoluble huntingtin protein levels we found in our juvenile HD subject HD86 are in concordance with the results by Gutekunst *et al* [8] who found that huntingtin aggregation was predominantly present within the cortex. In conclusion, the data from this pilot-study provide a proof-of-principle of the filter trap assay to be used as a quantitative assay for determining the level of huntingtin protein aggregation in *post-mortem* human brain tissue.

References

1. Roos, R.A., *Huntington's disease: a clinical review.* Orphanet J Rare Dis, 2010. **5**: p. 40.
2. *A novel gene containing a trinucleotide repeat that is expanded and unstable on Huntington's disease chromosomes. The Huntington's Disease Collaborative Research Group.* Cell, 1993. **72**(6): p. 971-83.
3. Aronin, N., et al., *CAG expansion affects the expression of mutant Huntingtin in the Huntington's disease brain.* Neuron, 1995. **15**(5): p. 1193-201.
4. Legleiter, J., et al., *Mutant huntingtin fragments form oligomers in a polyglutamine length-dependent manner in vitro and in vivo.* J Biol Chem, 2010. **285**(19): p. 14777-90.
5. DiFiglia, M., et al., *Aggregation of huntingtin in neuronal intranuclear inclusions and dystrophic neurites in brain.* Science, 1997. **277**(5334): p. 1990-3.
6. Yang, W., et al., *Aggregated polyglutamine peptides delivered to nuclei are toxic to mammalian cells.* Hum Mol Genet, 2002. **11**(23): p. 2905-17.
7. Costanzo, M., et al., *Transfer of polyglutamine aggregates in neuronal cells occurs in tunneling nanotubes.* J Cell Sci, 2013. **126**(Pt 16): p. 3678-85.
8. Gutekunst, C.A., et al., *Nuclear and neuropil aggregates in Huntington's disease: relationship to neuropathology.* J Neurosci, 1999. **19**(7): p. 2522-34.

9. Arrasate, M., et al., *Inclusion body formation reduces levels of mutant huntingtin and the risk of neuronal death.* Nature, 2004. **431**(7010): p. 805-10.
10. Heiser, V., et al., *Identification of benzothiazoles as potential polyglutamine aggregation inhibitors of Huntington's disease by using an automated filter retardation assay.* Proc Natl Acad Sci U S A, 2002. **99 Suppl 4**: p. 16400-6.
11. Scotter, E.L., et al., *High throughput quantification of mutant huntingtin aggregates.* J Neurosci Methods, 2008. **171**(1): p. 174-9.
12. Baldo, B., et al., *TR-FRET-based duplex immunoassay reveals an inverse correlation of soluble and aggregated mutant huntingtin in huntington's disease.* Chem Biol, 2012. **19**(2): p. 264-75.
13. Li, S.H. and X.J. Li, *Aggregation of N-terminal huntingtin is dependent on the length of its glutamine repeats.* Hum Mol Genet, 1998. **7**(5): p. 777-82.
14. Evers, M.M., et al., *Making (anti-) sense out of huntingtin levels in Huntington disease.* Mol Neurodegener, 2015. **10**: p. 21.

Chapter 6

Making (anti-) sense out of huntingtin levels in Huntington disease

Melvin M Evers[1#], Menno H Schut[1#], Barry A Pepers[1], Melek Atalar[2], Martine J van Belzen[3], Richard LM Faull[4], Raymund AC Roos[5] and Willeke MC van Roon-Mom[1*]

1 Department of Human Genetics, Leiden University Medical Center, Albinusdreef 2, Leiden 2333ZA, the Netherlands.

2 Galapagos B.V., Leiden, the Netherlands.

3 Department of Clinical Genetics, Leiden University Medical Center, Leiden, the Netherlands.

4 Centre for Brain Research and Department of Anatomy with Radiology, University of Auckland, Auckland, New Zealand.

5 Department of Neurology, Leiden University Medical Center, Leiden, the Netherlands.

* Corresponding author: Willeke M.C. van Roon-Mom, Department of Human Genetics, Leiden University Medical Center, Albinusdreef 2, 2333ZA Leiden, The Netherlands. Tel: +31 71 5269435; Fax: +31 71 5268285; Email: w.vanroon@lumc.nl

# Both authors contributed equally

Molecular neurodegeneration (2015)

Evers et al. Molecular Neurodegeneration (2015) 10:21
DOI 10.1186/s13024-015-0018-7

MOLECULAR NEURODEGENERATION

RESEARCH ARTICLE Open Access

Making (anti-) sense out of huntingtin levels in Huntington disease

Melvin M Evers[1†], Menno H Schut[1†], Barry A Pepers[1], Melek Atalar[2], Martine J van Belzen[3], Richard LM Faull[4], Raymund AC Roos[5] and Willeke MC van Roon-Mom[1*]

Abstract

Background: Huntington disease (HD) is an autosomal dominant neurodegenerative disorder, characterized by motor, psychiatric and cognitive symptoms. HD is caused by a CAG repeat expansion in the first exon of the *HTT* gene, resulting in an expanded polyglutamine tract at the N-terminus of the huntingtin protein. Typical disease onset is around mid-life (adult-onset HD) whereas onset below 21 years is classified as juvenile HD. While much research has been done on the underlying HD disease mechanisms, little is known about regulation and expression levels of huntingtin RNA and protein.

Results: In this study we used 15 human post-mortem HD brain samples to investigate the expression of wild-type and mutant huntingtin mRNA and protein. In adult-onset HD brain samples, there was a small but significantly lower expression of mutant huntingtin mRNA compared to wild-type huntingtin mRNA, while wild-type and mutant huntingtin protein expression levels did not differ significantly. Juvenile HD subjects did show a lower expression of mutant huntingtin protein compared to wild-type huntingtin protein. Our results in HD brain and fibroblasts suggest that protein aggregation does not affect levels of huntingtin RNA and protein. Additionally, we did not find any evidence for a reduced expression of huntingtin antisense in fibroblasts derived from a homozygous HD patient.

Conclusions: We found small differences in allelic huntingtin mRNA levels in adult-onset HD brain, with significantly lower mutant huntingtin mRNA levels. Wild-type and mutant huntingtin protein were not significantly different in adult-onset HD brain samples. Conversely, in juvenile HD brain samples mutant huntingtin protein levels were lower compared with wild-type huntingtin, showing subtle differences between juvenile HD and adult-onset HD. Since most HD model systems harbor juvenile repeat expansions, our results suggest caution with the interpretation of huntingtin mRNA and protein studies using HD cell and animal models with such long repeats. Furthermore, our huntingtin antisense results in homozygous HD cells do not support reduced huntingtin antisense expression due to an expanded CAG repeat.

Keywords: Huntington disease, Huntingtin, Huntingtin antisense transcript, Post-mortem HD brain tissue, HD patient-derived fibroblasts, Juvenile HD

Background

Huntington disease (HD) is an autosomal dominant neurodegenerative disorder, characterized by motor, psychiatric and cognitive symptoms [1]. HD is caused by a CAG repeat expansion in the first exon of the *HTT* gene on chromosome 4p16, resulting in an expanded polyglutamine (polyQ) tract at the N-terminus of the huntingtin (htt) protein. People carrying 40 or more CAG repeats will develop HD, whereas people with 36 to 39 repeats show reduced penetrance [2,3]. The mean disease onset lies between 30 and 50 years of age (adult-onset HD). HD patients carrying more than 50 CAGs will have a disease onset typically below 21 years of age (juvenile HD) [1]. The major neuropathology in HD occurs in the striatum and cerebral cortex but degeneration is seen throughout the brain as the disease progresses [4] and insoluble protein aggregates in the nucleus and cytoplasm of cells are a hallmark of the disease [5].

* Correspondence: w.vanroon@lumc.nl
†Equal contributors
[1]Department of Human Genetics, Leiden University Medical Center, Albinusdreef 2, Leiden 2333ZA, the Netherlands
Full list of author information is available at the end of the article

Knowledge on regulation of HTT RNA and htt protein expression is limited and inconsistent. In patient-derived lymphoblasts, no CAG repeat-related effect on total HTT mRNA was observed [6], suggesting that there is no difference in wild-type and mutant HTT RNA expression. On the other hand, upregulation of mutant HTT mRNA translation in HD was suggested by interaction of the expanded CAG repeat with the MID1-PP2A complex [7]. Upregulation of mutant HTT mRNA translation was also suggested by HTT antisense transcript regulation [8]. Two natural HTT antisense transcripts (HTTAS) were identified at the *HTT* locus, of which one HTTAS contains a CTG repeat. Overexpression of HTTAS resulted in reduced HTT transcript levels, whereas knockdown increased HTT transcript levels [8]. Furthermore, in post-mortem HD brain no HTTAS with an expanded CTG repeat could be detected. From these observations, it was suggested that HTTAS negatively regulated HTT transcript expression and that loss of HTTAS in HD increases mutant HTT mRNA levels [8]. Upregulation of mutant HTT mRNA in human post-mortem HD brain tissue was confirmed recently using an allele-specific quantitative (q)PCR [9]. However, endogenous mRNA expression levels have not been related to subsequent mutant and wild-type htt protein levels. Also the effect of the presence of insoluble protein aggregates on htt protein levels is not known.

In this study we have examined HTT mRNA and htt protein levels in HD patient-derived fibroblasts and post-mortem brain tissue with varying CAG repeat lengths. We find a decrease in mutant HTT mRNA levels compared to wild-type in adult-onset HD patients. However, this reduced mutant HTT mRNA expression did not result in lower mutant htt protein levels. In contrast, juvenile HD fibroblasts and brain tissue did show lower levels of mutant htt protein compared to wild-type htt protein, indicating subtle differences in htt protein expression between adult-onset and juvenile HD.

Results

Validation of RT-PCR amplification across the CAG repeat

To reliably measure both wild-type and mutant HTT mRNA we first optimized our PCR procedure to account for differences in amplification across the CAG repeat expansion. To exclude amplification bias across the CAG repeat in our PCR [10], we fitted a linear regression curve of both wild-type and mutant *HTT* genomic DNA (gDNA) with increasing PCR cycles (Figure 1A). PCR linearity was evaluated by determining the linear regression coefficient (r^2) of the band intensities versus the number of PCR cycles. Both wild-type and mutant PCR products showed a linear increase in gel electrophoresis band intensity with increasing PCR cycle number (wild-type, $r^2 = 0.8680$; mutant, $r^2 = 0.8282$). The slopes were not significantly different ($P = 0.6485$), indicating that the PCR was equally efficient for both wild-type and mutant *HTT*. Additionally, we always used gDNA as a reference since gDNA has a 1:1 ratio of normal and expanded *HTT*. Next, we performed RT-PCR expansion across the CAG repeat using four adult-onset HD patient-derived fibroblasts (Figure 1B). Reverse transcription without reverse transcription enzyme was taken along, verifying that there was no gDNA contamination in our RT-PCR (Figure 1C). For each fibroblast line the two PCR products corresponding to wild-type and mutant HTT mRNA were quantified and average expression levels of wild-type and mutant HTT mRNA calculated (Figure 1D). No significant difference ($P = 0.7642$) between wild-type and mutant HTT mRNA expression was observed in adult-onset HD patient-derived fibroblasts.

Less mutant HTT mRNA in human post-mortem HD brain material

Next, we investigated HTT mRNA expression levels in post-mortem brain tissue from HD patients with a wide range of repeat lengths. RNA and gDNA was isolated from frontal cortex or middle temporal gyrus and PCR was performed with primers flanking the CAG repeat (Figure 2A). The wild-type and mutant PCR products for each brain sample were quantified and normalized against PCR products from gDNA and individual wild-type versus mutant HTT mRNA expression levels were calculated. Next, the average expression levels of wild-type and mutant HTT mRNA in the frontal cortex (Figure 2B) and middle temporal gyrus (Figure 2C) of adult-onset HD patients were calculated. We found a significant 31.0% (SEM ± 6.1%) lower average mutant HTT mRNA compared to wild-type HTT mRNA expression in the frontal cortex from HD patients. In the middle temporal gyrus, a 22.1% (SEM ± 10.9%) lower average mutant HTT mRNA expression was found. When we combined all the brain samples and repeated the analysis we found a significant lower average mutant HTT mRNA expression of 26.6% (SEM ± 6.1%) compared to wild-type HTT mRNA (Figure 3A).

To validate our results with a different technique, we performed a single nucleotide polymorphism (SNP)-specific TaqMan qPCR, using probes for rs362273 SNP located at on the 3′ side of HTT in exon 57. Of our post-mortem brain samples, 6 out of 14 were heterozygous for rs362273. Next, SNP linkage by circularization (SLiC) [11] was performed to determine which allele has the guanine and which allele the adenine in exon 57. Due to the variable RNA quality of brain tissue, SLiC was only possible in 4 out of 6 samples. TaqMan qPCR showed an identical trend towards more wild-type HTT as was found for our RT-PCR analysis (Figure 3B), but due to the smaller number of brain samples did not

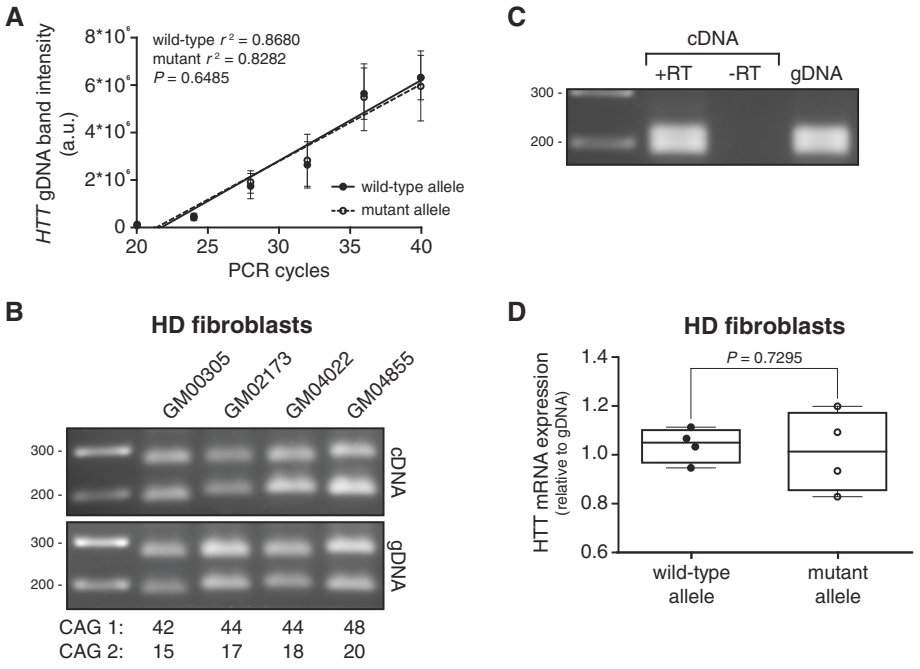

Figure 1 Validating RT-PCR amplification across the CAG repeat in HD patient-derived fibroblasts. Wild-type and mutant HTT were separated by gel electrophoresis. **(A)** Standard curve of wild-type and mutant HTT RT-PCR products with increasing PCR cycles from gDNA derived from post-mortem brain tissue of 7 HD patients. PCR linearity was evaluated by determining the individual linear regression coefficients (r^2) of the band intensities of wild-type and mutant HTT expression versus the number of PCR cycles, n = 7. **(B)** PCR products from cDNA of 4 HD (GM00305, GM02173, GM04022, GM04855) fibroblasts. CAG repeat sizes for the wild-type (lower band) and mutant alleles (upper band) are indicated below each lane. gDNA was used to examine differences in PCR amplification between the wild-type and mutant product due to the CAG repeat expansion. **(C)** RT-PCR products with input: cDNA (+RT), cDNA lacking reverse transcriptase (−RT) and gDNA of one control (GM04204). **(D)** Whisker boxplot of RT-PCR from HD patient-derived fibroblasts, comparing wild-type and mutant HTT mRNA expression levels, relative to gDNA. Line = mean, pair wise differences were evaluated using linear mixed model, n = 4.

reach significance, demonstrating that the RT-PCR quantification across the CAG repeat is an accurate technique to measure small allelic differences in mRNA expression.

Despite a lower RNA quality in our juvenile HD samples compared to the adult-onset HD samples, we were able to separate both alleles by amplification across the CAG repeat in cDNA and gDNA samples (Figure 4A). Consistent with adult-onset HD samples, we found a 22.6% (SEM ± 10.6%) lower mutant HTT mRNA expression compared to wild-type HTT mRNA in post-mortem brain tissue from juvenile HD patients (Figure 4B).

No difference in wild-type and mutant htt protein levels in adult-onset HD

To relate the observed differences in allelic HTT mRNA expression to wild-type and mutant htt protein levels, we analyzed SDS-soluble htt protein levels in both HD fibroblasts (Figure 5A) and post-mortem human HD brain homogenates (Figure 5B) using Western blot. Wild-type and mutant htt protein bands were quantified and both the individual wild-type and mutant htt protein levels were calculated as well as the average of all individual measurements. No significant difference between wild-type and mutant htt protein levels in patient-derived fibroblasts was found (Figure 5C). Likewise, in the post-mortem human HD brain homogenates there was no difference in wild-type and mutant htt protein levels (Figure 5D).

It is known that in post-mortem human HD brain, mutant htt aggregates in a polyQ length-dependent manner [12], while no mutant htt aggregates are present in HD patient-derived fibroblasts [13]. Our results show that the levels of soluble wild-type and mutant htt protein do not change in the absence or presence of htt protein aggregates.

Less mutant than wild-type htt protein in juvenile HD

Next, we analyzed SDS-soluble wild-type and mutant htt levels in juvenile HD samples. Htt protein levels from patient-derived fibroblasts with mutant polyQ lengths of 73, 99 and 181 were analyzed on Western blot (Figure 6A). Juvenile HD fibroblast lysates showed a significant 10.1% (SEM ± 2.7%) lower level of mutant htt protein compared to wild-type htt (Figure 6B).

Next, we analyzed SDS-soluble levels of wild-type and mutant htt protein in post-mortem juvenile HD brain

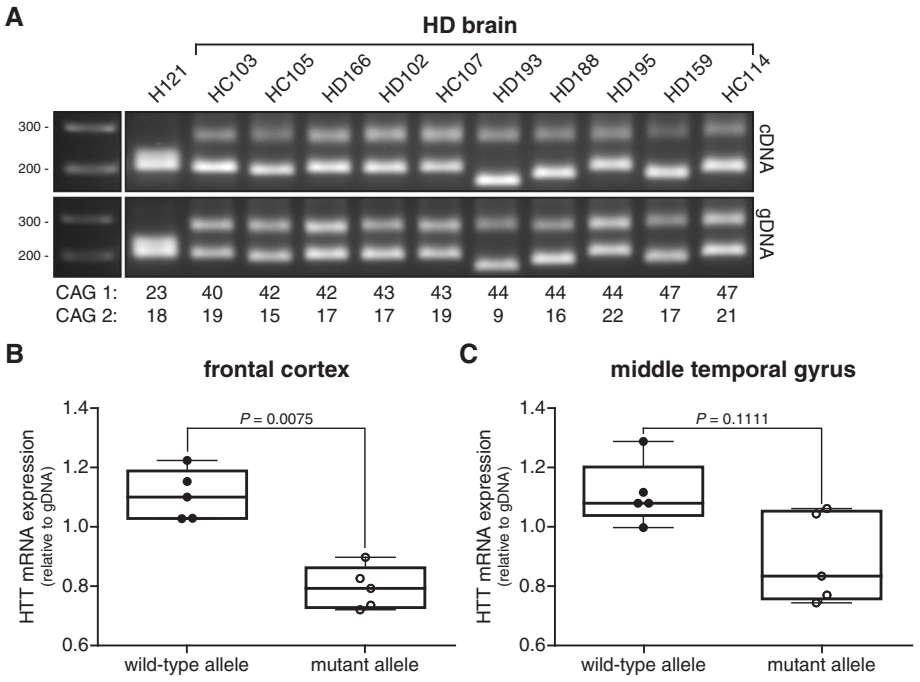

Figure 2 Wild-type and mutant HTT mRNA levels in adult-onset HD brain tissue. Wild-type and mutant HTT mRNA PCR products were separated on gel electrophoresis by differences in their CAG repeat length. **(A)** RT-PCR products from brain tissue derived from a control (H121) and 10 HD patients. Allelic CAG repeat sizes are indicated below each lane. gDNA from each sample was taken along to control for differences in PCR amplification efficiencies across the CAG repeat. **(B)** Whisker boxplot of allelic HTT mRNA expression levels in frontal cortex from 5 HD adult-onset HD patients. **(C)** Whisker boxplot of allelic HTT mRNA expression levels in middle temporal gyrus from 5 HD adult-onset HD patients. Expression levels relative to gDNA. Pair wise differences were evaluated using linear mixed model, n = 5.

lysates. Three of the four juvenile HD brain lysates showed multiple mutant htt protein products (Figure 6C). Despite of the reduced quality of the post-mortem juvenile HD brain lysates, we were able to quantify the protein bands and showed 16.4% (SEM ± 7.0%) lower mutant htt protein levels with respect to wild-type htt (Figure 6D).

These results show that in adult-onset HD samples, wild-type and mutant htt protein levels are equal, regardless of mutant htt protein aggregation. In juvenile HD there is a consistent lower level of mutant htt protein expression.

HTT antisense expression in HD patient-derived fibroblasts and post-mortem brain tissue

It is known that a lower expression of HTTAS that contains the CTG repeat can increase HTT mRNA expression [8]. To investigate if the lower mutant HTT mRNA levels we

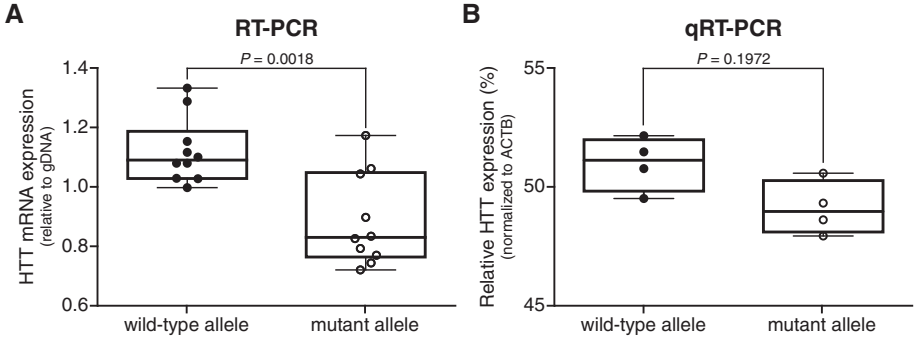

Figure 3 HTT mRNA quantification after RT-PCR amplification across the CAG repeat compared to SNP-specific quantitative RT-PCR. Whisker boxplots of wild-type versus mutant HTT mRNA expression levels in adult-onset HD post-mortem brain material. **(A)** Quantification after amplification across the CAG repeat, relative to gDNA. Pair wise differences were evaluated using linear mixed model, n = 10. **(B)** SNP rs362273-specific quantitative RT-PCR, normalized to β-actin (ACTB). Data were evaluated using a two-tailed student *t*-test, n = 4.

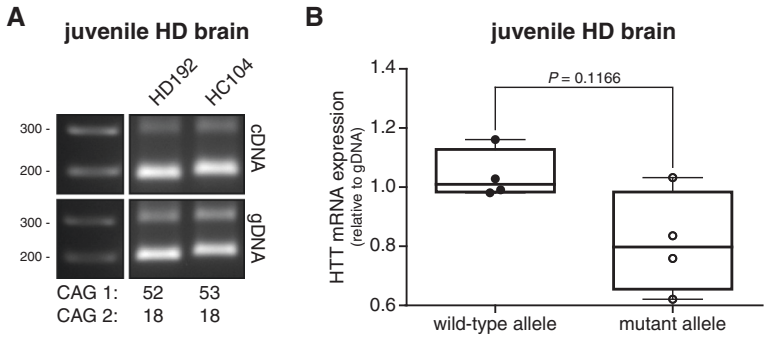

Figure 4 Wild-type and mutant HTT mRNA levels in juvenile HD brain. Wild-type and mutant HTT mRNA PCR products were separated by gel electrophoresis. **(A)** RT-PCR products from brain tissue derived from two juvenile HD patients (HD192 and HC104). CAG repeat sizes for the wild-type and mutant alleles are indicated below each lane. gDNA was used to control for differences in PCR amplification between the wild-type and mutant product due to the CAG repeat expansion. **(B)** Whisker box plot comparing wild-type and mutant HTT mRNA expression levels, relative to gDNA. Pair wise differences were evaluated using linear mixed model, n = 4.

observed were due to higher HTTAS expression we investigated HTTAS expression in fibroblasts and post-mortem brain tissue from HD patients. In post-mortem brain tissue we detected comparable levels of HTTAS in HD and control brain tissue (Figure 7A). We could also reliably detect HTTAS in all cell lines that we investigated, including the homozygous HD patient-derived fibroblasts (Figure 7B). Sanger sequencing confirmed that this was HTTAS with the expanded CTG repeat. This was unexpected since reduced expression of HTTAS with an expanded CTG repeat was reported in post-mortem HD brain [8], which would suggest no expression of this HTTAS when both *HTT* alleles contain an expanded repeat. We conclude that our observed variations in mutant and wild-type HTT mRNA levels in post-mortem brain are probably not caused by altered transcription of HTTAS with an expanded CTG repeat.

Discussion

In the current study we found that in post-mortem adult-onset HD brain material the levels of wild-type and mutant HTT mRNA were significantly different. We found lower levels of mutant HTT mRNA compared to wild-type in the frontal cortex and a trend towards lower mutant HTT mRNA levels in the middle temporal gyrus. In adult-onset HD patient-derived fibroblasts the levels of wild-type and mutant HTT mRNA did not differ. This is in concordance with results found in patient-

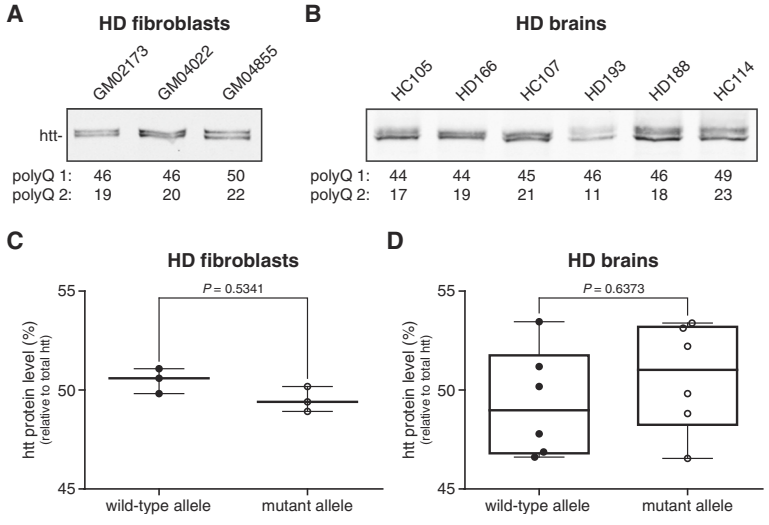

Figure 5 Wild-type and mutant htt protein levels in HD fibroblasts and brain tissue. **(A)** Western blot analysis of total protein lysates from human fibroblasts from three HD patients (GM02173, GM04022, GM04855). The lower band represents wild-type htt, the upper band mutant htt. PolyQ repeat lengths are indicated below each lane. **(B)** Western blot analysis of cortical brain homogenates from six HD subjects. **(C)** Whisker box plots comparing wild-type and mutant htt levels normalized against total htt in HD fibroblasts (n = 3) and **(D)** post-mortem brain tissue (n = 6). Pair wise differences were evaluated using linear mixed model.

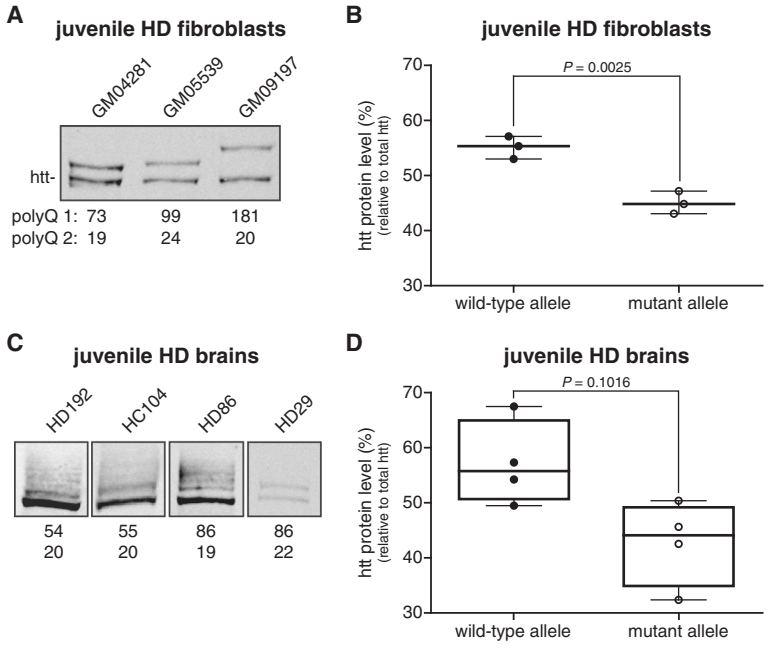

Figure 6 Wild-type and mutant htt protein levels in juvenile HD fibroblasts and brain tissue. **(A)** Western blot analysis of total protein lysates from human fibroblasts derived from three juvenile HD subjects (GM04281, GM05539, GM09197). The lower band represents wild-type htt, the upper band mutant htt. PolyQ repeat lengths are indicated below each lane. **(B)** Whisker box plot comparing wild-type and mutant htt levels normalized against total htt in juvenile HD fibroblasts (n = 3). **(C)** Post-mortem cortical brain tissue from four juvenile HD subjects (HD192, HC104, HD86, HD29). **(D)** Whisker box plot comparing wild-type and mutant htt levels normalized against total htt in juvenile HD post-mortem brain tissue (n = 4). Pair wise differences were evaluated using linear mixed model.

derived HD lymphoblasts, where it was shown that the expanded CAG repeat did not affect HTT mRNA expression [6]. Conversely, a small (~10%) upregulation of mutant HTT mRNA was recently shown in human post-mortem HD brain tissue using SNP-specific qPCR [9]. These contradictory results could be explained by the fact that the two SNP's used in this study were both located outside HTT Exon 1 (3′UTR, and Exon 50). Furthermore, the small upregulation of mutant HTT mRNA was most pronounced in post-mortem brain material derived from patients with early neuropathological grades (grades 1 and 2), whereas the material in our study was generally of later disease stages (grades 3 and 4).

Wild-type and mutant htt protein levels did not significantly differ in either fibroblasts or post-mortem brain samples of adult-onset HD patients. Soluble htt has a half-life of approximately 24 hours [14] and we hypothesize that with Western blot analysis we detect soluble htt that is present in the cells. Protein aggregation is an important feature in HD brain tissue, but does not occur in HD fibroblasts [13], our results show that protein aggregation does not affect the levels of soluble htt protein. However, we did find lower mutant HTT mRNA levels in brain. A possible explanation could be an enhanced translation of mutant HTT mRNA, resulting in equal htt protein levels. Recently, increased translation of mutant HTT was suggested [7]. Cells overexpressing N-terminal htt fragments with a normal and mutant polyQ repeat showed an enhanced protein synthesis of htt fragments with an expanded polyQ repeat. This more efficient translation of mutant HTT mRNA was proposed to be caused by enhanced binding of the MID1-complex to the expanded CAG repeat and mediated by mTOR and S6K kinases [7].

Two of the three juvenile HD brain lysates showed multiple mutant htt protein products. This could be due to somatic mosaicism of mutant htt in the brain of juvenile patients [15] or due to reduced protein quality caused by the post-mortem delay. These multiple mutant htt protein products were not present in the fibroblast samples. Nonetheless, we consistently, found that the levels of mutant htt protein were lower than wild-type in both fibroblasts and post-mortem brain tissue of juvenile HD patients. This is in contradiction with previous studies in knock-in HD mice carrying one or two alleles with 111 CAG repeats [7], which showed increased mutant htt protein levels. The lower mutant htt protein level in juvenile HD is consistent with lower levels of mutant HTT mRNA. Although juvenile HD is much rarer than adult-onset HD [16], for development of a rapid phenotype HD animal models generally carry a mutant *HTT* transgene with juvenile CAG repeats [17]. Our results indicate that wild-type and mutant htt protein

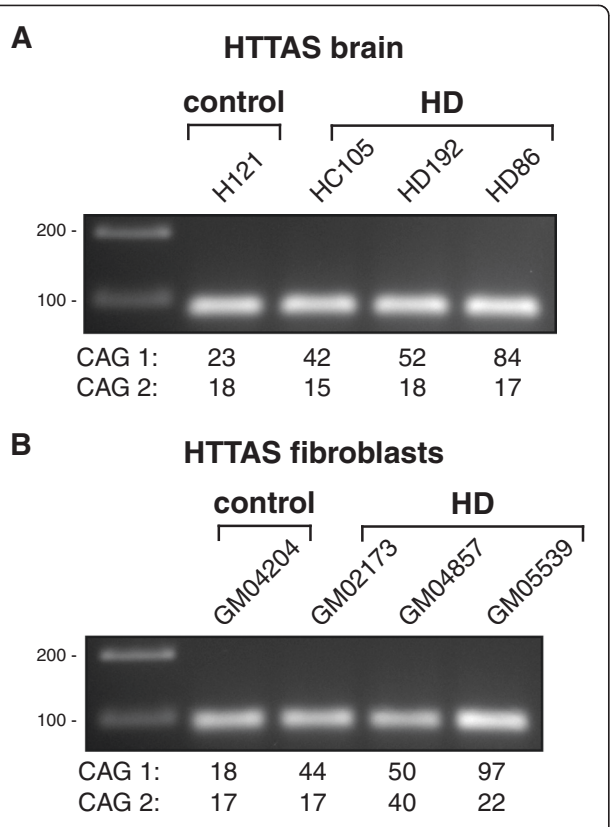

Figure 7 HTT antisense expression in HD patient-derived fibroblasts and brain tissue. Gel electrophoresis of HTTAS amplified using strand- and HTTAS isoform-specific primers. **(A)** RT-PCR of patient-derived fibroblasts from a control (GM04204), an HD patient (GM02173), an HD patient homozygous for the CAG repeat expansion (GM04857) and a juvenile HD patient (GM05539). **(B)** RT-PCR of post-mortem brain tissue from a control (H121), an HD patient (HC105), and 2 juvenile HD patients (HD192 and HD86). Allelic CAG repeat sizes below each lane.

ratios are different in juvenile HD and adult-onset HD brain samples and this should be taken into account when interpreting results from HD models carrying a juvenile repeat expansion.

Recently it has been suggested that in polyQ disorders bidirectional RNA transcription could play a role in the disease pathology by deregulation of the sense transcript [8,18]. It was hypothesized that a bidirectional RNA transcript called HTTAS, negatively regulates htt transcript expression [8]. In accordance, in HD patient-derived fibroblasts and brains HTTAS with the expanded CTG repeat could not be detected [8]. Our results show HTTAS expression in all HD samples and most notably in patient-derived fibroblasts homozygous for the CAG repeat expansion, suggesting that there is an HTTAS with expanded CTG repeat transcribed. We can conclude however that differences in allelic HTT transcript levels in post-mortem brain are probably not caused by lower levels of HTTAS.

Recent advances have shown the potential of reducing mutant htt levels with oligonucleotide-based therapeutics. Reduction of both wild-type and mutant htt up to 70% was well tolerated in HD rodent models and non-human primates [19]. Long-term suppression of wild-type and mutant htt might not be desirable because of htt's anti-apoptotic function [20] and importance for cell survival in the adult brain [21,22]. A different approach would be an allele-specific reduction of mutant htt. This could be achieved with oligonucleotides directed against SNPs unique to the mutant htt transcript, or by targeting the expanded CAG repeat directly [23]. Although our allelic HTT mRNA expression levels are in disagreement to that of Liu *et al.* [9], the overall differences in basal HTT mRNA in both studies are small. This shows that the levels of wild-type and mutant htt protein are not considerably different and provides feasibility for oligonucleotide therapeutics that are not completely specific for the mutant *HTT* allele.

Conclusions

Although we found significantly lower mutant HTT mRNA levels in adult-onset HD, wild-type and mutant htt protein levels did not differ significantly in adult-onset HD brain samples. Conversely, in juvenile HD brain samples mutant htt protein levels were lower compared with wild-type htt, showing subtle differences between juvenile HD and adult-onset HD. Since most HD model systems harbor juvenile repeat expansions, our results suggest caution with the interpretation of htt mRNA and protein studies using HD cell and animal models with such long repeats. Furthermore, our HTTAS results in homozygous HD cells do not support reduced HTTAS expression due to an expanded CAG repeat.

Methods

Patient-derived fibroblasts and human brain samples

Fibroblasts derived from HD patients and controls were purchased from Coriell Cell Repositories, Camden, USA (Table 1). Fibroblasts were cultured at 37°C and 5% CO_2 in Minimal Essential Medium (Gibco Invitrogen, Carlsbad, USA) with 15% heat inactivated Fetal Bovine Serum (Clontech, Palo Alto USA), 1% Glutamax (Gibco) and 100 U/ml penicillin/streptomycin (Gibco).

Post-mortem human brain tissue was obtained from the Neurological Foundation of New Zealand Human Brain Bank in the Centre for Brain Research, University of Auckland, and the brain bank from the department of Neurology, Leiden University Medical Center. Tissue was obtained with the families full consent and with the ethical approval of the various institutional Ethics Committees. For a complete list of samples and corresponding clinical information, see Table 2.

Table 1 Patient-derived fibroblasts

Name	CAG 1	CAG 2	Type	Age at sampling	Age of onset	Sex
GM00305	42	15	HD	56	46	F
GM02173	44	17	HD	52	NA	F
GM04022	44	18	HD	28	NA	F
GM04855	48	20	HD	11	26	M
GM04857	50	40	Homozygous HD	23	28	F
GM04281	71	17	Juvenile HD	20	14	F
GM05539	97	22	Juvenile HD	10	2	M
GM09197	179	18	Juvenile HD	6	NA	M
GM04204	18	17	Control	81	NA	M

M: male, F: female, NA: not assessed.
Samples ranked on CAG repeat size of the longest allele.

CAG repeat sizing

Genomic DNA samples were isolated from patient-derived fibroblasts and human brain using the Wizard Genomic DNA Purification Kit (Promega, Madison, USA) according to manufacturer's instructions and diluted to 50 μg/ml. The number of CAG repeats in the *HTT* gene was determined by PCR using primers "HD-1" and "HD-3" as described previously [24], followed by fragment analysis on an ABI 3130 Automated Capillary DNA Sequencer (Applied Biosystems, Life Technologies Corporation, Carlsbad, USA). The exact PCR conditions are available on request. The 3′ CAA and following CAG are not counted. For the polyQ repeat the CAA and CAG triplet are counted and the polyQ repeat is therefore 2 units longer than the CAG repeat size.

RNA and genomic DNA analysis

Post-mortem brain tissue was homogenized using ceramic MagNA Lyser beads (Roche, Mannheim, Germany) by grinding in a Bullet Blender (Next Advance, Averill Park, USA) according to manufacturer's instructions. Total RNA was isolated from fibroblast cells and brain tissue using the Aurum Total RNA Mini Kit (BioRad, Hercules, USA), with an on-column DNase treatment for 30 min. RNA was eluted in 40 μl elution buffer and cDNA was synthesized from 1 μg total RNA using the Transcriptor First Strand cDNA Synthesis Kit with oligo (dT) primers at 55°C for 90 min (Roche).

PCR was performed using 1 μl cDNA or genomic DNA, 10x Expand High Fidelity buffer with 15 mM $MgCl_2$ (Roche), 200 μM dNTPs (Roche), 1 M Betaine (Sigma-Aldrich, St. Louis, USA), 15 pmol of both forward primer

Table 2 Post-mortem human brain tissue

Name	CAG 1	CAG 2	Type	Tissue	PMD	Grade	Age of death	Age of onset	Sex
HC103	40	19	HD	MTG	11	1	41	35	M
HC105	42	15	HD	MTG	9	1	67	47	F
HD166	42	17	HD	FC	32	2	80	>70	M
HC102	43	17	HD	MTG	10	3	64	40	M
HC107	43	19	HD	MTG	3	3	75	58	M
HD193	44	9	HD	FC	18	3	68	44	M
HD188	44	16	HD	FC	NA	3	64	44	M
HD195	44	22	HD	FC	8.5	3	61	NA	F
HD159	47	17	HD	FC	42	3	41	26	F
HC114	47	21	HD	MTG	12	NA	53	30	F
HD192	52	18	Juvenile HD	FC	62	4	37	NA	M
HC104	53	18	Juvenile HD	MTG	15	3	40	15	M
HD86	84	17	Juvenile HD	FC	20	3	20	16	F
HD29	84	20	Juvenile HD	FC	11	NA	11	8	F
H121	23	18	Control	MTG	6	control	64	control	F

MTG: middle temporal gyrus, FC: frontal cortex, PMD: post-mortem delay (hours), Grade: neuropathological classification [28], M: male, F: female, NA: not assessed.
Samples ranked on CAG repeat size of the longest allele.

HttCAGFw: 5′-ATG GCG ACC CTG GAA AAG CTG AT-3′ and reverse primer HttCAGRev: 5′-TGA GGC AGC AGC GGC TG-3′ (Eurogentec, Liege, Belgium), 3 U Expand High Fidelity enzyme mix (Roche), and PCR grade water to a final volume of 30 μl. The PCR program started with a 2 min initial denaturation at 94°C, followed by 35 cycles of 15 sec denaturation at 94°C, 30 sec annealing at 60°C, 1 min elongation at 72°C, and final elongation step at 72°C for 7 min.

PCR products were loaded on a 2% agarose gel diluted in Tris/Borate/EDTA (TBE) buffer. DNA gel electrophoresis was performed for 1 hour at 100 V. Intensities of DNA bands were quantified using ImageJ software. Intensity of the HTT mRNA band was divided by the corresponding genomic DNA band to normalize for differences in PCR efficiency due to CAG repeat length.

SNP genotyping and SNP linkage by circularization (SLiC)

The procedure for SNPs rs362273 genotyping and SNP linkage by circularization on human brain tissue was adapted from Liu *et al*. [11]. One μg of DNase-treated total RNA, together with oligo (dT) primers, was used for cDNA synthesis using SuperScript III First-Strand Synthesis System (Invitrogen). To improve reverse transcription of long cDNA templates, 2 M betaine and 0.6 M trehalose (both Sigma-Aldrich) were added to the reaction mixture [25]. cDNA synthesis was performed at 42°C for 2.5 hours, followed by RNase H treatment at 37°C for 20 min. Next, 5 μl cDNA was used as template for long-range PCR and SLiC.

Taqman SNP assay

Quantitative PCR was performed using the LightCycler 480 II (Roche), according to manufacturer's instructions, using a mixture containing 45 ng cDNA, 1xTaqMan Universal PCR Master Mix, no AmpErase UNG (Applied Biosystems), 1xTaqMan SNP Genotyping Assay (Applied Biosystems), and nuclease-free water (Ambion) in a 20 μl reaction volume. ACTB (Applied Biosystems, cat#Hs99999903_m1) was included as reference gene. A standard curve was generated using pooled equal amounts of cDNA from all samples. Quantification of the dual-color hydrolysis of both allele-specific fluorescent reporter dyes, FAM ("G" allele) and VIC ("A" allele), was performed with the LightCycler 480 SW 1.5.1 software (Roche) using the 2^{nd} derivative method, according to manufacturer's instructions.

HTT antisense determination

RNA isolation as described above. PCR was performed using 1.5 μl cDNA, 10x PCR buffer with 20 mM $MgCl_2$ (Roche), 200 μM dNTPs (Roche), 6 pmol HTTAS_v1 primer, forward: 5′-CAC CGG GGC AAT GAA TGG-3′, reverse: 5′-GTG CGG ATG GCA AGG ACA G-3′, 2 U FastStart Taq DNA Polymerase (Roche), 1 M ethylene glycol (Sigma-Aldrich), and PCR grade water to a final volume of 30 μl. The PCR program started with a 3 min initial denaturation at 95°C, followed by 40 cycles of 10 sec denaturation at 95°C, 10 sec annealing at 60°C, 10 sec elongation at 72°C, after which a final elongation step was performed at 72°C for 7 min.

PCR products were loaded on a 3% TBE agarose gel and bands were extracted using the NucleoSpin Gel & PCR Clean-up kit (Machery Nagel, Düren, Germany). To confirm the sequence of HTTAS, PCR products were cloned into a pGEM-T Easy vector (Promega) and analyzed by Sanger sequencing using a T7-specific forward primer.

Protein isolation

Fibroblasts were detached from the culture surface with a 0.5% Trypsin/EDTA solution. After washing twice with HBSS, cells were resuspended in 200 μl ice cold lysis buffer, containing 50 mM HEPES, 50 mM NaCl, 10 mM EDTA, 10 mM DTT, 0.1% CHAPS, and 1 tablet Complete mini protease inhibitor EDTA free (Roche) per 10 ml buffer [26]. Next, samples were sonicated 3 times 5 sec using ultrasound with amplitude 60 at 4°C. After 1 hour head-over-head incubation at 4°C, extracts were centrifuged for 15 min at 10,000 × *g* and 4°C and supernatant was isolated.

For brain homogenates, slices from frozen unfixed human brain tissue were collected using a sliding microtome (Leica SM 2010R). Tissue was homogenized using ceramic MagNA Lyser beads (Roche) by grinding in a Bullet Blender (Next Advance) for 3 min at strength 8 in lysis buffer with pH 7.2, containing 1% CHAPS, 137 mM NaCl, 2.7 mM KCl, 4.3 mM Na2PO4, 1.4 mM KH2PO4, 5 mM EDTA, 5 mM EGTA, and 1 tablet Complete mini protease inhibitor EDTA free (Roche) per 10 ml buffer [27]. Homogenates were incubated for 1 hour in a head-over-head rotator at 4°C, and centrifuged for 15 min at 10,000 × *g* at 4°C.

Protein concentrations were determined with the bicinchoninic acid kit (BCA) (Thermo Fisher Scientific, Waltham, USA) using Bovine Serum Albumin (BSA) as a standard. After addition of 5% glycerol, samples were aliquotted, snap frozen and stored at −80°C.

Western blotting

SDS-PAGE separation of proteins was performed according to the "shorter CAG repeats" protocol as described previously [27]. Proteins were transferred to a 0.2 μm nitrocellulose membrane (Bio-Rad, #170-4159) using the Trans-blot Turbo (BioRad) at 2.5A (constant)/25 V for 10 min. Membranes were blocked for 15 min in tris buffered saline containing 5% non-fat milk (Nutricia, Schiphol, the Netherlands). Next, membranes were incubated with primary rabbit antibody EPR5526 (Abcam,

Cambridge, UK) that recognizes the N-terminus of the htt protein, diluted 1:5000 in blocking buffer, followed by secondary incubation with rabbit IRDye800 (LI-COR, Lincoln, USA) diluted 1:5000 in blocking buffer. Blots were analyzed on an Odyssey reader (LI-COR). Protein bands corresponding to were quantified using the Odyssey software version 3.0 (LI-COR). Background correction was performed by sampling an empty area of the blot of the same size as the area that contained the positive protein band. Quantification of wild-type and mutant htt protein relied on densitometry measurement of both western blot bands separately. In case separation was small, we could magnify our scanned blots using the software's "zoom" function to aid in a proper alignment of the densitometry calculation boxes over both separate bands. Wild-type and mutant htt protein expression levels relative to total htt protein expression were calculated by dividing wild-type and mutant htt band intensities with total htt band intensity (wild type + mutant).

Statistical analyses

Experiments were performed at least six times per subject (3 biological and 2 technical replicates). PCR linearity was evaluated by GraphPad Prism version 6.02 by determining the individual linear regression coefficients ($r2$) of the band intensities of wild-type and mutant HTT expression versus the number of PCR cycles.

GraphPad Prism version 6.02 was used to create whisker boxplots (whiskers = min to max), showing all mean values per sample. IBM SPSS Statistics Version 20.0.0 was used for statistical analysis. All datasets were tested for a Gaussian distribution by visual inspection after plotting the residuals. Significance of the pairwise differences was determined using a linear mixed model.

Competing interests

The authors declare that they have no competing interests.

Authors' contributions

MME wrote the article and performed the experiments and statistical analysis. MHS wrote the article and performed the experiments. BAP, MA and MJB contributed to the manuscript by providing analytical tools. RLMF and RACR contributed by providing post-mortem brain tissue. The project was supervised and designed by WMCRM. All authors read and approved the final manuscript.

Acknowledgements

The authors would like to thank David F. Fischer (BioFocus, a Galapagos company, Leiden, The Netherlands) and Michela A. Tessari (Galapagos B.V., Leiden, The Netherlands) for the TaqMan SNP assay, Ron Wolterbeek (Medical Statistics) for statistical review, Marlous van der Weijden for technical assistance and Marika Eszes and Ingrid Hegeman for providing us with the relevant clinical information.

This work was supported by the Center for Biomedical Genetics (the Netherlands), the Prinses Beatrix Spierfonds (the Netherlands), and Integrated European Project in Omics Research of Rare Neuromuscular and Neurodegenerative Diseases (Neuromics). The funders had no role in study design, data collection and analysis, decision to publish, or preparation of the manuscript.

Author details

[1]Department of Human Genetics, Leiden University Medical Center, Albinusdreef 2, Leiden 2333ZA, the Netherlands. [2]Galapagos B.V., Leiden, the Netherlands. [3]Department of Clinical Genetics, Leiden University Medical Center, Leiden, the Netherlands. [4]Centre for Brain Research and Department of Anatomy with Radiology, University of Auckland, Auckland, New Zealand. [5]Department of Neurology, Leiden University Medical Center, Leiden, the Netherlands.

Received: 4 December 2014 Accepted: 17 April 2015
Published online: 28 April 2015

References

1. Roos RA. Huntington's disease: a clinical review. Orphanet J Rare Dis. 2010;5:40.
2. Kremer B, Weber B, Hayden MR. New insights into the clinical features, pathogenesis and molecular genetics of Huntington disease. Brain Pathol. 1992;2:321–35.
3. Losekoot M, van Belzen MJ, Seneca S, Bauer P, Stenhouse SA, Barton DE. EMQN/CMGS best practice guidelines for the molecular genetic testing of Huntington disease. Eur J Hum Genet. 2013;21:480–6.
4. Vonsattel JP, DiFiglia M. Huntington disease. J Neuropathol Exp Neurol. 1998;57:369–84.
5. Difiglia M, Sapp E, Chase KO, Davies SW, Bates GP, Vonsattel JP, et al. Aggregation of huntingtin in neuronal intranuclear inclusions and dystrophic neurites in brain. Science. 1997;277:1990–3.
6. Lee JM, Galkina EI, Levantovsky RM, Fossale E, Anne AM, Gillis T, et al. Dominant effects of the Huntington's disease HTT CAG repeat length are captured in gene-expression data sets by a continuous analysis mathematical modeling strategy. Hum Mol Genet. 2013;22:3227–38.
7. Krauss S, Griesche N, Jastrzebska E, Chen C, Rutschow D, Achmuller C, et al. Translation of HTT mRNA with expanded CAG repeats is regulated by the MID1-PP2A protein complex. Nat Commun. 2013;4:1511.
8. Chung DW, Rudnicki DD, Yu L, Margolis RL. A natural antisense transcript at the Huntington's disease repeat locus regulates HTT expression. Hum Mol Genet. 2011;20:3467–77.
9. Liu W, Chaurette J, Pfister EL, Kennington LA, Chase KO, Bullock J, et al. Increased Steady-State Mutant Huntingtin mRNA in Huntington's Disease Brain. J Huntingtons Dis. 2013;2:491–500.
10. Stine OC, Li SH, Pleasant N, Wagster MV, Hedreen JC, Ross CA. Expression of the mutant allele of IT-15 (the HD gene) in striatum and cortex of Huntington's disease patients. Hum Mol Genet. 1995;4:15–8.
11. Liu W, Kennington LA, Rosas HD, Hersch S, Cha JH, Zamore PD, et al. Linking SNPs to CAG repeat length in Huntington's disease patients. Nat Methods. 2008;5:951–3.
12. Legleiter J, Mitchell E, Lotz GP, Sapp E, Ng C, DiFiglia M, et al. Mutant huntingtin fragments form oligomers in a polyglutamine length-dependent manner in vitro and in vivo. J Biol Chem. 2010;285:14777–90.
13. Sathasivam K, Woodman B, Mahal A, Bertaux F, Wanker EE, Shima DT, et al. Centrosome disorganization in fibroblast cultures derived from R6/2 Huntington's disease (HD) transgenic mice and HD patients. Hum Mol Genet. 2001;10:2425–35.
14. Persichetti F, Carlee L, Faber PW, Mcneil SM, Ambrose CM, Srinidhi J, et al. Differential expression of normal and mutant Huntington's disease gene alleles. Neurobiol Dis. 1996;3:183–90.
15. Gonitel R, Moffitt H, Sathasivam K, Woodman B, Detloff PJ, Faull RL, et al. DNA instability in postmitotic neurons. Proc Natl Acad Sci U S A. 2008;105:3467–72.
16. Quarrell O, O'Donovan KL, Bandmann O, Strong M. The Prevalence of Juvenile Huntington's Disease: A Review of the Literature and Meta-Analysis. PLoS Curr. 2012;4:e4f8606b742ef3.
17. Pouladi MA, Morton AJ, Hayden MR. Choosing an animal model for the study of Huntington's disease. Nat Rev Neurosci. 2013;14:708–21.
18. Sopher BL, Ladd PD, Pineda VV, Libby RT, Sunkin SM, Hurley JB, et al. CTCF regulates ataxin-7 expression through promotion of a convergently transcribed, antisense noncoding RNA. Neuron. 2011;70:1071–84.
19. Kordasiewicz HB, Stanek LM, Wancewicz EV, Mazur C, McAlonis MM, Pytel KA, et al. Sustained Therapeutic Reversal of Huntington's Disease by Transient Repression of Huntingtin Synthesis. Neuron. 2012;74:1031–44.
20. Rigamonti D, Bauer JH, De-Fraja C, Conti L, Sipione S, Sciorati C, et al. Wild-type huntingtin protects from apoptosis upstream of caspase-3. J Neurosci. 2000;20:3705–13.

21. Zhang Y, Li M, Drozda M, Chen M, Ren S, Mejia Sanchez RO, et al. Depletion of wild-type huntingtin in mouse models of neurologic diseases. J Neurochem. 2003;87:101–6.
22. Dragatsis I, Levine MS, Zeitlin S. Inactivation of Hdh in the brain and testis results in progressive neurodegeneration and sterility in mice. Nat Genet. 2000;26:300–6.
23. Appl T, Kaltenbach L, Lo DC, Terstappen GC. Targeting mutant huntingtin for the development of disease-modifying therapy. Drug Discov Today. 2012;17:1217–23.
24. Warner JP, Barron LH, Brock DJ. A new polymerase chain reaction (PCR) assay for the trinucleotide repeat that is unstable and expanded on Huntington's disease chromosomes. Mol Cell Probes. 1993;7:235–9.
25. Spiess AN, Ivell R. A highly efficient method for long-chain cDNA synthesis using trehalose and betaine. Anal Biochem. 2002;301:168–74.
26. Evers MM, Tran HD, Zalachoras I, Meijer OC, den Dunnen JT, van Ommen GJ, et al. Preventing formation of toxic N-terminal huntingtin fragments through antisense oligonucleotide-mediated protein modification. Nucleic Acid Ther. 2014;24:4–12.
27. Hu J, Matsui M, Gagnon KT, Schwartz JC, Gabillet S, Arar K, et al. Allele-specific silencing of mutant huntingtin and ataxin-3 genes by targeting expanded CAG repeats in mRNAs. Nat Biotechnol. 2009;27:478–84.
28. Vonsattel JP, Myers RH, Stevens TJ, Ferrante RJ, Bird ED, Richardson EP. Neuropathological classification of Huntington's disease. J Neuropathol Exp Neurol. 1985;44:559–77.

Chapter 7

Discussion

Huntington disease, simple yet complex

In 1993, the cause of Huntington disease (HD) was revealed to be one single mutation in one gene which allowed for the immediate development of a straightforward genetic test to determine if someone carried the HD-mutation [1-3]. Due to the simplicity of the mutation, hope arose that a therapeutic intervention against HD could soon be developed. Unfortunately, a simple cause does not always imply a simple cure. Since the discovery of the *HTT* gene, it has been well established that the htt protein has many cellular functions. The HD mutation leads to a cascade of pathological effects resulting in a variety of HD symptoms. HD combination treatments separately targeting all HD symptoms are complex. A single therapy that intervenes at the root-cause level in the HD pathological cascade is expected to alleviate all HD symptoms. In addition, such a therapy could delay HD symptom onset and/or prevent neurological damage when already applied during the presymptomatic phase of HD. Developing a cure for HD or even a therapeutic intervention that could delay symptom onset is the highest pinnacle of HD research [4]. Developing such therapies, which should prevent or block toxicity of the mutant htt protein, is challenging. The therapeutic intervention should be able to discriminate mutant htt from normal htt as the latter has many important functions within the cell. In addition, methods to deliver the therapeutic agent at areas affected by HD pathology should be developed. Furthermore, a reliable HD biomarker should be established to follow disease progression before symptom onset in order to be able to assess therapeutic efficacy in early stages of HD. Due to these challenges, no approved HD therapy that directly intervenes with the htt protein is available 24 years after discovery of the *HTT* gene. In addition to these challenges, the idea of the mutant htt protein as the sole pathogenic agent in HD was challenged by de Mezer *et al* whom suggested effects of RNA toxicity [5].

VHH antibodies, simple yet versatile

In 1993, the heavy chain-only antibody (HCA)-class was discovered in *Camelidae*. The VHH is a very versatile antibody fragment derived from HCA. Selection of suitable VHH from phage display banks is a lengthy process that involves pre-screening of recombinant clones for identical ones before sequencing. In **chapter 2**, we developed high-resolution melting curve analysis (HRMA) as a pre-screening tool for VHH selection from Llama phage-display banks. HRMA is a widely applicable technique [6], capable of accurately pre-screening recombinant clones in a timely manner. HRMA was utilized in **chapter 3**, were we describe a successful selection and characterization of anti-huntingtin VHH antibodies. In HD research, much attention has been focussed on N-terminal htt fragments. In **chapter 3**, huntingtin-specific VHH were selected from a phage display bank originating from Llamas (*Llama glama*) immunized with an N-terminal huntingtin fragment. We showed that, next to binding the N-terminal htt fragment on ELISA and western blot, our VHH were also capable of precipitating full length htt from human brain lysates. Hence, the VHH epitope is accessible in both the N-terminal

htt fragment, and the full length htt protein. This makes our VHH potentially useful in studies on both N-terminal htt fragments and the full-length protein. For example, immunoprecipitation commonly utilizes an antibody for antigen precipitation and another antibody to detect the precipitated antigen on western blot. If both antibodies are from the same host species, the antibody used for precipitation could result in strong western blot bands at around 50 kDa from the IgG heavy chain [7]. This could obscure smaller N-terminal htt fragments. The use of camelid VHH as a precipitation antibody could solve this issue. A drawback of using immunized banks is that the immunization process narrows the field of binding VHH. This drawback is reflected in the homogeneity of the protein sequences from our anti huntingtin VHH. Although immunization generally results in VHH with strong epitope affinities, immunization does not necessarily result in VHH that give the desired biological effect. To increase the chance of obtaining biologically relevant VHH, peptide based immunizations (e.g. with the N17 peptide) could be performed in the future. Detailed knowledge of the structural features of htt would aid in the development of peptides for these future immunizations. Recently, De Genst *et al* used x-ray crystallography and NMR to describe how Scfv, an antibody fragment consisting of a fusion between the variable light and heavy chain domains from a regular IgG, binding to N17 affects htt aggregation [8]. Due to its tendency to aggregate however, mutant htt crystallization without modifications is notoriously difficult even under microgravity conditions [9].

The huntingtin protein in post mortem human brain tissue.

Model systems are an integral part of HD research. They offer many benefits above human subjects such as flexibility, speed, a uniform genetic background, controlled conditions and the possibility to study early pathogenic processes. For example, HD mouse models with large CAG repeats offer an early onset HD phenotype that allows results to be obtained within the animals life span. To be useful in research aimed at developing HD therapies, the model system should fit with the therapeutic mechanism of action. The widely used R6/2 mouse model for example, cannot be used to test HD therapies from which the mechanism-of-action is targeted towards more C-terminal htt domains (e.g. caspase-cleavage) as these are not present on the pathogenic N-terminal mutant htt fragment expressed in the R6/2 mouse. HD model systems do not necessarily correlate well to HD pathology in human brain tissue. For example, aggregation of mutant htt is a hallmark for HD in human brain tissue but is not detected in human-derived HD fibroblasts. Hence, interpretation of results obtained from HD model systems should be performed carefully and if possible, validated in human HD brain tissue. However next to ethical issues, using *post mortem* brain tissue in HD research is challenging. Possible effects on the htt protein due to *post mortem* delay (PMD) or a freeze-thaw cycle are not known and could influence results. In **chapter 4**, we have addressed how *post mortem* delay (PMD) affects the presence of N-terminal htt protein fragments in human brain tissue. Therefore we mimicked PMD effects in individual control and HD cases. In a recent study, PMD was mimicked in a similar way in

hippocampal brain tissue [10]. Blair *et al* reported that most variance in results is caused by interpersonal differences rather than PMD, and that the severity of PMD effects vary between different proteins (e.g. no discernible effect on actin and GAPDH, but levels of alpha tubulin are drastically lowered). For htt, we found similar results. Interpersonal variance on htt levels and N-terminal fragments was apparent, and lower htt levels were detected at longer PMD's (>24hr). Moreover, we found that PMD effects on N-terminal htt protein fragments in human brain tissue are small and can be defined. This allows for an accurate interpretation of western blot results. A review of previous western blot results on N-terminal htt fragments in human brain tissue raised an intriguing point. Western blot results using an anti N17-huntingtin antibody presented in **chapter 4** include striatal tissue from an HD subject, and indicate that a 43 kDa N-terminal htt fragment is associated with PMD. An earlier study performed in 2001 also detected a 43 kDa N-terminal htt fragment in striatal HD tissue lysates using western blot [11]. However, another study performed in 2002 did not detect this band in striatal HD tissue lysates [12]. A review of the material and methods section reveals that the experimental procedures of both studies were very similar. Both utilized subjects between 55-75 years of age with an average PMD of 9 to 16 hr from the Harvard brain tissue resource centre but no clinical data of individual subjects was shown. Furthermore, western blotting by both studies was performed as described in [13, 14]. Although these similarities do not fully exclude the possibility that the difference between [11] and [12] is due to subject-to-subject variation, some other factor of variance (e.g. biological or technical) should be considered.

The quantification of htt aggregates in human brain tissue is important to elucidate the role of htt aggregation in HD pathology. However, quantification of htt aggregates by counting them on brain tissue slides stained with an anti-htt antibody is a slow and subjective process that counts visible (i.e. larger) aggregates. In **chapter 5** we present the results of a small-scale pilot study involving a filter retardation assay to quantify huntingtin aggregates in human brain tissue. Although more data is needed to fully determine the correlation between the number of aggregates in the brain and the amount of insoluble protein in this filter retardation assay, our results are promising. Using the filter-binding test, we observed a correlation between the subjects polyQ-length and htt aggregation. Furthermore, we observed that aggregation within the cortical region was more abundant with respect to the striatal region in a juvenile HD-case which is in agreement with earlier studies [15, 16]. Hence, our results indicate that the filter-binding test could be useful for quantification of htt aggregation in different brain regions which will aid in further elucidating its role in HD pathogenicy.

Levels of normal huntingtin versus mutant huntingtin.

Selective silencing of the mutant *HTT* gene is a promising potential intervention. However, complete selectivity towards mutant *HTT* without silencing of normal *HTT* is very difficult as the two alleles mainly differ in the length of their CAG sizes. Furthermore, a sufficient level of normal htt protein must remain for proper cellular function. Therefore, knowledge regarding basal expression levels of normal versus mutant *HTT* RNA and htt protein in human tissue is needed in order to pre-assess the safety and efficacy of huntingtin lowering therapies with partial selectivity towards mutant *HTT*. In **chapter 6**, the ratio of normal versus mutant *HTT* RNA and htt protein in human fibroblasts and brain tissue was assessed. Here, we found that the level of mutant *HTT* RNA was equal compared to normal *HTT* RNA in human-derived HD fibroblasts. In *post-mortem* human brain, levels of mutant *HTT* RNA were lower compared to normal *HTT* RNA. On protein level, we found that expression of the mutant htt protein was equal to (adult-onset HD) or lower (juvenile HD) with respect to the normal htt protein in both human-derived HD fibroblasts and *post-mortem* HD brain tissue. These results have several implications. First, our results suggest that some a-specific lowering of normal htt by therapeutic interventions aimed at lowering mutant htt protein levels is acceptable. Furthermore, it is suggested that adult-onset HD and juvenile HD pathologies are probably not alike, as juvenile HD symptoms generally present according to the Westphal-variant. Our results support this and indicate that there are subtle differences in RNA and protein expression levels between adult-onset HD and juvenile HD. This further emphasizes the importance of including HD models with a non-juvenile CAG repeat in molecular studies to match the adult-onset HD situation. In addition, we detected the *HTT* antisense transcript (*HTTAS_v1)* in a patient-derived homozygous HD fibroblast cell line. This suggests that the *HTTAS_v1* antisense transcript with the expanded GTC repeat is not reduced in HD as suggested by Chung *et al* who were unable to detect *HTTAS_v1* from the mutant *HTT* allele [17]. The *HTTAS_v1* antisense transcript represses *HTT* expression. Hence, reduced levels of *HTTAS_v1* with an expanded GTC repeat would result in upregulation of mutant *HTT* expression, which is unfavourable for therapeutic interventions that aim to lower mutant *HTT* expression. Chung *et al* based their findings on a PCR encompassing the CAG/GTC repeat which is known to be technically challenging [18]. Coupled with the low expression level of *HTTAS_v1* compared to *HTT*, the lack of *HTTAS_v1* with an expanded repeat detected by Chung *et al* could be explained by a non-optimal PCR protocol, which was also acknowledged by the authors. Because we used fibroblasts from a homozygous HD subject, we could perform a PCR that did not encompass the repeat because both alleles were mutant, thus eliminating PCR artefacts. In this homozygous cell line we were able to detect *HTTAS_v1* with an expanded GTC repeat suggesting that there is no reduction in *HTTAS_v1* expression containing an expanded repeat. this implies that *HTT* expression, and thus also mutant *HTT*, is not elevated in HD. In addition, *HTTAS_v1* would be an interesting prospective therapeutic agent in itself, as Chung *et al* showed the regulating effect is repeat-length dependent. Hence, overexpression of *HTTAS_v1* could

lower the levels of mutant htt. Finally, our results from chapter 6 also suggest that htt protein aggregation does not affect the ratio of soluble full-length wild-type versus soluble full-length mutant huntingtin. Because soluble huntingtin is considered the most toxic, htt aggregation might represent a defensive cellular response to lower htt toxicity. Combined with literature, our results in HD fibroblast cells and human brain tissue suggest that htt aggregation does not affect soluble htt protein levels.

Conclusion

The research described in this thesis sheds light onto the huntingtin protein in the *post-mortem* human brain. The assessment of mutant and wild-type htt levels should aid in developing htt lowering therapies. Understanding PMD-related effects on huntingtin in *post-mortem* human brain supports the interpretation of results from brain tissue with longer PMD's and could allow for a better understanding of N-terminal htt protein fragments in the human brain. The suggested filter-retardation assay might allow a more precise understanding of htt aggregation HD pathogenesis. The anti-huntingtin VHH that we selected using HRMA as a companion test could find use as a scientific tool to track the huntingtin protein within the living cell. This thesis has contributed to knowledge regarding the levels, aggregation and proteolytic cleavage products of the htt protein in human brain. In addition, we have selected htt specific VHH. This can contribute to obtain the ultimate goal; the development of a cure for HD.

References

1. *A novel gene containing a trinucleotide repeat that is expanded and unstable on Huntington's disease chromosomes. The Huntington's Disease Collaborative Research Group.* Cell, 1993. **72**(6): p. 971-83.
2. Gusella, J.F., et al., *Molecular genetics of Huntington's disease.* Arch Neurol, 1993. **50**(11): p. 1157-63.
3. Simpson, S.A. and A.E. Harding, *Predictive testing for Huntington's disease: after the gene. The United Kingdom Huntington's Disease Prediction Consortium.* J Med Genet, 1993. **30**(12): p. 1036-8.
4. Zielonka, D., M. Mielcarek, and G.B. Landwehrmeyer, *Update on Huntington's disease: advances in care and emerging therapeutic options.* Parkinsonism Relat Disord, 2015. **21**(3): p. 169-78.
5. de Mezer, M., et al., *Mutant CAG repeats of Huntingtin transcript fold into hairpins, form nuclear foci and are targets for RNA interference.* Nucleic Acids Res, 2011. **39**(9): p. 3852-63.
6. Vossen, R.H., et al., *High-resolution melting analysis (HRMA): more than just sequence variant screening.* Hum Mutat, 2009. **30**(6): p. 860-6.
7. Weiss, A., et al., *Mutant huntingtin fragmentation in immune cells tracks Huntington's disease progression.* J Clin Invest, 2012. **122**(10): p. 3731-6.
8. De Genst, E., et al., *Structure of a single-chain Fv bound to the 17 N-terminal residues of huntingtin provides insights into pathogenic amyloid formation and suppression.* J Mol Biol, 2015. **427**(12): p. 2166-78.
9. Owens, G.E., et al., *Comparative analysis of anti-polyglutamine Fab crystals grown on Earth and in microgravity.* Acta Crystallogr F Struct Biol Commun, 2016. **72**(Pt 10): p. 762-771.

10. Blair, J.A., et al., *Individual Case Analysis of Postmortem Interval Time on Brain Tissue Preservation.* PLoS One, 2016. **11**(3): p. e0151615.
11. Mende-Mueller, L.M., et al., *Tissue-specific proteolysis of Huntingtin (htt) in human brain: evidence of enhanced levels of N- and C-terminal htt fragments in Huntington's disease striatum.* J Neurosci, 2001. **21**(6): p. 1830-7.
12. Toneff, T., et al., *Comparison of huntingtin proteolytic fragments in human lymphoblast cell lines and human brain.* J Neurochem, 2002. **82**(1): p. 84-92.
13. Hook, V.Y., et al., *Evidence for functional localization of the proenkephalin-processing enzyme, prohormone thiol protease, to secretory vesicles of chromaffin cells.* Endocrinology, 1999. **140**(8): p. 3744-54.
14. Hook, V.Y., et al., *The kunitz protease inhibitor form of the amyloid precursor protein (KPI/APP) inhibits the proneuropeptide processing enzyme prohormone thiol protease (PTP). Colocalization of KPI/APP and PTP in secretory vesicles.* J Biol Chem, 1999. **274**(5): p. 3165-72.
15. Gutekunst, C.A., et al., *Nuclear and neuropil aggregates in Huntington's disease: relationship to neuropathology.* J Neurosci, 1999. **19**(7): p. 2522-34.
16. Kuemmerle, S., et al., *Huntington aggregates may not predict neuronal death in Huntington's disease.* Ann Neurol, 1999. **46**(6): p. 842-9.
17. Chung, D.W., et al., *A natural antisense transcript at the Huntington's disease repeat locus regulates HTT expression.* Hum Mol Genet, 2011. **20**(17): p. 3467-77.
18. Stine, O.C., et al., *Expression of the mutant allele of IT-15 (the HD gene) in striatum and cortex of Huntington's disease patients.* Hum Mol Genet, 1995. **4**(1): p. 15-8.

Chapter 8

Appendix

Nederlandse samenvatting

De ziekte van Huntington (ZvH) is een autosomaal dominant overerfbare neurodegeneratieve ziekte gekenmerkt door motorische symptomen (chorea) en stemmingsstoornissen. Voor de ZvH is thans geen effectieve therapie beschikbaar. De ZvH wordt veroorzaakt door de aanwezigheid van een verlengde CAG repeat in het *huntingtine*-gen (HD-gen). Deze mutatie resulteert in de vorming van een mutant huntingtine eiwit met een verlengde polyQ.

In **hoofdstuk 1** wordt, na een historisch intermezzo, de frequentie, symptomen, genetische achtergrond en de hersenpathologie van de ZvH beschreven. Klinisch waarneembare symptomen van de ZvH openbaren zich meestal op middelbare leeftijd en in zeldzame gevallen al op vroege leeftijd. Dit laatste wordt *juveniele* ZvH genoemd. Pathologie van de ZvH kenmerkt zich door ophopingen (aggregatie) van mutant huntingtine en een vroege specifieke atrofie van het striatum. In diermodellen van de ZvH en MRI-scans van personen met het HD-gen is deze ziektepathologie al pre-symptomatisch waarneembaar. Tevens wordt ingegaan op het gevaar van het ontstaan van *de novo* zaken door intergenerationele overdracht. Vervolgens wordt ingegaan op het huntingtine-eiwit. Normaal huntingtine vertolkt verschillende rollen in de cel en is essentieel voor embryonale ontwikkeling. Uit experimenten met een knock-out muismodel blijkt dat mutant huntingtine het gemis van normaal huntingtine op kan vangen. Dit suggereert dat ZvH pathologie wordt gestuurd door een “gain-of-function” mechanisme, waarbij het mutante eiwit een of meerdere toxische additionele (inter)acties uitvoert. Experimenten in verschillende ZvH dier- en celmodellen geven een wisselend beeld met betrekking tot de expressielevels van het normale versus mutante huntingtine-eiwit. De vorming van met name N-terminale mutante huntingtine-fragmenten speelt een belangrijke rol in de ZvH pathologie. Echter, kennis van expressie-levels en N-terminale huntingtine fragmenten in humaan brein weefsel is beperkt. Deze kennis is belangrijk voor de ontwikkelingen van therapieën die gericht zijn op verlaging van het expressielevel van mutant huntingtine, of het verhinderen van de vorming van N-terminale huntingtine fragmenten. Als laatst wordt in **hoofdstuk 1** het mogelijke nut van VHH antilichaamfragmenten, afgeleid van een speciaal type antilichaam afkomstig uit kameelachtigen, als therapie of onderzoeksmiddel voor de ZvH besproken. In **hoofdstuk 2** wordt een techniek gepresenteerd genaamd “high resolution meltingcurve analysis” (HRMA) welke is gebaseerd op DNA smeltcurve analyse. Met HMRA kunnen verzamelingen van recombinante klonen snel en nauwkeurig worden gescreend op identieke klonen. Deze techniek is in **hoofdstuk 3** toegepast waarin de selectie en karakterisatie van VHH antilichaamfragmenten tegen een N-terminaal mutant huntingtine eiwitfragment uit een geïmmuniseerde Lama faag-display bank wordt beschreven. De VHH binden zowel aan een normaal als mutant N-terminaal huntingtine fragment op ELISA en Western blot, en zijn in staat om endogeen normaal en mutant huntingtine te immunoprecipiteren uit humaan breinlysaat. De VHH hebben een epitoop tussen aminozuur 49 en 148. Deze VHH kunnen gebruikt

worden voor verder onderzoek naar de ZvH. In **hoofdstuk 4** is gekeken naar het effect van *post-mortem* delay, een vries-dooi cyclus en interpersoonlijke verschillen op het patroon van N-terminale huntingtine fragmenten in *post-mortem* humaan brein. Het effect van *post-mortem* delay op dit patroon was beperkt. Een vries-dooi cyclus op humaan breinweefsel (niet ZvH) had effect op signaalintensiteit, maar niet op het patroon van N-terminale huntingtine fragmenten. Het grootste effect op dit patroon kwam van interpersoonlijke verschillen. De resultaten van **hoofdstuk 4** kunnen worden gebruikt voor het (her)interpreteren van studies naar N-terminale huntingtine fragmenten. Vervolgens is in **hoofdstuk 5** een korte studie gepresenteerd naar huntingtine aggregatie in *post-mortem* humaan brein. Aggregatie is kwalitatief bepaald met behulp van immunohistochemie, en kwantitatief met behulp van een filter bindingstest. De resultaten van de filter bindingstest zijn op kwalitatief niveau vergelijkbaar met immunohistochemie. Op kwantitatief niveau liet de filterbindingstest een correlatie zien met polyQ lengte, en in één casus juveniele ZvH liet de filter bindingstest een significant hogere hoeveelheid aggregatie zien in cortex versus striatum. Deze resultaten suggereren dat de filter bindingstest een bruikbare tool is voor het kwantitatief bepalen van aggregatie in ZvH *post-mortem* brein. In **hoofdstuk 6** is met behulp van PCR en western-blot technieken gekeken naar expressiehoeveelheden van normaal en mutant huntingtine mRNA en eiwit in fibroblast cellijnen afkomstig van ZvH patieënten, en *post-mortem* humaan ZvH brein. Onze resultaten tonen geen verschil in de hoeveelheid mRNA tussen normaal en mutant huntingtine in fibroblast cellijnen. In *post-mortem* brein was de hoeveelheid mutant huntingtine mRNA lager dan de hoeveelheid normaal huntingtine mRNA. Op eiwit niveau werden gelijke hoeveelheden normaal en mutant huntingtine gevonden in zowel fibroblast cellijnen alsmede *post-mortem* brein. Echter, minder mutant dan normaal huntingtine was aanwezig in juveniele ZvH fibroblast cellijnen en *post-mortem* brein weefsel. Deze resultaten suggereren het bestaan van subtiele verschillen in expressie tussen gewone ZvH en de juveniele variant. Verder onderbouwen onze resultaten de toepasbaarheid van therapieën gericht op het verlagen van de hoeveelheid mutant huntingtine. In **hoofdstuk 7** wordt het in dit proefschrift beschreven onderzoek bediscussieerd in het licht van de aanwezige literatuur.

Het in dit proefschrift beschreven onderzoek heeft het kennisveld met betrekking tot expressielevels, aggregatie en fragmentatie van het huntingtine eiwit in *post-mortem* humaan brein (iets) vergroot, en reikt de VHH aan als gereedschap om ook in de toekomst op innovatieve wijze onderzoek te doen met als uiteindelijk doel een behandeling voor de ZvH.

English summary

Huntington disease (HD) is an autosomal dominant neurodegenerative disease with a variety of symptoms spanning from motor-related problems (chorea) to psychological issues. No effective HD therapy is yet available. HD is caused by expansion of a CAG repeat within the *huntingtin*-gene, resulting in a mutant huntingtin protein with an expanded polyQ.

After a historic intermezzo, **chapter 1** describes the frequency of occurrence, clinical symptoms, genetic background and brain pathology of HD. Onset of HD clinical symptoms typically starts around mid-life, but in rare cases HD symptoms occur at a young age which is referred to as *juvenile* HD. HD pathology is characterized by the presence of mutant huntingtin protein aggregations and an early specific atrophy of the striatum. HD pathology was detected before the onset of clinical symptoms in HD animal models and MRI-scans on persons who carry the HD mutation. Also, the risk of developing *de novo* HD through genetic anticipation is addressed. The huntingtin protein is discussed next. Huntingtin has a variety of functions within the cell and is essential for embryonic development. Experiments with knock-out mouse models showed that mutant huntingtin is capable of compensating for the loss of normal huntingtin. This suggests HD pathology exists through a “gain-of-function” mechanism where mutant huntingtin gains one or more toxic (inter)actions. Studies on HD animal and cell models show mixed results regarding the expression level of normal versus mutant huntingtin protein. The formation of especially N-terminal mutant huntingtin fragments is important for HD pathology. However, knowledge regarding protein expression levels or N-terminal huntingtin fragments in human brain tissue is limited. This knowledge is important with respect to- the development of therapies aimed at reducing expression of mutant huntingtin, or preventing the formation of N-terminal huntingtin fragments. At last, **chapter 1** describes how VHH antibody fragments, derived from a special type of antibody found in camelids, could be useful as potential HD therapy or research tool. **Chapter 2** describes “high resolution melting curve analysis”, or HRMA as a clone screening method. HRMA is based on DNA melting curve analysis and provides a fast and accurate screening of recombinant clones for the presence of identical ones. HRMA was used in **chapter 3** that describes the selection and characterization of VHH antibody fragments against an N-terminal mutant huntingtin fragment from an immunized Llama phage display library. The VHH binds normal and mutant N-terminal huntingtin fragments on ELISA and western blot and are capable of immunoprecipitating endogenous normal and mutant huntingtin from human HD brain lysate. The VHH epitope was mapped between amino acids 49 to 148 and is useful for HD research. In **chapter 4**, effects of *post mortem* delay, one freeze-thaw cycle and interpersonal variation on the pattern of N-terminal huntingtin fragments in post mortem human brain were assessed. We found that the effect of *post mortem* delay is small. One freeze-thaw cycle on (non-HD) human brain tissue affected signal intensity, but did not affect the pattern of N-terminal htt fragments which was mainly affected by

interpersonal differences. Hence, the results described in **chapter 4** could be used to (re)interpret study results regarding N-terminal huntingtin fragments. **Chapter 5** presents a pilot-study into huntingtin aggregation in *post mortem* human brain tissue. Aggregation was qualitatively determined using immunohistochemistry, and quantitatively using a filter trap assay. On the qualitative level, results from the filter-trap assay are comparable with immunohistochemistry. On the quantitative level, a correlation was seen between the filter trap assay results and polyQ-length. Also, a significantly higher level of aggregation was shown with the filter trap assay within cortex compared with striatum. These results suggest that the filter trap assay is useful to quantify huntingtin aggregation in *post mortem* human tissue. **Chapter 6** describes a PCR and western blot study into expression levels of normal versus mutant huntingtin RNA and protein in HD patient-derived fibroblasts and *post mortem* human HD brain tissue. Our results show no difference in mRNA quantities in fibroblasts between normal and mutant huntingtin. In *post mortem* brain tissue, quantities of mutant huntingtin mRNA was lower compared with normal huntingtin mRNA. On protein-level, no differences in normal versus mutant huntingtin was detected in either fibroblasts or *post mortem* brain tissue. However, when juvenile HD was considered, lower levels of mutant huntingtin were shown in both fibroblasts and *post mortem* brain. These results suggest that there are subtle differences in expression between regular and juvenile HD. Furthermore, our results support applicability of potential therapeutic interventions aimed at lowering mutant huntingtin levels. **Chapter 7** discusses the results from this thesis against literature findings.

The research described in this thesis has (modestly) broadened knowledge regarding expression levels, aggregation and fragmentation of the huntingtin protein in *post mortem* human brain tissue. Moreover, the VHH is presented as a new research-tool for future HD research with the ultimate goal of developing a cure for HD.

List of publications

Schut MH, Patassini S, Kim EH, Bullock J, Waldvogel HJ, Faull RLM, Pepers BA, den Dunnen JT, van Ommen GJB, and van Roon-Mom WMC. Effect of Post-Mortem Delay on N-terminal Huntingtin Protein Fragments in Human Control and Huntington Disease Brain Lysates. *PLoS One. 2017 Jun 1;12(6):e0178556. doi: 10.1371/journal.pone.0178556. eCollection 2017.*

Jansen AH, van Hal M, Op den Kelder IC, Meier RT, de Ruiter AA, **Schut MH**, Smith DL, Grit C, Brouwer N, Kamphuis W, Boddeke HW, den Dunnen WF, van Roon WM, Bates GP, Hol EM, Reits EA. Frequency of nuclear mutant huntingtin inclusion formation in neurons and glia is cell-type-specific. *Glia. 2017 Jan; 65(1): 50–61.*

Evers MM[#], **Schut MH**[#], Pepers BA, M. Atalar M, van Belzen MJ, Faull RLM, Roos RAC, van Roon-Mom WMC. Making (anti-) sense out of huntingtin levels in Huntington disease. *Molecular Neurodegeneration (2015) 10:21.*

Schut MH, Pepers BA, Klooster R, van der Maarel SM, el Khatabi M, Verrips T, den Dunnen JT, van Ommen GJB, van Roon-Mom WMC. Selection and characterization of llama single domain antibodies against N-terminal Huntingtin. *Neurol Sci (2015) 36:429–434.*

Pepers BA, **Schut MH**, Vossen RH, van Ommen GJB, den Dunnen JT, van Roon-Mom WMC. Cost-effective HRMA pre-sequence typing of clone libraries; application to phage display selection. *BMC Biotechnol. 2009 May 22;9:50.*

Moolenaar GF, **Schut M**, Goosen N. Binding of the UvrB dimer to non-damaged and damaged DNA: residues Y92 and Y93 influence the stability of both subunits. *DNA Repair (Amst). 2005 Jun 8;4(6):699-713.*

Curriculum Vitae

Menno Harm Schut is geboren op 4 Juni 1980 te Voorburg. Na het behalen van zijn VWO diploma aan College het Loo te Voorburg in 1998 is hij begonnen aan de studie Scheikunde te Leiden. In 2004 behaalde hij zijn doctoraaldiploma met als afstudeerrichting Biochemie na een stage in de groep van Dr. Nora Goosen onder begeleiding van Geri F. Moolenaar. Het onderwerp van zijn stage betrof “Nucleotide excision repair in E.Coli”, waar met behulp van verschillende puntmutaties in het UvrB-eiwit getracht is om het schadeherkenningsmechanisme te ontrafelen. Datzelfde jaar begon hij als QC analist bij het toenmalige Centocor te Leiden. In 2007 heeft hij een jaar als laborant gewerkt bij Sanquin te Amsterdam, waarna hij in 2008 als research analist bij het LUMC startte in de onderzoeksgroep van Dr. Willeke van Roon-Mom alwaar hij van 2009 tot 2013 als OIO heeft gewerkt wat uiteindelijk heeft geresulteerd in het in dit proefschrift beschreven onderzoek. Sinds 2014 werkt hij op detacheerbasis via Ajilon bij MSD te Oss.

Dankwoord

C'est fini…

Eindelijk is mijn proefschrift af. Echter de totstandkoming hiervan is allesbehalve een solistische aangelegenheid geweest, en ik wil hier dan ook van de gelegenheid gebruikmaken om allen die een bijdrage hebben geleverd daarvoor te bedanken.

Mijn promotor: **Gert-Jan**. Bedankt dat u bereid bent geweest om als mijn promotor op te treden. Uw nuchtere, al dan niet van een kwinkslag voorziene commentaren werden door mij immer gewaardeerd. Dank u wel!

Vanzelfsprekend wil ik ook mijn co-promotor **Willeke** bedanken. Naast de kans die je mij geboden hebt om te gaan promoveren, jouw uitstekende wetenschappelijke begeleiding en de mogelijkheid om in Nieuw Zeeland te werken, was je tevens cruciaal om mijn soms iets te negatieve insteek op argumenten te pareren. Daar heb ik op meerdere vlakken baat bij.

Mijn direkte collega's: **Melvin**; *"serieus maar met een glimlach"* is mijns inziens wel een goede omschrijving, en ik heb ook van jou veel geleerd. Bedankt voor alle gezelligheid en leuk dat je mijn paranimf wilt zijn. **Barry**; jou zou ik het best kunnen omschrijven als *"kundig en grondig"*. Mede door jouw adviezen en hulp is mijn proefschrift uiteindelijk tot stand gekomen. Bedankt voor alles! **Lodewijk**; De expert met betrekking tot *in vivo* experimenten en het presenteren daarvan. Succes met de laatste loodjes van jouw PhD. **Tassos**; Congratulations with finishing your PhD and I wish you all the best in the future.

Ik heb de eer mogen hebben om een aantal studenten te begeleiden; **Carlijn** en **Louise**, bedankt voor jullie noeste arbeid op het lab. Also, **Fausta** thank you for all your work.

I would also like to thank my other Leiden colleagues for providing assistance and/or a good and open working environment **Alex**, **Annemieke**, **Astrid**, **Christa**, **Cor**, **Curtis**, **Dwi**, **Eleonora**, **Ellen**, **Emile**, **Emmelien**, **Eve**, **Guido**, **Hans**, **Henk**, **Herman**, **Ingrid H**, **Ingrid V**, **Irina**, **Isabella**, **Ivo**, **Jeroen L**, **Jeroen N**, **Johan**, **José**, **Julie**, **Juliette**, **Laura**, **Laure**, **Leonie**, **Linda**, **Maaike**, **Maarten**, **Maartje**, **Majella**, **Marcel**, **Margriet**, **Marlous**, **Monika**, **Neil**, **Nisha**, **Omar**, **Peter-Bram**, **Petra**, **Pietro**, **Piet**, **Polina**, **Rolf**, **Raymund**, **Sandra**, **Silvana**, **Silvère**, **Simon**, **Steven**, **Svetlana**, **Tim**, **Timo**, **Vered**, **Willem**, **Wouter**, **Yahja**, **Yavuz**, and everyone whom I might have forgotten to put on this long list!

Babs en **Pauline**; Dank voor alle hulp met Converis en de formele promotieprocedure.

During my PhD, I had the wonderful opportunity to work in New Zealand. I would like to express my gratitude to **Henry** and **Richard** from the University of Auckland, New Zealand for their kind hospitality and keen advice. **Jocelyn** and **Marika**, thank you for providing all the help. **Stefano** and **Eric**; thank you for further assisting me with my project. **Malvindar**, **Nassim**, **Mike**, **Russel,**
Kevin, **Ray, Vicky** and **Maurice** thanks for the excellent working environment and all hospitality.
Kia Ora!

Bij dezen wilde ik tevens het Leids Universitair Medisch Centrum, alsmede de universiteit van Auckland bedanken en de respectievelijke afdelingen waar ik heb mogen werken.

Een bedankje gaat ook uit naar **Laura**. Jouw sport, en wijze lessen hielden mij fit en de geest scherp gedurende mijn promotieonderzoek.

Rutger, al 26 jaar zijn wij vrienden waarvoor ik via deze weg mijn waardering wil laten blijken.

Mijn beider families wil ik bedanken voor hun niet-aflatende steun en interesse gedurende deze lange weg. Oom **Paul**, je bent een voorbeeld voor mij. Mijn zus **Jurma** en mijn zwager **Peter**, jullie ondernemerschap verdient bewondering en jullie hulp heeft mij de broodnodige rust gegeven in een onrustige tijd. **Niels**, mijn zwager bij wie ik het proces van de laatste loodjes van het promoveren heb kunnen afkijken. Mijn zus **Maaike**; wij hebben altijd boeiende gesprekken. Bedankt dat je bereid bent om mijn paranimf te zijn!

Als laatste wil ik mijn ouders, **Harry** en **Jane** bedanken. Zonder de door jullie geleverde basis had ik nu niet gestaan waar ik sta. Ik heb veel geluk gehad jullie als ouders te hebben!